

Main-Sequence Effective Temperatures from a Revised Mass-Luminosity Relation Based on Accurate Properties

Z. Eker¹, F. Soydugan^{2,3}, E. Soydugan^{2,3}, S. Bilir⁴, E. Yaz Gökçe⁴, I. Steer⁵, M. Tüysüz^{2,3},
T. Şenyüz^{2,3} and O. Demircan^{3,6}

Akdeniz University, Faculty of Sciences, Department of Space Sciences and Technologies,
07058, Antalya, Turkey

Çanakkale Onsekiz Mart University, Faculty of Arts and Sciences, Department of Physics,
Terzioğlu Kampüsü, TR-17020 Çanakkale, Turkey

Çanakkale Onsekiz Mart University, Astrophysics Research Centre and Ulupınar
Observatory, Terzioğlu Kampüsü, TR-17020 Çanakkale, Turkey

Istanbul University, Faculty of Science, Department of Astronomy and Space Sciences,
34119, University-Istanbul, Turkey

NASA/IPAC Extragalactic Database, Pasadena, California, USA

Çanakkale Onsekiz Mart University, Faculty of Arts and Sciences, Department of Space
Science and Technologies,
TR-17020 Çanakkale, Turkey

eker@akdeniz.edu.tr

Received _____; accepted _____

ABSTRACT

The mass-luminosity ($M - L$), mass-radius ($M - R$) and mass-effective temperature ($M - T_{eff}$) diagrams for a subset of galactic nearby main-sequence stars with masses and radii accurate to $\leq 3\%$ and luminosities accurate to $\leq 30\%$ (268 stars) has led to a putative discovery. Four distinct mass domains have been identified, which we have tentatively associated with low, intermediate, high, and very high mass main-sequence stars, but which nevertheless are clearly separated by three distinct break points at 1.05, 2.4, and $7M_\odot$ within the mass range studied of $0.38 - 32M_\odot$. Further, a revised mass-luminosity relation (MLR) is found based on linear fits for each of the mass domains identified. The revised, mass-domain based MLRs, which are classical ($L \propto M^\alpha$), are shown to be preferable to a single linear, quadratic or cubic equation representing as an alternative MLR. Stellar radius evolution within the main-sequence for stars with $M > 1M_\odot$ is clearly evident on the $M - R$ diagram, but it is not clear on the $M - T_{eff}$ diagram based on published temperatures. Effective temperatures can be calculated directly using the well-known Stephan-Boltzmann law by employing the accurately known values of M and R with the newly defined MLRs. With the calculated temperatures, stellar temperature evolution within the main-sequence for stars with $M > 1M_\odot$ is clearly visible on the $M - T_{eff}$ diagram. Our study asserts that it is now possible to compute the effective temperature of a main-sequence star with an accuracy of $\sim 6\%$, as long as its observed radius error is adequately small ($< 1\%$) and its observed mass error is reasonably small ($< 6\%$).

Subject headings: Stars: fundamental parameters – Stars: binaries: eclipsing – Stars: binaries: spectroscopic – Astronomical Database: catalogues

1. Introduction

One of the fundamental secrets of the cosmos, the famous stellar mass-luminosity relation (MLR), was discovered empirically in the beginning of the 20th century independently by Hertzsprung (1923) and Russell, Adams & Joy (1923) from the masses of visual binaries. Eclipsing binaries were included in MLRs later. There were only 13 eclipsing binaries available together with 29 visual binaries and 5 Cepheids to Eddington (1926), while McLaughlin (1927) was able to include 41 eclipsing binaries in his plots.

Investigations of the MLR continued as the quantity and quality of data increased (Kuiper 1938; Petrie 1950a,b; Strand & Hall 1954; Eggen 1956; Cester, Ferluga & Boehm 1983; Henry & McCarthy 1993). Especially noteworthy was the critical compilation of absolute dimensions of binary components by Popper (1967, 1980). Only after the mid 20th century however, did studies involving the empirical stellar mass-radius relation (MRR) begin to appear in the literature (McCrea 1950; Plaut 1953; Huang & Struve 1956; Lacy 1977, 1979; Kopal 1978; Patterson 1984; Gimenez & Zamorano 1985; Harmanec 1988; Demircan & Kahraman 1991). There were five resolved binaries, 14 visual binaries and 12 O-B binaries with less accuracy in the MRR by Gimenez & Zamorano (1985). Demircan & Kahraman (1991) studied both MLR and MRR using 140 stars (70 eclipsing binaries) including the main-sequence components of detached, semi-detached binaries and the components of OB-type contact and near-contact binaries

Andersen (1991) collected detached double-lined eclipsing systems having masses and radii with uncertainties within 3%. Henry & McCarthy (1993) used masses of 37 visual binaries with main-sequence components from the fourth catalog of orbits of visual binary stars (Worley & Heintz 1983) in order to study the MLR for stars of mass 0.08 to $1M_{\odot}$ at near-infrared wavelengths, J (1.25 μm), H (1.6 μm), and K (2.2 μm). For the mass-absolute magnitude relation at visual wavelengths, where the upper mass limit

extended to $2M_{\odot}$, Henry & McCarthy (1993) combined the visual/speckle binary sample with the eclipsing binary data of 24 systems taken from Andersen (1991) and Popper (1980). Gorda & Svechnikov (1998) collected stellar masses and radii with accuracies within 2-3% from photometric, geometric, and absolute elements of 112 eclipsing binaries with both components on the main sequence for studying $(\log m - M_{bol})$ and $(\log m - \log R)$ relations, where m , R and M_{bol} stand for stellar mass, radius and absolute bolometric magnitude.

Ibanoglu et al. (2006) studied 74 detached and 61 semi-detached Algols on $M - R$, $M - T_{eff}$, $R - T_{eff}$, and $M - L$ diagrams separately. Collecting masses, luminosities, radii and temperatures from 114 (215 stars) detached main-sequence eclipsing binaries, Malkov (2007) constructed MLR and other relations [$M_V(\log m)$, $\log m(M_V)$, $\log L(\log m)$, $\log m(\log L)$, $\log T_{eff}(\log m)$, $\log m(\log T_{eff})$, $\log R(\log m)$, $\log m(\log R)$] by polynomials validated for the ranges of data. Recently, Torres, Andersen & Giménez (2010) updated the critical compilation of accurate, fundamental determinations of binary masses and radii. Studying metallicity and age contributions to the MLR for main-sequence FGK stars, Gafeira, Patacas, & Fernandes (2012) worked with only 13 binary systems, all taken from Torres et al. (2010).

Mass and chemical composition are two independent basic parameters from which various stellar evolution models are constructed. Radius (R), luminosity (L), and effective temperature (T_{eff}) are prime products of these models, and parameters by which stellar evolution can be followed. From the observational point of view, M and R are first order observable parameters. In the last decade, the number of accurately determined M and R has increased by hundreds. Further, their accuracy has reached the level needed to indicate stellar evolution, even within the main-sequence band. Chemical composition (or metallicity $[M/H]$) and T_{eff} are not as accurate as M and R , as present data indicates for binary stars. “Spectroscopic metal abundance determinations are available for a handful of systems”

says Andersen (1991). Unlike M and R , L is a second step product obtained from either observed magnitudes and distance, or from the relation $L = 4\pi R^2 \sigma T^4$. Both are problematic however, because both require accurate determinations of effective temperatures and such temperatures are rarely accurate because they are indirectly inferred. This study asserts that a revised main-sequence MLR can provide an easy and effective estimate of stellar effective temperatures directly from masses and radii.

Table 1 summarizes MLRs, MRRs and related improvements within the last two decades, where contributions from detached eclipsing-double lined binaries appear dominant. According to Table 1, the number of stars first decreased from 140 (70 eclipsing pairs) to 90 by eliminating unreliable ones. Demircan & Kahraman (1991) kept contact and semi-contact systems in calculating empirical $M - M_{bol}$ (mass-absolute bolometric magnitude) and MRRs within the mass range $0.63 < M/M_\odot < 18.1$ for the sake of statistical significance. Afterwards, the number of stars increased to 188, where 149 of them were from detached eclipsing main-sequence binaries in the study of Henry (2004), who also extended the mass range to $0.07 < M/M_\odot < 33$. Numbers increased further: 215 stars (114 pairs) by Malkov (2007) and 190 stars (94 eclipsing and α Cen) by Torres et al. (2010). An online database of detached binaries known as DEBCat¹ (Southworth 2014), which is periodically updated and commonly referenced, currently includes 342 stars (171 pairs). For this study, the latest compilation of detached eclipsing binaries given by Eker et al. (2014), was chosen as a calibration sample. It features 514 stars in 257 detached double-lined eclipsing binary systems.

Table 1 makes clear that the most recent updates of MLR and MRR are from Malkov (2007). It is noteworthy that despite having the most accurate and sufficient number of data, Andersen (1991) and Torres et al. (2010) did not pursue revising the classical MLRs

¹<http://www.astro.keele.ac.uk/jkt/debcat/>

& MRRs. “The scatter on the mass-luminosity diagram is not due to observational errors but most likely abundance and evolutionary effects” was a genuine message in both studies. Andersen (1991) claimed “... departures from a unique relation are real”. Therefore, declining to define a unique M - L function, Torres et al. (2010) preferred to express $\log M$ by the simplest possible polynomials containing the parameters T_{eff} , $\log g$ and $[Fe/H]$ as variables rather than a classical approach as Malkov (2007), who expressed $\log L$ as a function of $\log M$. Similarly, a unique MRR was not defined by Torres et al. (2010) but instead $\log R$ was expressed as a function of T_{eff} , $\log g$ and $[Fe/H]$, unlike in Malkov (2007), who expressed $\log R$ ($\log M$) and/or vice versa $\log M$ ($\log R$).

Fortunately, it is always possible to define a unique function to express a band of data by a least squares method. Moreover, the classical MLR and MRR have been proven to be useful and are widely applied. For example, the MLR and MRR of Malkov (2007) has been used by Catanzaro & Ripepi (2014), Fumel & Böhm, (2012), Ripepi et al. (2011), and Zasche & Wolf (2011). The MLR and MRR of Demircan & Kahraman (1991) were used by Jiang et al. (2009), Kraus et al. (2009), Hunter et al. (2008), and Li et al. (2005). Of course, usage is not limited to these authors. There are many more examples; indeed too many for all to be cited here. Therefore, revisions of classical MLR and MRR with modern and more accurate data are periodically necessary. As a preparatory work, Eker et al. (2014) have already compiled basic stellar parameters (i.e. M , R , T_{eff} and L) for 257 detached binaries (514 stars), mostly main-sequence, and with masses and radii recomputed based on the most up to date values in use of the solar gravitational constant and solar radius of $GM_{\odot} = 1.3271244 \times 10^{20} \text{ m}^3\text{s}^{-2}$ (Standish 1995) and $R_{\odot} = 6.9566 \times 10^8 \text{ m}$ (Haberreiter, Schmutz & Kosovichev 2008). Stellar temperatures and luminosities were also revised and homogenized (Table 2 of Eker et al. 2014). Compared with previous lists in Table 1, the number of stars with masses and radii, which are accurate to within 3%, is increased by 50%. Not only the number and quality, but also the range of the data was

improved to: $0.2 < M/M_{\odot} < 32$, and $0.23 < R/R_{\odot} < 9.36$. All of these improvements motivated us to revise the $M - L$, $M - R$ and $M - T_{eff}$ relations based on the increased quantity and quality of data, and the fact that it is now available in a homogenized form.

Critically, most light curve solutions for eclipsing binaries require an effective temperature for at least one component as an input. However, in most critical cases that is not available. Therefore, some authors such as Helminiak et al. (2009) and Zasche (2011), avoid using roughly estimated values, and are satisfied with solutions without temperatures. Such solutions contain only temperature ratios, not absolute temperatures. Since detached double-lined eclipsing binaries are basic sources of reliable stellar parameters (M , R), this study asserts that by revising the MLR, and making use of $L = 4\pi R^2 \sigma T^4$, direct estimates of stellar temperatures can be obtained. Direct estimates can be used in problematic cases where no estimate is available, and can provide an important, independent calibration of temperatures obtained by indirect means.

2. The Data

The number of stars with dependable parameters was so limited just a quarter of a century ago, that even solutions based on contact and semi-contact eclipsing systems could not constrain uncertain parameters sufficiently to produce revised MLRs and MRRs, as shown in Table 1. Thanks to modern detectors, observing techniques and high speed computers, the number of accurate and precise solutions from detached eclipsing spectroscopic binaries has increased rapidly. Today we are able to select stars with the most reliable stellar parameters of any desired criteria. Therefore, the first step of this study was to form a calibration sample containing a larger number of stars with more reliable parameters distributed over a greater range than was available to previous studies (Table 1).

2.1. Calibration Sample

A calibration sample was formed by selecting main-sequence stars with the most accurate masses, radii and effective temperatures from Table 2 of “The Catalogue of Stellar Parameters ...” by Eker et al. (2014), which is already reprocessed and homogenized. In the first step, our preliminary criteria involved finding stars where both mass and radius with errors of less than or equal to 3%, and luminosities with errors less than or equal to 30% were available. Among 514 stars (257 binaries), 296 stars were found fulfilling the criteria. In the second step, 25 stars outside of the main sequence were removed.

The process of removing non-main-sequence stars was completed by using the mass-radius diagram. Compared to effective temperatures and luminosities, which can only be inferred indirectly, masses and radii provide much more reliable indicators of stellar properties, and a highly improved diagnostic tool for analyzing stellar evolution. Fig. 1 shows 271 main-sequence stars selected for the calibration sample and 25 non main-sequence stars on the $M - R$ diagram. Theoretical ZAMS (Zero Age Main Sequence) and TAMS (Terminal Age Main Sequence) lines for metallicity zero from Bertelli et al. (2008, 2009) were used as border lines to secure the stars within the main-sequence band.

Although metallicity data is missing in the catalogue of Eker et al. (2014), the thin-disk field stars in the solar neighborhood are known to have solar metallicity on average, with upper and lower limits of ± 0.5 dex in metallicity (Cox 2000). It is also known that the thin disk stars in the solar neighborhood could be polluted by about 6-8% by thick disk and halo stars (Karaali et al. 2003; Karataş et al. 2004; Bilir et al. 2005, 2006, 2008; Ak et al. 2010, 2013). TAMS lines for zero metallicity, therefore, do not limit the upper border sharply. Consequently, there could be a negligible number of non-main sequence stars remaining in the calibration sample. Such a small amount of pollution however, is too small to alter the general characteristics of the sample stars, which are solar neighborhood main-sequence

stars with an average metallicity of zero.

Table 2 gives basic astrophysical parameters (M , R , T_{eff} , and L) and their relative errors. The columns are self explanatory to indicate sequence number, name, coordinates, component (primary or secondary), mass, relative error in mass, radius, relative error in radius, published effective temperature, error in temperature, luminosity, relative error in luminosity, the Roche lobe filling factor and remark. A filling factor (FF) for a star in a binary, which is defined as $FF = \bar{r}/\bar{r}_{RL}$, where \bar{r} is average radius, and \bar{r}_{RL} is Roche Lobe radius relative to the semi-major axis of the orbit, is a parameter that indicates its sphericity. Eker et al. (2014) have concluded that deviations from sphericity could be ignorable for small FF , as big as 75%, a value corresponding to the difference between $r(\text{point})$ and $r(\text{pole})$ being less than 1% of the star radius. $r(\text{point})$ and $r(\text{pole})$ are the deformed radii of the star towards the other component and towards the rotation axis, respectively.

Fig. 2 shows how filling factors distribute among the stars of the calibrating sample. Accordingly, 89% of the stars in the calibrating sample are spherical within 1% of radius. The rest, or 11%, are deformed more than 1% but still respectively detached, so that one can assume all of the calibrating stars are from binaries in which mass transfer has not occurred. All of the stars in the calibrating sample should have evolved as if they were single with a corresponding rotation as indicated in the catalogue of Eker et al. (2014).

2.2. Stellar mass domains

The main sequence MLR, discovered by Hertzsprung (1923) and Russell et al. (1923) in the first half of the 20th century, is one of the most fundamentally confirmed, and universally recognized astronomical relations. The relation can be expressed in different

ways, based on the relation between M and L , or between M and M_{bol} for example. Various forms of it are found. However, the most fundamental and basic form is $L \propto M^\alpha$, where the power (α) is the slope on the logarithmic $M - L$ diagram. With early limited data, it was possible to express the MLR of main-sequence stars with a single power law. However, as the quantity, quality, and range of data increased, it became increasingly clear that the MLR could not be expressed with a single linear fit. Consequently, many authors (Kuiper 1938; Cester et al. 1983; Andersen 1991; Demircan & Kahraman 1991; Henry & McCarthy 1993; Malkov 2003, 2007; Fang & Yan-ning 2010) preferred to express the MLR for various mass ranges; thus there could be various values of α for various mass ranges, usually arbitrary.

When pre-exploring different forms of the relation using M and L of 271 stars (Table 2), we identified natural stellar mass intervals, where α is constant on the $\log M - \log L$ diagram. Their identification came as a surprise, since we were exploring the amount of stellar energy production rate as a function of stellar mass. Being a parameter expressing the efficiency of stellar furnaces, that is L/M , the luminosity per stellar mass (in solar units) was plotted against the stellar mass in Fig. 3. The distribution appears linear only in distinct mass ranges. There are break points as indicated on the figure at $M = 1.05$, 2.4 and $7M_\odot$. Linear distributions are clearly visible before, between and after the break points.

The reciprocal of L/M , that is M/L , which is known as the mass to light ratio, is a parameter commonly used among extragalactic astronomers (Faber & Gallagher 1979; Bell & de Jong 2001; Girardi et al. 2002). In global meaning, mass to light ratio implies a variety of galactic compositions (stellar) and depends on the relative number of stars of different types. As it is used for spiral galaxy rotation curve decomposition and band-pass dependent slope of the galaxy magnitude-rotation velocity relation (Tully-Fisher

relation, Tully & Fisher 1977), it is also recognized as a parameter to indicate dark matter (Blumenthal et al. 1984). Although usage of M/L by extragalactic astronomers appears to be conceptually different than L/M investigated in this study, M/L cannot be independent of L/M . We believe updated information of the energy generation efficiency as a function of varying stellar types on the main sequence will be used in improving models for future extragalactic studies.

We tried many simple functions to express L/M in terms of M . However, when we plotted $\log(L/M)$ versus M , the appearance of natural stellar mass intervals caught our attention. In Fig. 3 for example, a sharp linear increase of $\log(L/M)$ up to $1.05M_{\odot}$ is clear. For stars with masses greater than $1.05M_{\odot}$ however, that increase continues less steeply up to $2.4M_{\odot}$. The p-p chain is the main energy source for stars less massive than the Sun, while the CNO cycle becomes dominant for stars more massive than the Sun. Thus, we surmise that the break point at $1.05M_{\odot}$ is just an indication of this change. There could be similar reasoning related to the efficiency of stellar energy production mechanisms at the other break points, where the rate of linear increase of $\log(L/M)$ suddenly decreases. The preliminary conclusion, based on Fig. 3, is that the change of energy production rate per stellar mass (efficiency, L/M) for stars of a given mass is a stronger function of a star’s mass than of its temporal evolution. Nevertheless, the prime concern of the present work is to study classical MLR in general and/or in between those break points, which can be defined in terms of stellar mass domains: low mass ($0.2 < M/M_{\odot} \leq 1.05$), intermediate mass ($1.05 < M/M_{\odot} \leq 2.4$), high mass ($2.4 < M/M_{\odot} \leq 7$), and very high mass ($M/M_{\odot} > 7$). We encourage theoreticians especially nuclear astrophysicists, to further investigate the physical facts and reasoning behind these break points.

3. Calibrations

3.1. Classical MRL

The improved data of the present study permits us to apply a classical approach thanks to the recognition of stellar mass domains when updating classical MLRs. Recent studies, by comparison, were more limited (Demircan & Kahraman 1991; Henry & McCarthy 1993; Malkov 2003, 2007; Fang & Yan-ning 2010). At best, the existing mass range could be divided at $M = 1.7M_{\odot}$, since stars of $M > 1.7M_{\odot}$ have convective cores with radiative envelope while stars of $M < 1.7M_{\odot}$ are vice versa. At worst, the range in masses was handled arbitrarily when determining the power of M for the classical MLRs. Fig. 4 gives the distribution of the sample stars on the $\log L - \log M$ diagram. The break points in Fig. 3 are marked as vertical dashes at 0.021, 0.38 and 0.845 in $\log M$, which corresponds to 1.05, 2.4 and $7M_{\odot}$ in mass. The first one at $1.05M_{\odot}$ is obvious but other break points are not as clear as before when compared to Fig. 3, where the mass axis was linear. With a careful look at Fig. 4, one can nevertheless still detect by eye the linear orientation of the data before, between and after these break points, even with the mass axis changed to logarithmic and vertical axis changed to $\log L$.

The linear distributions of $\log L$ within the four mass domains are clearly displayed in the four panels of Fig. 4 (Fig. 4b, c, d and e) below the main panel (Fig. 4a). The four panels contain M and L of the stars from the calibrating sample within each stellar mass domain, which was defined according to the brake points in Fig. 3. The classical MLR ($L \propto M^{\alpha}$) for stars within each of the four stellar mass domains have been determined by fitting a linear equation by the least squares method. The statistics, mass domains and linear MRLs are summarized in Table 3. The linear equations given in column 4 represent the best fitting lines, which are displayed in the lower four panels in Fig. 4. High degrees of correlations indicated by the data within the lines of 1σ limit are very clear. Notice that

the three stars with the smallest masses, the components (A and B) of CM Dra and the secondary of LSPM J1112+7626, do not seem to obey the linear trend of the MLR line in the low mass domain ($0.2 < M/M_{\odot} \leq 1.05$). Therefore, those three stars were excluded from the analysis and the lower limit of the low mass domain was changed to $0.38M_{\odot}$ as indicated in Table 3. Obviously, those three stars with lowest masses in the calibration sample belong to another domain, which could be called very low mass domain. The break point between the very low and low mass domains is not clear because of insufficient data. We leave clarification of this point for the future, when more data will be available.

As in earlier studies, we also asked if there is a single unique function to represent all stars in the calibrating sample. Consequently, a linear, a quadratic and a cubic equation were fitted to the masses and luminosities of the calibration sample using the least squares method. The results are summarized in Table 4. The correlations of all three fits are the same, but the linear function has considerably larger standard deviation than the quadratic and cubic functions. It is interesting that quadratic and cubic functions give the same standard deviations. This means that a quadratic function, as given in Table 4, fits the present sample sufficiently and there is no need for cubic and higher order polynomials. The quadratic MLR found in this study is compared with the most recent quadratic MLRs in Fig. 5. While deviation from Demircan & Kahraman (1991) is apparent, there is very little difference between Malkov (2007) and the present study.

As in earlier studies, it could be practical to define a single function to represent the MLR for stars in the calibration sample as a whole. However, if such a function is a quadratic, cubic or a higher order polynomial, the classical meaning ($L \propto M^{\alpha}$) implied by a linear fit is lost. In revising the classical MLR based on the calibration sample, the linear fits found within the four mass domains can be considered as due to physically real if not yet physically understood divisions. Quadratic MLRs by comparison are only useful

for inter-comparing the results of current and previous studies in terms of how improved the quantity and quality of data is compared to previous studies. In this study we assert therefore, that the linear MLRs as suggested in Table 3, are best to represent the calibration sample in particular and, nearby main-sequence field stars in general.

The residuals due to the four piece linear MRL (Table 3) and residuals due to quadratic and cubic MRL (Table 4) are inter-compared in Fig. 6. The quality of all fits is very similar, but the four-piece linear function, with physical background, is preferable.

3.2. Mass-Radius and Mass-Effective Temperature

The MRR and the mass-effective temperature (MTR) relations found from the present sample are displayed in Fig. 7. The radius evolution within the main-sequence band, especially for the stars $M > 1M_{\odot}$, is clearly visible on the $M - L$ plot. The appearance of data on the $M - R$ diagram is very different than the appearance on the $M - L$ diagram, which rather looks like a band of data expressible by a function. However, with a very narrow distribution of radii for masses $M < 1M_{\odot}$ and a broad band of radii for stars with $M > 1M_{\odot}$, a single function to express a MRR would be odd and meaningless. A continuous line in Fig. 4a indicates the theoretical ZAMS according to Bertelli et al. (2008, 2009). However, the temperature evolution within the main-sequence band is not that obvious on the $M - T_{eff}$ diagram. At first look, it resembles the MLR shown in Fig. 4a. Therefore, one may think, it is possible to express a MTR by a polynomial or by various linear fits as was done for the MLRs of the four mass domains.

The temperatures of stars are determined mostly by a few methods including intrinsic colors, atmosphere modeling, spectral fitting to selected spectral line(s) or region(s), and/or from spectral line depth ratios. When applied to binary stars, however, those methods

face severe difficulties since colors and spectra obtained are usually for the system, not for the components separately. Recent methods, like CCF fitting or spectral analysis give accurate, and reliable temperatures, but it is only quite recently. In many previous studies, including light curve analyses of eclipsing binaries, the temperatures of the primary components were adopted according to roughly estimated spectral types and colors determined from de-reddened *UBVRI* photometry (e.g. Ren et al. 2011; Li & Qian 2013; Elkhateeb, Nouh & Saad 2014). Spectral types and colors for eclipsing binaries however, are mostly given for the system, not for the components separately. In addition, low resolution spectra do not provide reliable spectral types. As a result, some researchers have preferred to use temperature ratios to avoid unreliable temperature values (e.g. Hełminiak et al. 2009; Zasche 2011). Therefore, practical and reliable methods for determining component temperatures in eclipsing binaries are needed.

3.3. Calculating T_{eff} using MLRs

An effective temperature for a star may be calculated using the well known Stephan-Boltzmann relation: $L = 4\pi R^2 \sigma T_{eff}^4$. Solving it for T_{eff}

$$T_{eff} = 5777 \times \sqrt[4]{\frac{L/L_\odot}{(R/R_\odot)^2}}, \quad (1)$$

where 5777 K is the effective temperature of the Sun (Cox 2000). Only the L and R of the star are needed. The solar luminosity and radius (L_\odot and R_\odot) are also needed if L and R are not in solar units. Assuming M and R of a star are available together with relative errors, one may use the proper MLR in Table 3 to compute L/L_\odot for the full range of stellar masses of the calibration sample of this study $0.38 < M/M_\odot < 32$. After calculating the effective temperature of a star using Eq. (1), the accuracy would be estimated as following:

$$\frac{\Delta T_{eff}}{T_{eff}} = \sqrt{\left(\frac{\Delta L}{4 \times L}\right)^2 + \left(\frac{\Delta R}{2 \times R}\right)^2}. \quad (2)$$

The vector form of Eq. (2) is $\frac{\Delta L}{L} = 2\frac{\Delta R}{R} + 4\frac{\Delta T_{eff}}{T_{eff}}$, which may be obtained from $L = 4\pi R^2 \sigma T_{eff}^4$ by a proper differentiation. The relative uncertainty of the radius was assumed to come from observational random errors. On the other hand, the relative uncertainty of the luminosity comes from dispersions of L on $M - L$ diagram. Using the logarithmic differentiation rule $\Delta \log L = (\log e)\frac{\Delta L}{L}$ and making the standard deviations (σ) equal to $\Delta \log L$, then the relative uncertainty of the luminosity is

$$\frac{\Delta L}{L} = \frac{\sigma}{0.4343}. \quad (3)$$

For a star of a given mass, the standard deviations and corresponding relative uncertainties are summarized in Table 5. The columns are self explanatory to indicate stellar mass domains, mass ranges, standard deviations, and corresponding uncertainties of the luminosities ($\Delta L/L$) in the first four columns. One fourth of $\Delta L/L$ and half of $\Delta R/R$ are in columns five and six. Since the largest uncertainty of a stellar radius is 3% in the calibration sample, the $\Delta T/T$ in column seven is an upper limit. Actual $\Delta T/T$ could be as small as one fourth of $\Delta L/L$ depending on the value of the relative errors associated with the radius of the star.

According to Table 5, relative error of a radius ($\Delta R/R$) contributes little to the uncertainty of the effective temperature ($\Delta T/T$). The uncertainty of the predicted luminosity ($\Delta L/L$) dominates. The standard deviations from MLRs are not the results of individual relative errors associated with observed parameters of the stars. In fact, we have chosen stars in the calibration sample with relative luminosity errors of 30% or less. Assuming a uniform error distribution, this would have given us a mean uncertainty on the MLRs of less than 15%. However, the predicted relative uncertainties in Table 5 (column 4) from the standard deviations are nearly twice as large. This would clearly indicate that the standard deviations from MLRs are affected more from the natural dispersions within a band defined by ZAMS and TAMS luminosities. “... scatter is highly significant and not

due to observational uncertainties” say Torres et al. (2010). Metallicity is also contributing by shifting ZAMS and TAMS. Negligibility of observed errors in comparison to metallicity and evolutionary effects on $M - L$ diagram are already confirmed by Andersen (1991), Torres et al. (2010) and even on the observed H-R diagram by Eker et al. (2014). Indeed many of the error bars of individual points in Fig. 4 are much smaller than the printed symbols.

Because uncertainties of MLR luminosities dominate over errors associated with observed radii according to the data in Table 5, one may take it as an advantage to tolerate less accurate stellar radii. Increasing the relative error of radius from 3% to 6%, the uncertainty of the predicted temperature would still be less than 8%, except for the high mass and very high mass domains, which would be extended to 10%.

According to Table 5, the method of computing T_{eff} using present MLRs would tolerate less accurate radii, but what about the tolerance associated with the mass of the star? The following equation could be used to propagate the uncertainty associated with the MLR luminosity to the mass of the star as

$$\frac{\Delta L}{L} = \alpha \frac{\Delta M}{M} \quad (4)$$

where the values of $(\Delta L/L)$ and α are given in Table 5. Note that α is available only for MLRs with classical mass luminosity relation ($L \propto M^\alpha$). For the stellar mass domains defined in this study, the propagated uncertainty to the mass of the star is computed and recorded in the last column of Table 5. For stellar masses up to $M = 2.4M_\odot$, about 6% error in mass is tolerable. Tolerance level increases to 8% and then to 13% as the mass of the star increases to 7 and then up to $32M_\odot$, respectively. Consequently, it can be concluded that: when predicting the luminosity for a star of a given mass from the revised classical MLR in this study, the observational errors associated with mass could be tolerable up to 6% for the stellar masses up to $2.4M_\odot$ and even up to 10% for stars with larger masses as

indicated in the last column of Table 5.

The method is still applicable to stars with less accurate mass and radius. With a mass having less accuracy, one must propagate the uncertainty of the mass back to the luminosity using Eq. (4). Such a propagated uncertainty ($\Delta L/L$) is expected to be poorer than the uncertainty ($\Delta L/L$) estimated from the standard deviations on MLRs through Eq. (3). Otherwise one must compare those propagated and MLR uncertainties of $\Delta L/L$ and then must insert the worst one in Eq. (2). The MLRs and the standard deviations predicted in this study from the most accurate stellar parameters ($\Delta L/L \leq 30\%$, $\Delta M/M \leq 3\%$, $\Delta R/R \leq 3\%$) reveal that it is possible to calculate the effective temperature of a star with an accuracy better than 8% if the mass and the radius of the star have accuracies up to 6%. With a negligible radius error, the temperature error could be reduced to as low as 6%. For sun-like stars, that means 300-400 K. Such accuracy is lower than, admittedly, the accuracy available using other methods including spectroscopy, line depth ratios, template fitting, cross correlation or non-LTE spectral synthesis, at typically 100-200 K. However, an effective temperature with few (or several) hundred degrees uncertainty is very useful in cases where such information is not given, like Helminiak et al. (2009) and Zasche (2011). Further, the method based on the Stephan-Boltzmann law, identified mass domains and revised MLR has the advantage over other methods of being practical and easy to apply if M and R are available. In comparison, other methods suffer from problems with de-reddening, issues with decomposition, and various other complexities common with spectroscopic techniques.

4. Applications and results

4.1. Comparison with published temperatures and errors

Our simple method for calculating effective temperatures based on the Stephan-Boltzmann law has been tested using updated MLRs. Temperatures calculated were compared with temperatures published. For the low mass domain, the revised MLR is based on 57 stars in the calibration sample, since we excluded the three lowest mass stars already mentioned as outliers from our analysis (primary and secondary of CM Dra and the secondary of LSPM J1112+7626). The low mass MLR therefore applies to main sequence stars in the mass range $0.38 < M/M_{\odot} \leq 1.05$. Fig. 8 shows calculated (vertical) and published (horizontal) temperatures for 268 stars in the calibrating sample. The mean standard differences ($\sqrt{\langle(T_{cal} - T_{pub})^2\rangle}$) for the temperature ranges 2750-5000 K, 5000-10000K, 10000-15000K and 15000-43000K are marked as dashed lines in Fig. 8b. Those standard differences were compared to the standard deviations of calculated (mean calculated error) and published (mean published error) temperatures in Table 6.

The stellar Mass-Luminosity relation is a well determined universal law discovered in early 20th century and since later confirmed by stellar structure and evolution theory. The empirical $M - L$ diagrams produced within the last two decades indicate observational errors have little contribution to the true shape of the luminosity distribution (thickness of the band) for main-sequence stars. The width of MLRs is mostly affected by metallicity and evolution (Andersen 1991; Torres et al. 2010). In this respect, our computed effective temperatures must be independent from the published temperatures because: 1) the uncertainty contribution of the dispersion on M-L diagrams is a dominant factor and it is mostly due to evolution and metallicity, not because of observational errors. Consequently, 2) observed temperature errors do not propagate back to calculated temperatures because they have negligible contribution to the dispersion.

The results in Table 6 indicate that mean calculated errors are about the same order as the mean calculated differences. This further supports the temperature calculating method used here. It also demonstrates that the calculated temperatures are all in close agreement with the published temperatures obtained by other methods, most based on optical photometry (color or brightness temperatures) and some involving spectroscopic techniques (excitation, ionization, or kinetic temperatures).

The results in Table 6 also indicate that mean published errors are about three times smaller than mean calculated errors. That is, a significant fraction of the published temperatures are underestimated. Underestimated temperature errors are very obvious in some studies, e.g. the effective temperatures of AE For $T_{eff}(sec) = 4055 \pm 6$ K (Rozyczka et al. 2013), XY UMa $T_{eff}(sec) = 4125 \pm 7$ K (Pribulla et al. 2001), and DV Psc $T_{eff}(sec) = 3614 \pm 8$ K (Zhang & Zhang 2007). These stars are not the only examples. Most light curve solutions require a temperature for a component, and then solutions provide a temperature and its uncertainty for the other component. The internal temperature errors given by such light curve solutions, usually, are not realistic, but underestimated. Occasionally, the same internal errors are assumed for both temperatures (Ribas, Jordi & Torra 1999; Clausen et al. 2010; Kraus et al. 2011). There are 31 systems, which temperature errors of the secondary is identical to the temperature error of the primary, among the 45 detached binaries listed by Andersen (1991). Similarly, among the 95 binaries of Torres et al. (2010), the number of such systems is 67.

The present sample is very heterogeneous in the sense that Table 1 of Eker et al. (2014), from where they were taken, lack a common treatment. Temperatures given in older papers are based on only rough fits. Those given in many recent studies, by comparison, are much more rigorously derived. To compare the agreement between the calculated and published effective temperatures in terms of older versus recent papers, we have plotted

published temperatures from the last seven years with a different symbol and color. Note that the number of recently determined temperatures dominates. 46% of temperatures in the calibration sample (124 stars) were taken from papers published in the last seven years. The better agreement between the calculated temperatures and those published recently compared to those published less recently is shown in Fig. 8.

For a better comparison between the calculated and published temperatures, the photometric distances were computed for the limited number (20) of binaries with most reliable *Hipparcos* parallax within 100 parsecs to avoid interstellar reddening. The method of computing can be summarized as: first luminosity of each component was calculated using its radius and effective temperature. The luminosities were transformed to bolometric absolute magnitudes. Bolometric absolute magnitudes were, then, transformed to visual absolute magnitudes with proper bolometric corrections (Cox 2000) corresponding to the temperatures used. The visual absolute magnitudes of the two stars (components) were combined to find absolute visual magnitude of the binary itself. From the apparent and absolute visual magnitudes (distance modulus), the photometric distances were computed and compared to the *Hipparcos* distances of the selected binaries in Fig. 9. The standard deviations of the differences from the diagonal indicate that calculated temperatures are slightly less accurate than the published temperatures.

4.2. Accuracy and Utility

Figure 10 compares both $M - T_{eff}$ diagrams with published and calculated temperatures. Note that the $M - T_{eff}$ diagram with published temperatures is shifted up in vertical scale by +0.3 dex in order to compare both on a single diagram. Heterogeneity of the published temperatures and homogeneity of the calculated temperatures can be deduced. The published temperatures appear mostly contained within the main-sequence

band for stars with $M > 1M_{\odot}$, while for the same stars the calculated temperatures appear to be scattered more and outside the main-sequence band. By comparison, the homogeneity and larger uncertainties makes the distribution of calculated temperatures relatively thicker than published ones (see, Fig. 10).

The classical MLR is a thin, well defined function, while the main-sequence evolution is rather a band. Therefore, calculating effective temperatures using such a function propagates the half thickness of the band as a dominant uncertainty, more than at least 6%. Thus there are more points outside the ZAMS and TAMS lines of Bertelli et al. (2008, 2009) for the stars with $M > 1M_{\odot}$. In comparison, for stars with $M \ll 1M_{\odot}$, the main-sequence lifetimes are much greater than the age of our Galaxy. Evolutionary effects therefore, do not impact lower mass stars as greatly as they do higher mass stars. MLR as a thin well defined function appears to be very successful in representing low mass stars. Notice that the scatter in calculated temperatures is much narrower compared to the scatter in published temperatures for stars with $M \ll 1M_{\odot}$, as shown in Fig. 10. However, low mass stars in eclipsing binaries show a well known discrepancy of temperatures and radii with respect to the models, most likely related to the activity (Çakırlı, İbanoğlu, & Dervişoğlu 2010; Morales et al. 2010; Hełminiak et al. 2011; Bass et al. 2012; Stassun 2013). This may partially explain the larger spread in the low-mass regime for the published temperatures. Apparently, radii of the sample stars in the same low-mass regime were not affected as indicated on $M - R$ diagram (Fig. 7a), a smooth and narrow distribution is produced in the same low-mass region of stars in Fig. 10.

Any well defined MLR provides a single L for a given M . Metallicity and evolution information contained on the $M - L$ diagram, will be lost with this single value of L . This may appear as a draw back. On the contrary, this study asserts that the information lost by defining a MLR could be re-introduced into the $M - T_{eff}$ diagram by calculating

effective temperatures using MLR and R . Accurately determined radii constrain the effects of metallicity and evolution because R is one of the primary products of the evolution theory, which uses M and metallicity as free initial parameters. One does not need to know age and chemical composition of the star because it naturally propagates to T_{eff} calculated. Since the same applies to all stars in the calibration sample, all calculated temperatures as calculated are homogeneous to reflect the evolution and metallicity information contained on $M - R$ diagram. In addition to this propagated effect of evolution, further thickening of the distribution for the stars $M > 1M_\odot$ is introduced by errors. Therefore, the difference between ZAMS and TAMS reaches to 0.2 dex (in $\log T_{eff}$), rather than 0.15 dex implied by ZAMS and TAMS lines of Bertelli et al. (2008, 2009).

4.3. Applications with less accurate M and R

The presented method of calculating effective temperatures has been applied to a larger sample (371 stars) containing less accurate M and R . The sample has been chosen from the 514 stars in the same catalogue from which the calibration sample was selected. For this larger sample there were only two selection rules: 1) both M and R could have errors up to 6%, 2) both components had to be on the main sequence. Unlike for the calibration stars, there is no limitation on the accuracy of the luminosities here. There are 408 stars with M and R having errors less than or equal to 6%. That number is reduced to 371 after removing non main-sequence stars. This new list naturally contains the calibration sample. The new calculated effective temperatures and published temperatures for these stars are listed in Table 7. Columns are self explanatory to indicate sequence number, name of the binary, equatorial coordinates, component (primary or secondary), relative errors in mass and radius, published temperature and its error, computed temperature and the upper limit of its error. Notice that in this new list there are 12 stars with no effective temperatures.

New temperature estimates were calculated for these stars, and calculated temperatures for the entire sample are homogenized to a single method. Calculated temperatures have accuracies mostly better than 8%.

Figure 11a shows the $M - R$ diagram for the 371 main-sequence stars. Fig. 11b shows their distribution on the $M - L$ diagram. Finally, Fig. 11c illustrates the $M - T_{eff}$ diagram with effective temperatures computed. All temperatures are homogenized and despite having accuracies that are $\Delta T/T \leq 8\%$, stellar evolution within the main-sequence is also noticeable on the $M - T_{eff}$ diagram in the same fashion as in Fig. 10.

Figure 11 also demonstrates why main-sequence MLR is fundamentally confirmed and universally recognized, but the same is not true for the $M - R$ and $M - T_{eff}$ relations. If mass loss is neglected during the main-sequence lifetime, radius evolution pulls the star upward on the $M - R$ diagram, while corresponding temperature evolution is downward on the $M - T_{eff}$ diagram. This is at least what is happening in Fig. 11, where a single value of L of a given M is used according to derived MLR's in this study. A single value of L means there is no evolutionary and metallicity effects on L . Evolutionary and metallicity effects are main contributing factors to the uncertainty of L . In fact, as discussed in previous sections, the observational uncertainties of R and T , which propagate to L , are negligible compared to evolutionary and metallicity effects. The upward evolutions seen for the stars $M > 1M_\odot$ on $M - R$ diagrams become downward evolutions on the $M - T_{eff}$ diagram as a consequence of a fixed L . One should still keep in mind that the evolutionary and metallicity information contained in $M - R$ diagrams must also be contained in $M - T_{eff}$ diagrams, albeit exaggerated by errors of the computed temperatures.

If we look at stellar evolution theory in general, the stars with $M > 1M_\odot$ the luminosity increases but in such a way that the surface temperature drops relatively little because of the expanding radius (Clayton 1968) except in the final stages of MS evolution when the

central convection zone starts to shrink and disappear by the depletion of hydrogen in the center. In this final stage, surface effective temperatures increase a little such that, the overall effect is that the star is brighter but cooler at TAMS than when it is at ZAMS. On the contrary, for the stars with $M < 1M_{\odot}$, the temperature rises initially, to drop a little later while L is continuously increasing from ZAMS to TAMS. Reversals of the theoretical ZAMS and TAMS lines of Bertelli et al. (2008, 2009) on Fig. 10 at about $M = 1.05M_{\odot}$ are just indicating this fact. Notice that, for the stars with $M > 1.05M_{\odot}$, the TAMS line indicates lower, but for the stars with $M < 1.05M_{\odot}$ the TAMS line indicates higher temperature than the temperature at the ZAMS.

Vertical spread of T_{eff} in Fig. 11c is about one order of magnitude between coolest to hottest stars, while the vertical spread of radii is about two orders of magnitude in Fig. 11a. Consequently, the Stefan Boltzmann law requires L to spread about 8 orders magnitudes between the limiting values of L on Fig. 11b because L is proportional to the fourth power of the temperature and square of the radius. With such a large spread in vertical, the distribution of L values is more suitable than R and T_{eff} distributions to be expressed by a single thin function, which is called MLR. Squeezing the three different scales on the figure into a similar paper scale, makes the thickness of L smallest of all. The organization of stars in a sufficiently narrow band across the diagonal on the $M - L$ diagram clearly demonstrates the well-recognized universal MLR, and secret of the stellar realm discovered in the beginning of the 20th century. This study indicates that the universal MLR for stars in the solar neighborhood is not a continuous curve but rather a continuous sequence of four lines.

Absolute values of the differences between the calculated and published temperatures of Fig. 8 were divided by the published temperatures and analyzed as absolute relative differences, as shown in Fig. 12a. Most of the calculated temperatures agree with the

published temperatures to within 10%. Few cases show differences greater than 20%. The calculated and published temperature errors of Fig. 8 are displayed as percentages in Fig. 12b and Fig. 12c, respectively. The relative errors of calculated temperatures appear as a nearly horizontal distribution because uncertainty contributions of M and R are negligible, and the four levels of dispersions shown are those based on the four MLRs given in Table 3. Distributions of M and R errors in Eker et al. (2014) indicates the peak of the distribution is at 1% and 2% respectively, and for a smaller number of stars increases rapidly up to 5% in both distributions. Therefore, allowing more stars with radius errors of up to 6%, does not significantly change the distribution of errors for calculated temperatures since the error contribution of the dispersions on the $M - L$ diagram dominates.

5. Conclusions

A calibration sample has been formed to study $M - L$, $M - R$ and $M - T_{eff}$ diagrams of nearby main-sequence stars. The stars were selected from Table 2 of Eker et al. (2014) with three basic conditions: 1) Stars must be on the main-sequence, 2) masses and radii relative errors must be less than or equal to 3%, and 3) luminosity errors must be less than or equal to 30%. Being components of detached double-lined eclipsing binaries, the sample stars have not yet experienced any mass transfer. All can be taken as evolved as single stars.

The efficiency of stellar furnaces, that is $\log(L/M)$, is found to increase linearly from 0.38 to $1.05M_\odot$. The quantity $\log(L/M)$ continues increasing, but with a smaller slope from $1.05M_\odot$ to $2.4M_\odot$. We have found three break points, dividing the present sample into four subsamples, which we identified as stellar mass domains: low mass ($0.38 < M/M_\odot \leq 1.05$), intermediate mass ($1.05 < M/M_\odot \leq 2.4$), high mass ($2.4 < M/M_\odot \leq 7$), and very high mass ($M/M_\odot > 7$).

Those stellar mass domains were used to revise the classical MLR ($L \propto M^\alpha$). Lines with different α were fit to the masses and luminosities in each domain and best fitting lines were determined by the least squares method. The quality of all fits is very similar, but the four-piece linear function stands out with a physical background. The $M - R$ and $M - T_{eff}$ diagrams of the present sample have also been studied. Stellar evolution within the main-sequence band is clearly apparent in the $M - R$ diagram. Corresponding evolution could not be seen however, on the $M - T_{eff}$ diagram based on published temperatures.

A well known method of calculating stellar effective temperatures for main-sequence stars has been discussed and analyzed. The calculated temperatures should have accuracies of $\pm 8\%$ if M and R errors are less than or equal to 6% . The method is still applicable to less accurate stars. With less accurate stars, one must propagate observational errors of the mass to the predicted luminosity. The method produces correspondingly less accurate temperatures with increasingly less accurate mass and radius as inputs.

The method has been applied to a calibration sample and a wider sample containing 12 stars without published temperatures. The main-sequence evolution, which was clear on the $M - R$ diagram, but not seen on the $M - T_{eff}$ diagram with published temperatures, becomes clearly visible with the empirical effective temperatures calculated. Stellar temperatures based on this method are real effective temperatures, obtained directly from absolute stellar properties (M, R). In comparison, published temperatures are based on apparent properties, including colors or spectral lines, or through Pogson's formula using parallax and apparent magnitude. Alternative temperature estimates therefore, as previously published, require bolometric corrections. We believe that stellar temperatures calculated by the method based on the detached double-lined eclipsing binaries in the present study have relatively larger errors than published ones, but have potential in calibrating bolometric corrections needed to estimate the stellar temperatures of main

sequence stars in general, including in single, multiple, and other kinds of binary systems.

6. Acknowledgments

Authors are grateful to the anonymous referee whose comments were very useful in improving the manuscript. This work has been supported in part by the Scientific and Technological Research Council (TÜBİTAK) grant numbers 106T688 and 111T224. This research has made use of the SIMBAD database, operated at CDS, Strasbourg, France and NASA's Astrophysics Data System Bibliographic Services.

REFERENCES

- Ak, T., Bilir, S., Ak, S., Coşkunoğlu, K.B., & Eker, Z. 2010, NewA, 15, 491
- Ak, T., Bilir, S., Güver, T., Çakmak, H., & Ak, S. 2013, NewA, 22, 7
- Andersen, J. 1991, A&ARv, 3, 91
- Bass G., Orosz J. A., Welsh W. F., Windmiller G., Ames Gregg T., Fetherolf T., Wade R. A., & Quinn S. N., 2012, ApJ, 761, 157
- Bell, E. F., & de Jong R. S. 2001, ApJ, 550, 212
- Bertelli, G., Girardi, L., Marigo, P., & Nasi, E. 2008, A&A, 484, 815
- Bertelli, G., Nasi, E., Girardi, L., & Marigo, P. 2009, A&A, 508, 355
- Blumenthal, G. R., Faber, S. M., Primack, J. R., & Rees, M. J. 1984, Nature, 311, 517
- Bilir, S., Karataş, Y., Demircan, O., & Eker, Z. 2005, MNRAS, 357, 497
- Bilir, S., Karaali, S., & Gilmore, G. 2006, MNRAS, 366, 1295
- Bilir, S., Cabrera-Lavers, A., Karaali, S., Ak, S., Yaz, E., & López-Corredoira M. 2008, PASA, 25, 69
- Catanzaro, G., & Ripepi, V. 2014, MNRAS, 441, 1669
- Cester, B., Ferluga, S., & Boehm, C. 1983, Ap&SS, 96, 125
- Clausen, J. V., Olsen, E. H., Helt, B. E., & Claret, A., 2010, A&A, 510A, 91
- Clayton D. D., 1968, Principles of stellar evolution and nucleosynthesis, New York: McGraw-Hill

- Cox, A. N. 2000, Allen's astrophysical quantities, New York: AIP Press; Springer, Edited by Arthur N. Cox. ISBN: 0387987460
- Çakırlı Ö., İbanoğlu C., & Dervişoğlu A., 2010, RMxAA, 46, 363
- Demircan, O., & Kahraman, G. 1991, Ap&SS, 181, 313
- Eddington, A. S. 1926, The Internal Constitution of the Stars, Cambridge: Cambridge University Press, ISBN 9780521337083
- Eggen, O. J. 1956, AJ, 61, 361
- Eker, Z., Bilir, S., Soydugan, F., Yaz Gökçe, E., Soydugan, E., Tüysüz, M., Şenyüz, T., & Demircan, O. 2014, PASA, 31, e024
- Elkhateeb, M. M., Nouh, M. I., & Saad, S. M. 2014, NewA, 26, 102
- Faber, S. M., & Gallagher, J. S. 1979, ARA&A, 17, 135
- Fang, X., & Yan-ning, F. 2010, Chinese Astronomy and Astrophysics, 34, 277
- Fumel, A., & Böhm, T. 2012, A&A, 540, 108
- Gafeira, R., Patacas, C., & Fernandes, J. 2012, Ap&SS, 341, 405
- Gimenez, A., & Zamorano, J. 1985, Ap&SS, 114, 259
- Girardi, M., Manzato, P., Mezzetti, M., Giuricin, G., & Limboz, F. 2002, ApJ, 569, 720
- Gorda, S. Y., & Svechnikov, M. A. 1998, ARep, 42, 793
- Haberreiter, M., Schmutz, W., & Kosovichev, A. G. 2008, ApJ, 675L, 53
- Harmanec, P. 1988, BAICz, 39, 329

Helminiak, K. G., Konacki, M., Ratajczak, M., & Muterspaugh, M. W. 2009, MNRAS, 400, 969

Hełminiak K. G., & et al. 2011, A&A, 527, AA14

Hertzsprung, E. 1923, Bulletin of the Astronomical Institutes of the Netherlands, 2, 15

Henry, T. J., & McCarthy, D. W. 1993, AJ, 106, 773

Henry, T. J. 2004, In Spectroscopically and Spatially Resolving the Components of the Close Binary Stars, Proceedings of the Workshop held 20-24 October 2003 in Dubrovnik, Croatia. Edited by R. W. Hilditch, H. Hensberge and K. Pavlovski. ASP Conference Series, Vol. 318. San Francisco: Astronomical Society of the Pacific, 2004, p.159-165

Huang, S. S., & Struve O. 1956, AJ, 61, 300

Hunter, T. R., Brogan, C. L., Indebetouw, R., & Cyganowski, C. J. 2008, ApJ, 680, 1271

Ibanoğlu, C., Soydugan, F., Soydugan, E., & Dervişoğlu, A. 2006, MNRAS, 373, 435

Jiang, De., Han, Z., Jiang, T., & Li, L. 2009, MNRAS, 396, 2176

Karaali, S., Ak, S. G., Bilir, S., Karataş, Y., Gilmore, G. 2003, MNRAS, 343, 1013

Karataş, Y., Bilir, S., Eker, Z., & Demircan, O. 2004, MNRAS, 349, 1069

Kraus, S., Weigelt, G., Balega, Y. Y., & et al. 2009, A&A, 497, 195

Kraus, A. L., Tucker, R. A., Thompson, M. I., Craine, E. R., & Hillenbrand, L. A. 2011, ApJ, 728, 48

Kopal, Z. 1978, Dynamics of close binary systems, Dordrecht, D. Reidel Publishing Co. (Astrophysics and Space Science Library. Volume 68)

Kuiper, G. P. 1938, ApJ, 88, 472

- Lacy, C. H. 1977, ApJS, 34, 479
- Lacy, C. H. 1979, ApJ, 228, 817
- Li, L., Han, Z., & Zhang, F. 2005, PASJ, 57, 187
- Li, K., & Qian, S.-B. 2013, NewA, 21, 46
- Malkov, O. Y. 2003, A&A, 402, 1055
- Malkov, O. Y. 2007, MNRAS, 382, 1073
- McCrea, W. H. 1950, Physics of the sun and stars, London, New York, Hutchinson's University Library
- McLaughlin, D. B. 1927, AJ, 38, 21
- Morales J. C., Gallardo J., Ribas I., Jordi C., Baraffe I., & Chabrier G. 2010, ApJ, 718, 502
- Patterson, J. 1984, ApJS, 54, 443
- Petrie, R. M. 1950a, Publications of the Dominion Astrophysical Observatory, 8, 341
- Petrie, R. M. 1950b, AJ, 55, 180
- Popper, D. M. 1967, ARA&A, 5, 85
- Popper, D. M. 1980, ARA&A, 18, 115
- Plaut, L. 1953, Publications of the Kapteyn Astronomical Laboratory Groningen, 55, 1
- Pribulla, T., Chochol, D., Heckert, P. A., Errico, L., Vittone, A. A., Parimucha, Š., & Teodorani, M. 2001, A&A, 371, 997
- Ren, A. B., Zhang, X. B., Luo, C. Q., Luo, Y. P., Deng, L. C., & Luo, Z. Q. 2011, NewA, 16, 194

- Ribas, I., Jordi, C., & Torra, J. 1999, MNRAS, 309, 199
- Ripepi, V., Cusano, F., di Criscienzo, M., & et al. 2011, MNRAS, 416, 1535
- Rozyczka, M., Pietrukowicz, P., Kaluzny, J., Pych, W., Angeloni, R., & Dékány, I. 2013, MNRAS, 429, 1840
- Russell, H. N., Adams, W. S., & Joy, A. H. 1923, PASP, 35, 189
- Southworth, J. 2014, arXiv1411.1219S
- Standish, E. M. 1995, Highlights of Astronomy, 10, 180
- Stassun K. G. 2013, EAS Publications Series, 64, 363
- Strand, K. Aa., & Hall, R. G. 1954, ApJ, 120, 322
- Torres, G., Andersen, J., & Giménez, A. 2010, A&ARv, 18, 67
- Tully, R. B., & Fisher, J. R. 1977, A&A, 54, 661
- Worley, C. E., & Heintz, W. D. 1983, Publications of the United States Naval Observatory; 2nd ser., 24, Washington: U.S. G.P.O.
- Zasche, P., & Wolf, M., 2011, A&A, 527, 43
- Zasche, P. 2011, NewA, 16, 157
- Zhang, X. B., & Zhang, R. X. 2007, MNRAS, 382, 1133

Table 1: Comparison of data samples for earlier MLRs and MRRs.

Sample		Accuracy	Mass-Luminosity	Mass-Radius	Ranges
This Study	268 stars (all components of detached double-lined eclipsing), homogenized	$M\&R \leq 3\%$ $L \leq 30\%$	Four broken lines, linear and quadratic	—	$0.2 < M/M_{\odot} < 32$ $0.23 < R/R_{\odot} < 9.36$
Torres et al. (2010)	190 stars (94 eclipsing+ α Cen) homogenized	$M\&R \leq 3\%$	$\log M$ - $\log L$ diagram displayed	$\log M$ - $\log R$ diagram displayed	$0.21 < M/M_{\odot} < 27.27$ $0.24 < R/R_{\odot} < 9.35$
Malkov (2007)	215 stars (114 detached eclipsing), as published	$M\&R \leq 10\%$	Quadratic $\sigma = 0.12$	Cubic $\sigma = 0.08$	$0.63 < M/M_{\odot} < 31.6$ $0.63 < R/R_{\odot} < 25.1$
Henry (2004)	188 stars (139 detached main-sequence, 49 visual pairs), as published	$M\&R \leq 15\%$	Mass- M_V , plot		$0.07 < M/M_{\odot} < 33$
Andersen (1991)	90 stars (45 detached eclipsing binaries), as published	$M\&R \leq 2\%$	$\log M$ - $\log L$ diagram displayed		$0.58 < M/M_{\odot} < 22.90$ $0.61 < R/R_{\odot} < 9.35$
Demircan & Kahraman (1991)	140 stars (70 eclipsing binaries including contact, semi-contact and detached)	—	Mass- M_{bol} Linear, quadratic, cubic	Linear, quadratic, cubic	$0.63 < M/M_{\odot} < 18.1$ $0.15 < R/R_{\odot} < 9$

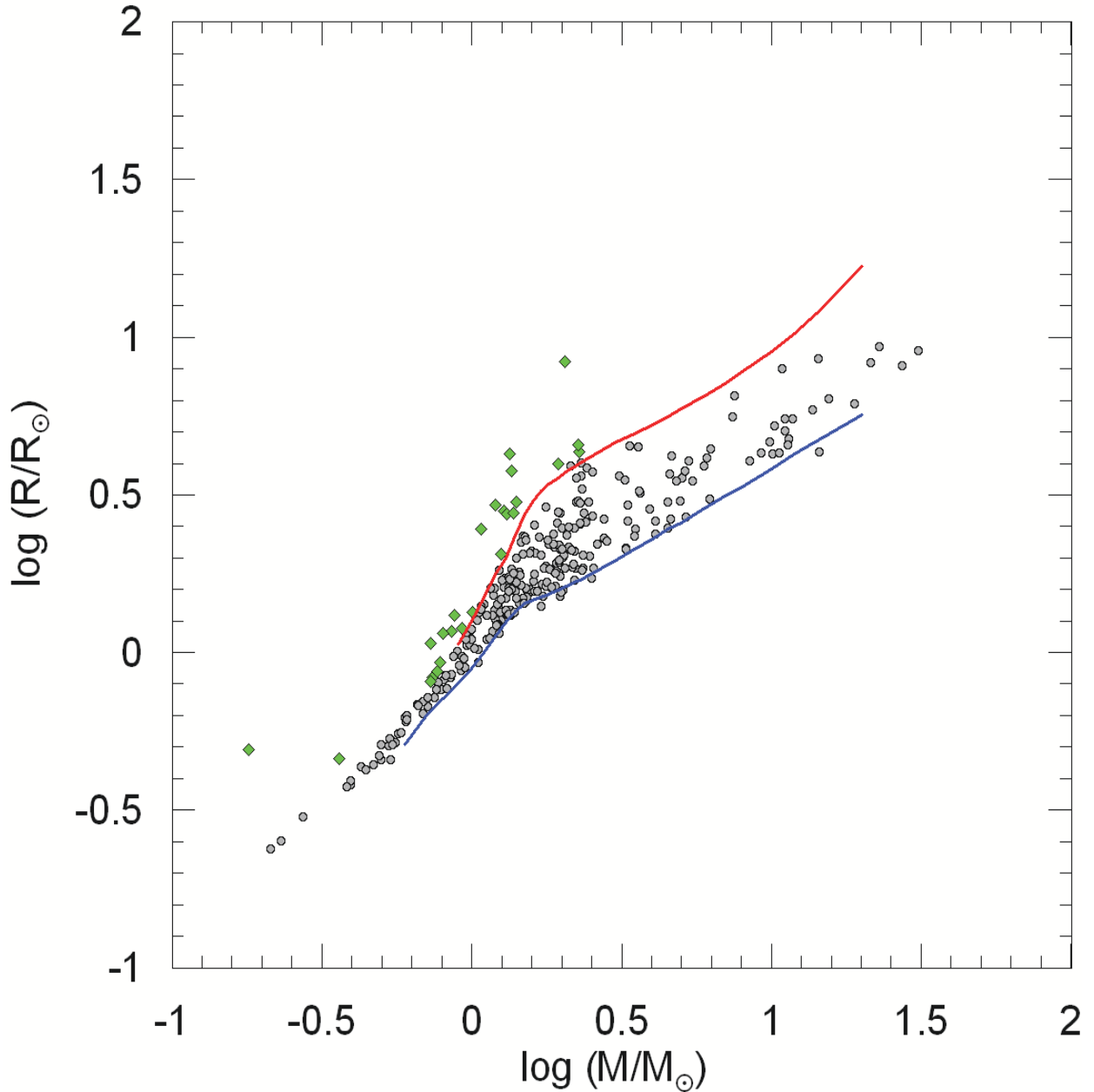


Fig. 1.— The masses and radii of main-sequence stars (filled circles) in the calibration sample is secured according to their positions in between ZAMS and TAMS lines for zero metallicity from Bertelli et al. (2008, 2009). The stars above TAMS line (diamonds) were designated to be probable non-main-sequence stars.

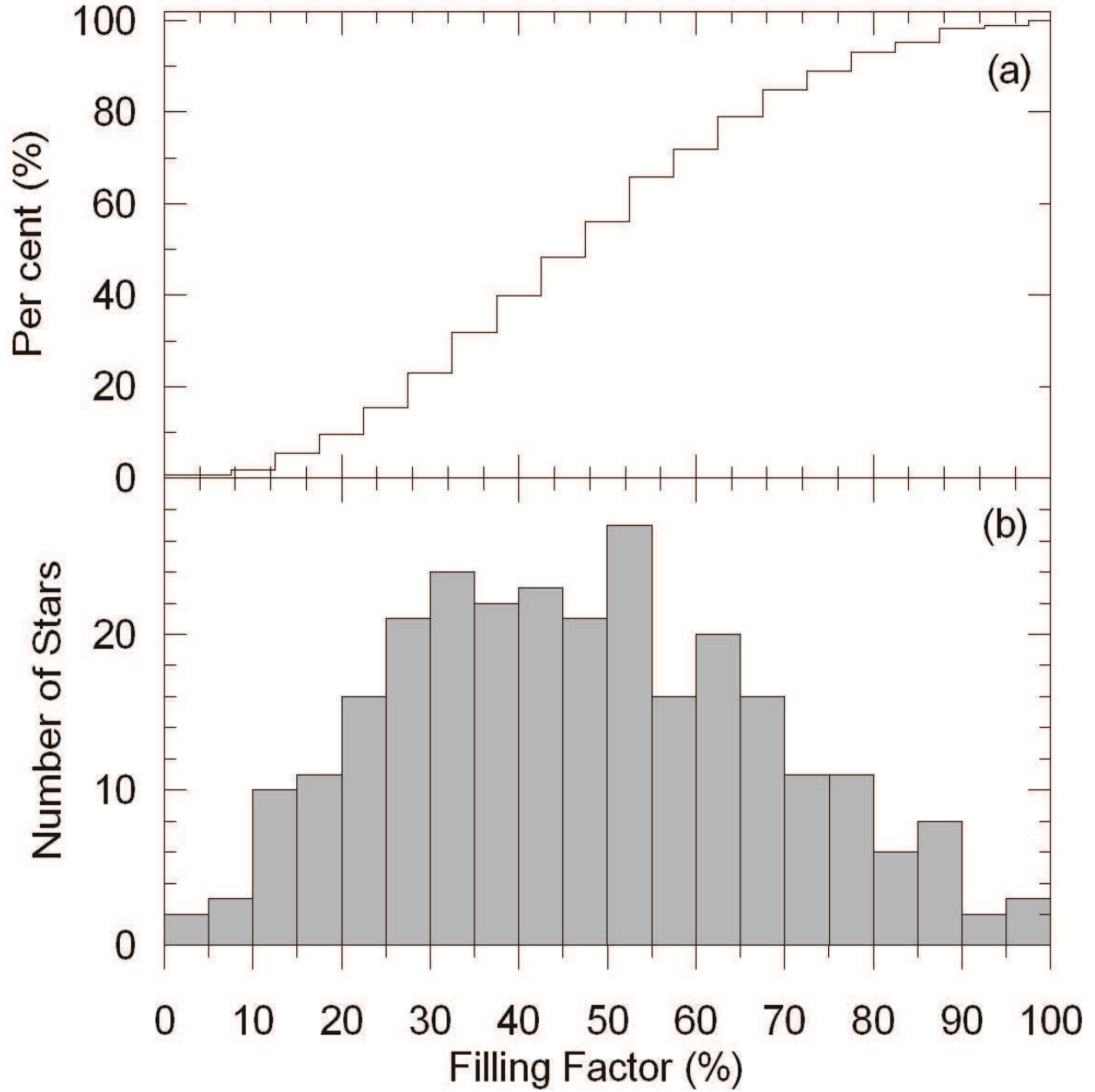


Fig. 2.— Cumulative (a) and histogram (b) distribution of the filling factors for the stars in the calibration sample. Stars are spherical within 1% of radius up to a filling factor of 75% (Eker et al. 2014).

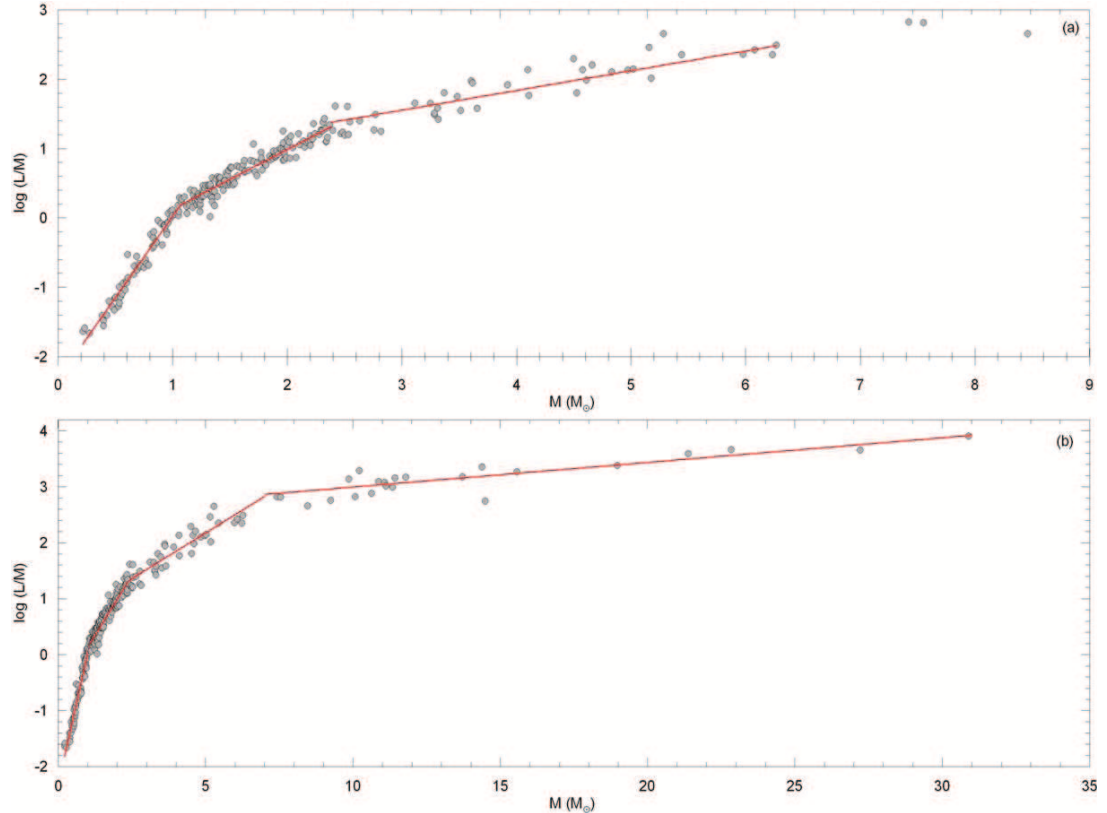


Fig. 3.— Energy production rate per stellar mass (L/M). Separate linear distributions in $\log(L/M)$ versus M are clear. Break points are at 1) $M = 1.05M_\odot$, 2) $M = 2.4M_\odot$, and 3) $M = 7M_\odot$.

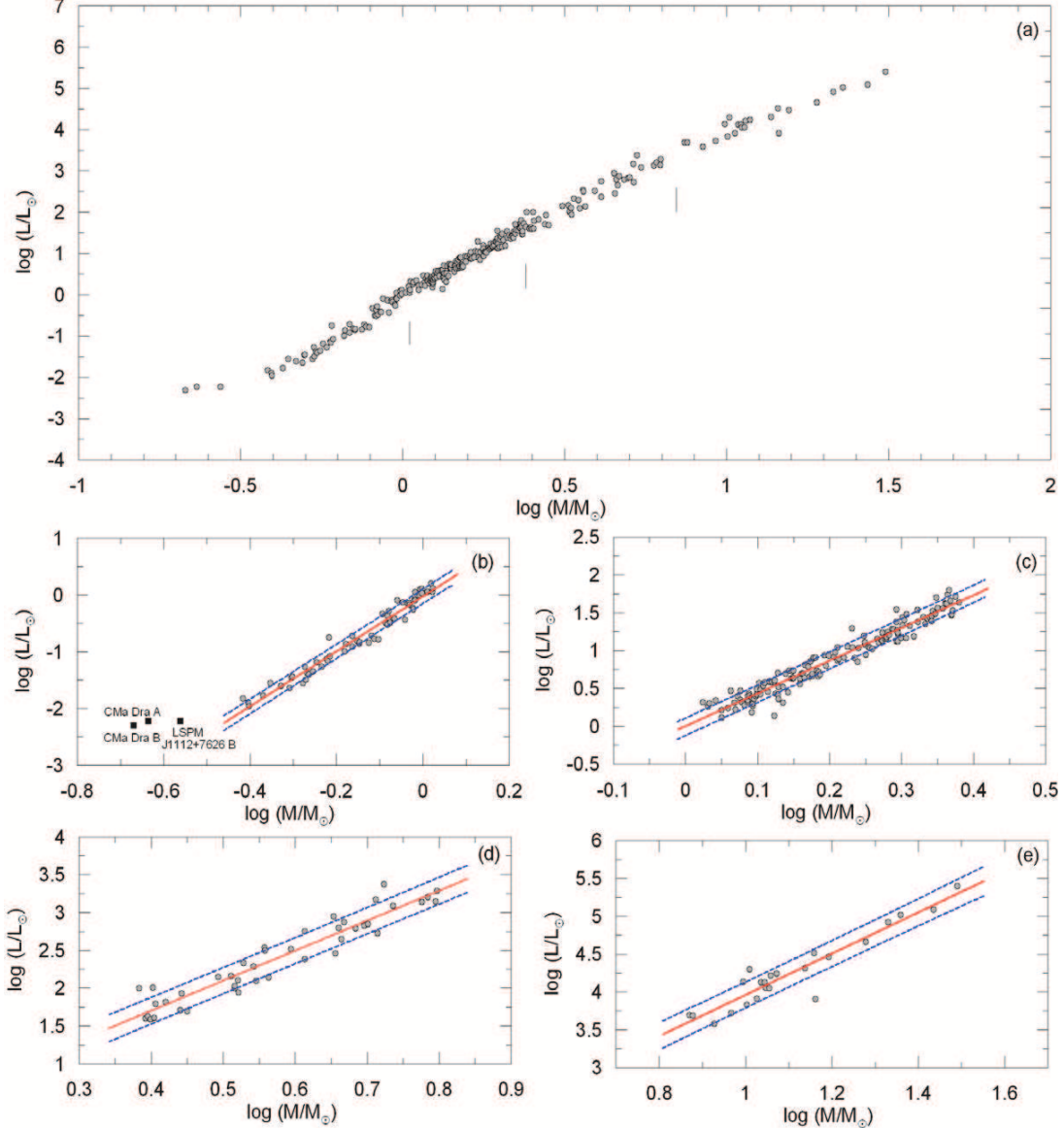


Fig. 4.— The $M - L$ diagram of the calibration sample (a). The three vertical dashes corresponding to the break points in Fig. 3 mark low mass ($0.2 < M/M_\odot \leq 1$), intermediate mass ($1.05 < M/M_\odot \leq 2.4$), high mass ($2.4 < M/M_\odot \leq 7$) and very high mass ($7 < M/M_\odot < 32$) domains. The lower four panels (b, c, d, e): show best fitting lines and 1σ limits in those domains. Note: lower three points indicated for low mass domain were excluded from the analysis.

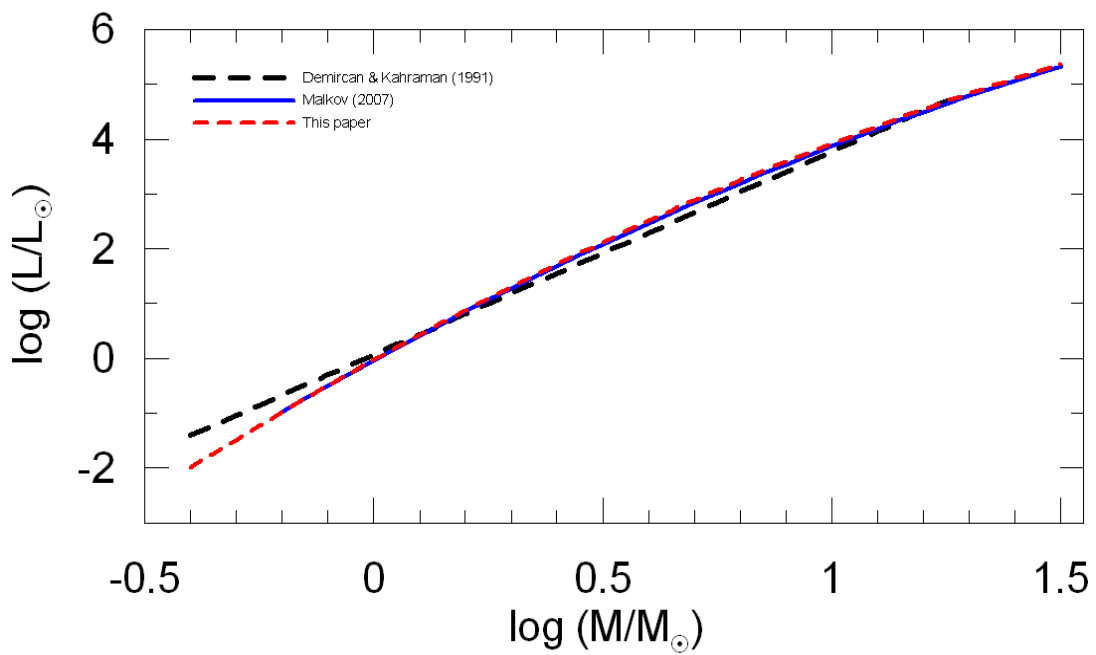


Fig. 5.— A best fitting quadratic curve as the MLR for the whole sample compared to the quadratic MLRs of Malkov (2007) and Demircan & Kahraman (1991).

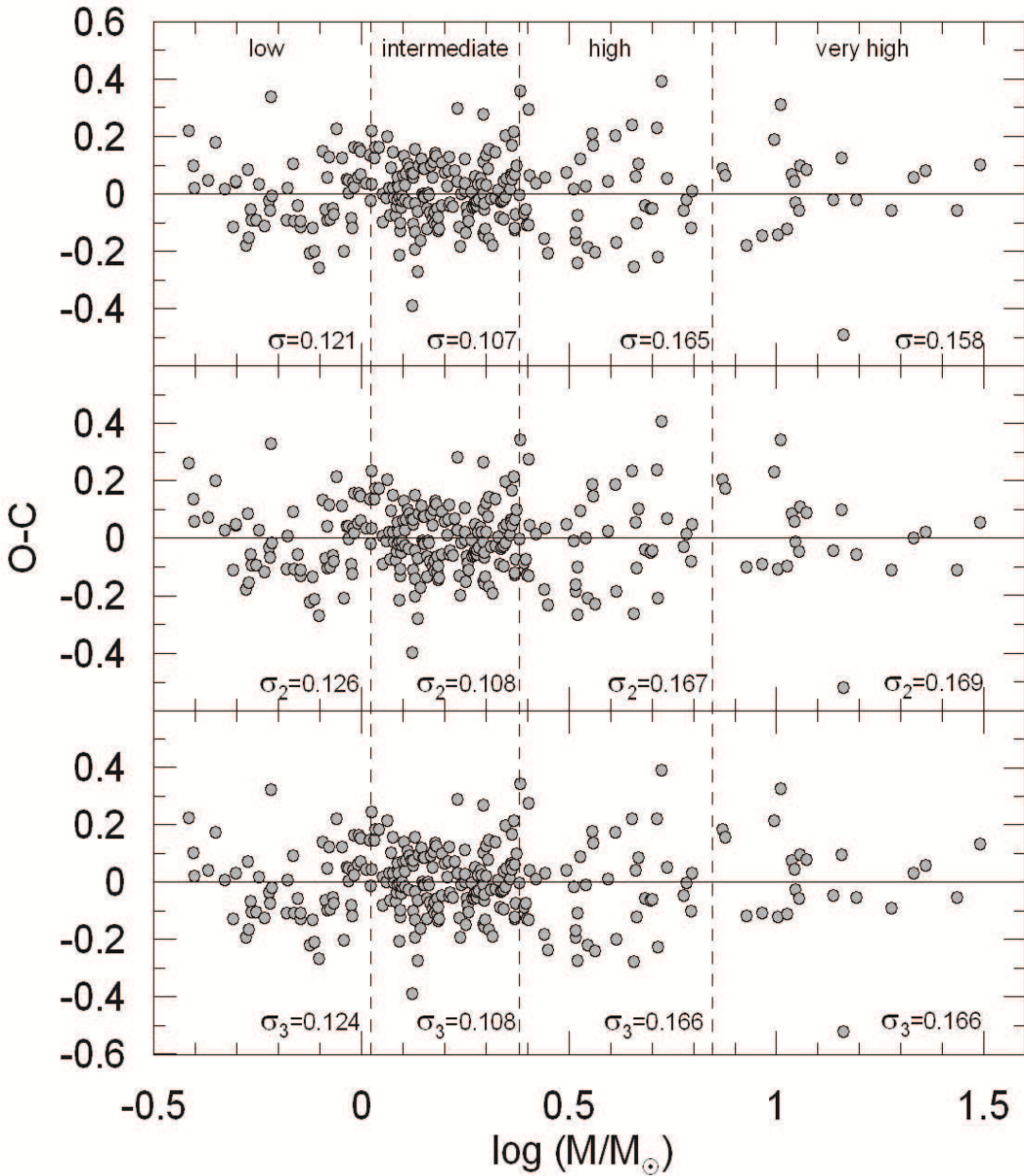


Fig. 6.— The $O-C$ dispersions of the four piece linear MRLs (upper) compared to quadratic (middle) and cubic (lower) MRLs. Low, intermediate, high and very high mass intervals separated by vertical dashed lines. Standard deviations of each segment (σ) indicates that the four piece linear MRLs (upper) are best to represent $M - L$ diagram in Fig. 4.

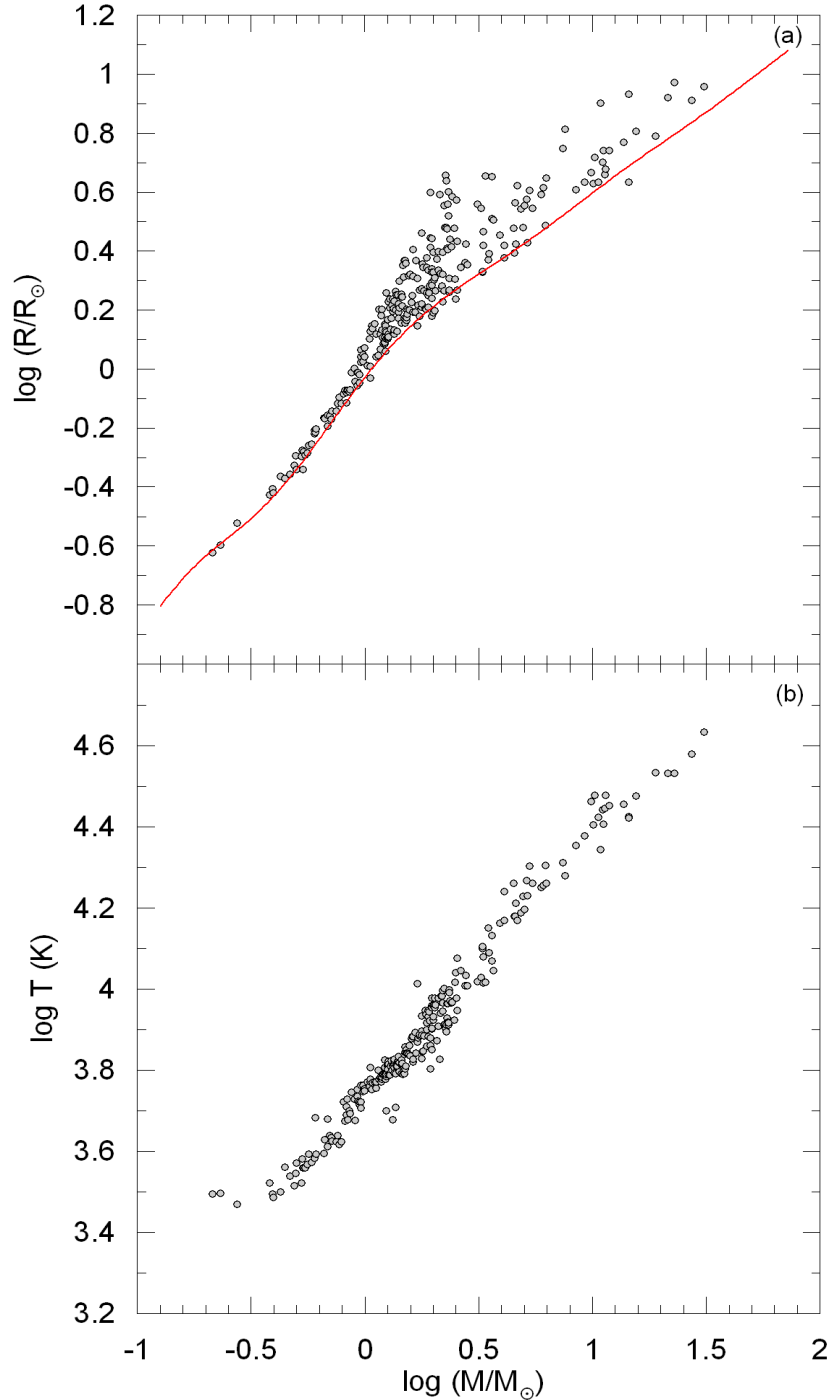


Fig. 7.— Observational a) radii and b) effective temperatures versus mass. The continuous line on the mass-radius plot is theoretical ZAMS of Bertelli et al. (2008, 2009).

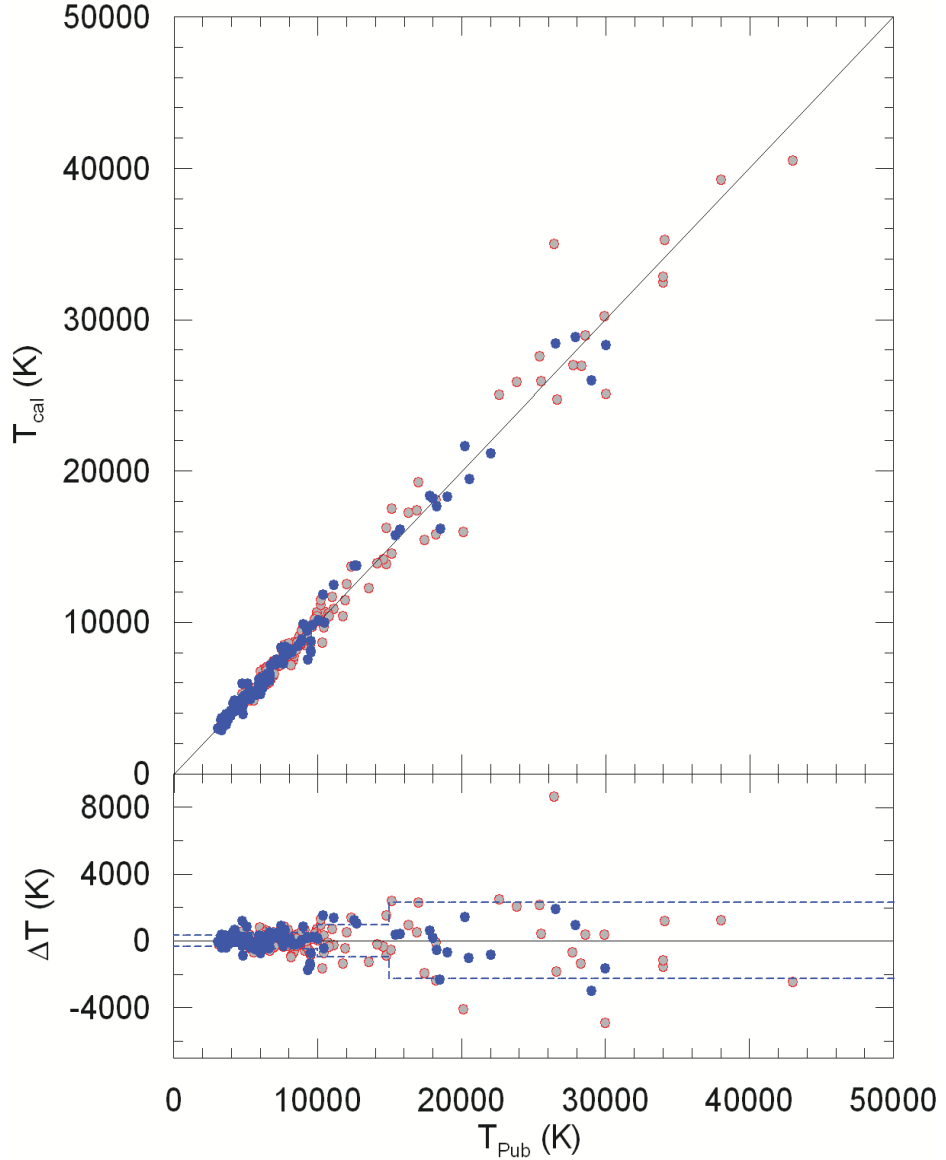


Fig. 8.— Comparing the calculated (empirical) T_{eff} and published T_{eff} temperatures (above) and ($\Delta T = T_{cal} - T_{pub}$) the difference between them (below). Dashed: the mean standard differences ($\sqrt{\langle (T_{cal} - T_{pub})^2 \rangle}$), the filled and empty circles: temperatures published within the last seven years and those published earlier, respectively.

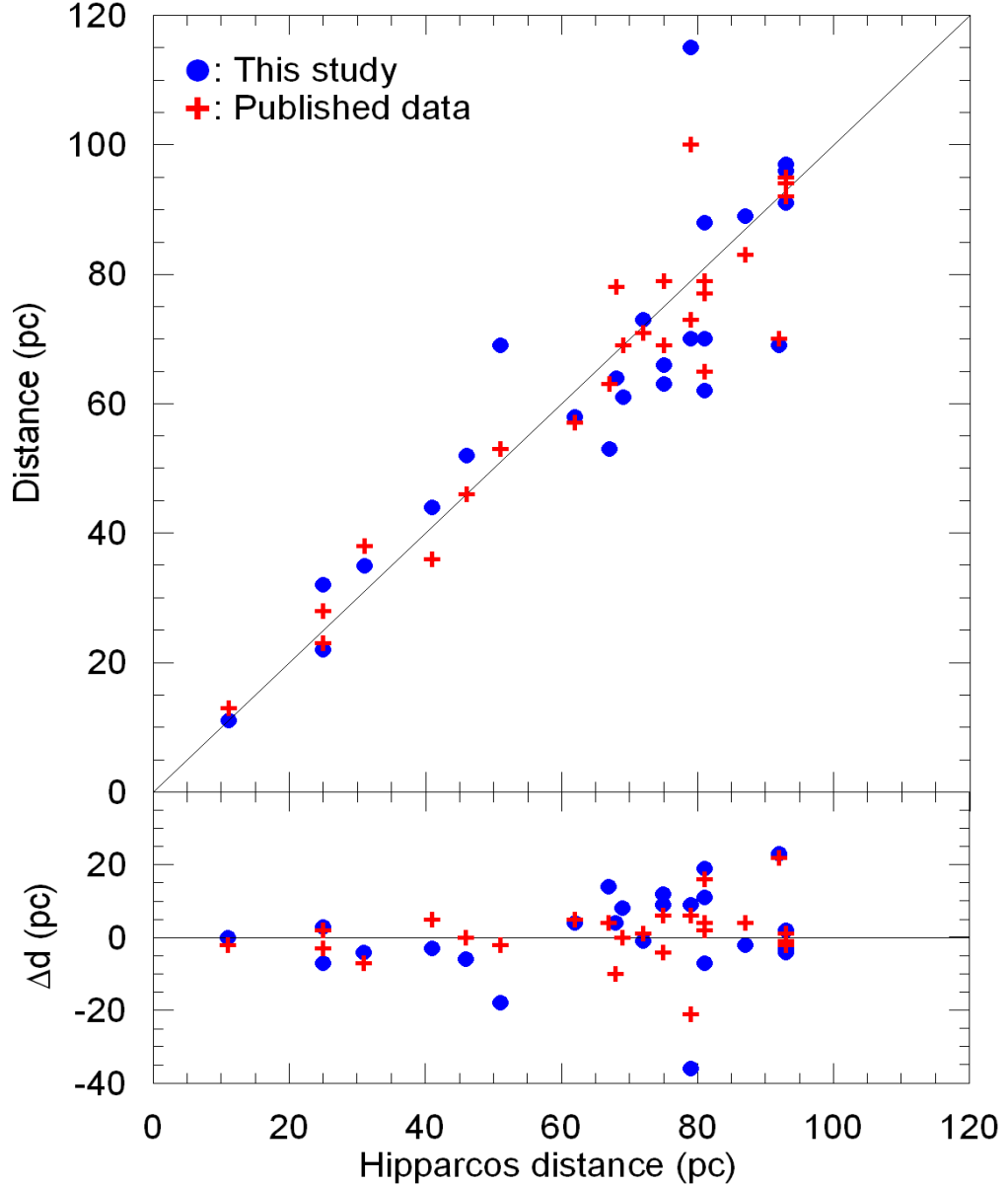


Fig. 9.— Photometric distances of some selected stars ($\sigma_{\pi}/\pi < 0.15$) in the calibration sample were compared to *Hipparcos* distances. Photometric distances were estimated as explained in the text using calculated temperatures (circles) and published temperatures (plus). Photometric and *Hipparcos* distances (above) and ($\Delta d = d_{Hip} - d_{Pho}$) the difference from the *Hipparcos* distances (below).

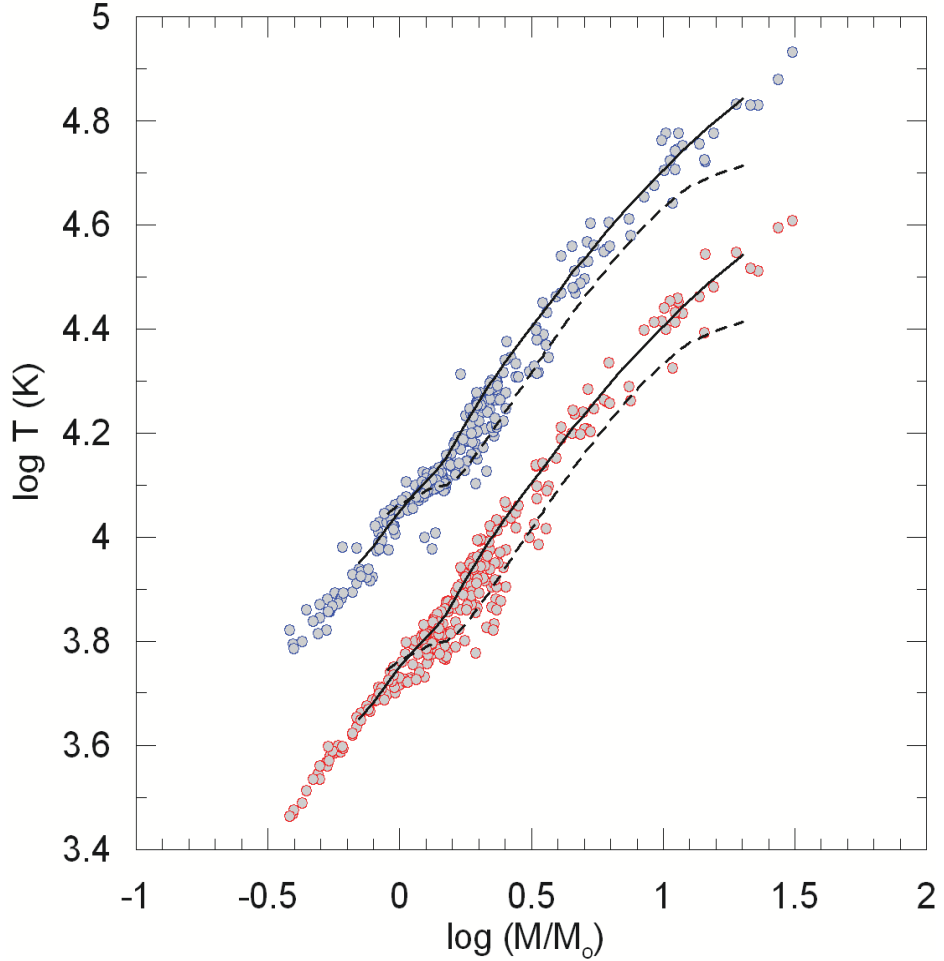


Fig. 10.— $M - T_{eff}$ diagrams. The upper shows published temperatures, as shown in Fig. 7b, but shifted up in vertical scale by +0.3 dex for side-by-side comparison. The lower shows calculated temperatures with empirical T_{eff} calculated according to Eq. (1). ZAMS (solid) and TAMS (dashed) lines of Bertelli et al. (2008, 2009) indicates theoretical thicknesses of $M - T_{eff}$ diagram for main-sequence stars. Larger errors of calculated temperatures makes main-sequence thicker, while a thin MRL better represents main-sequence stars with $M < 1M_\odot$, so the large degree of scattering (upper) for stars with $M < 1M_\odot$.

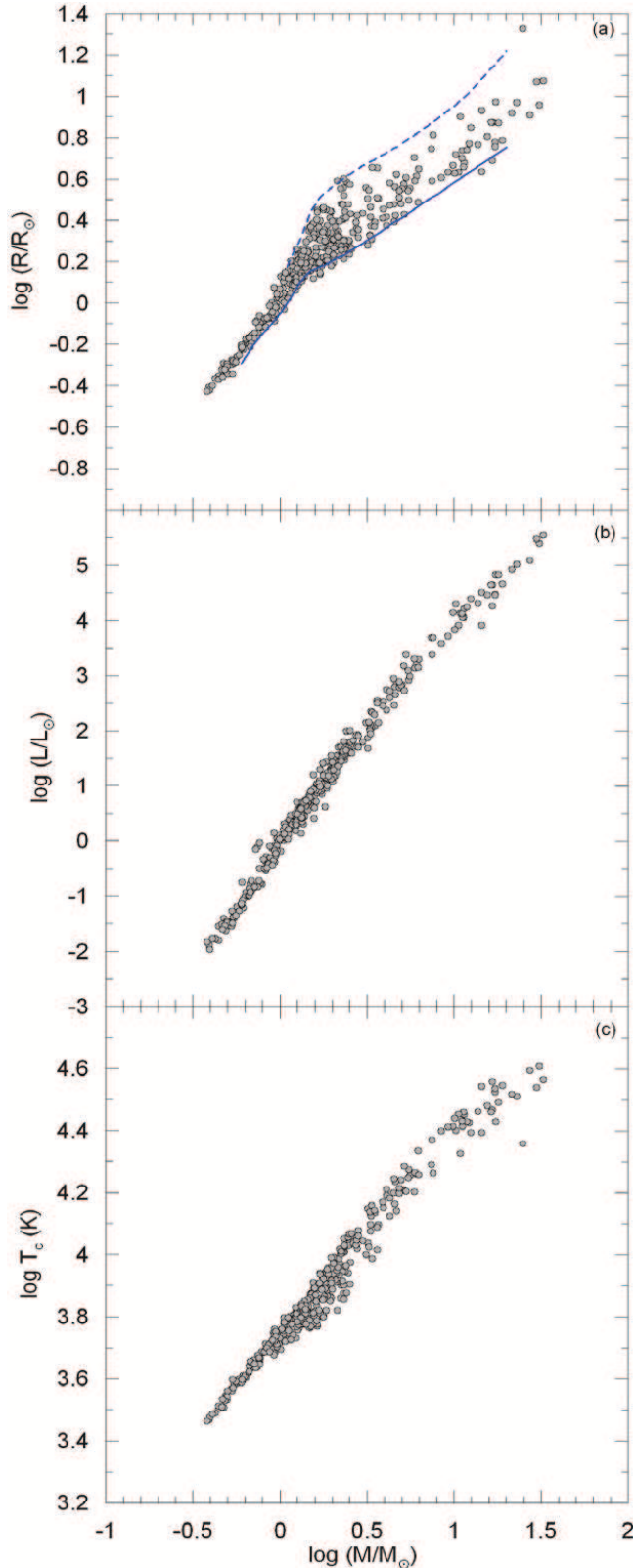


Fig. 11.— a) Larger sample ($N = 371$) of main-sequence stars on $M - R$ diagram. b) Their $M - L$ diagram (excluding 12 without published T_{eff}) and c) their $M - T_{eff}$ diagram with calculated effective temperatures. The solid lines and dashed are theoretical ZAMS and

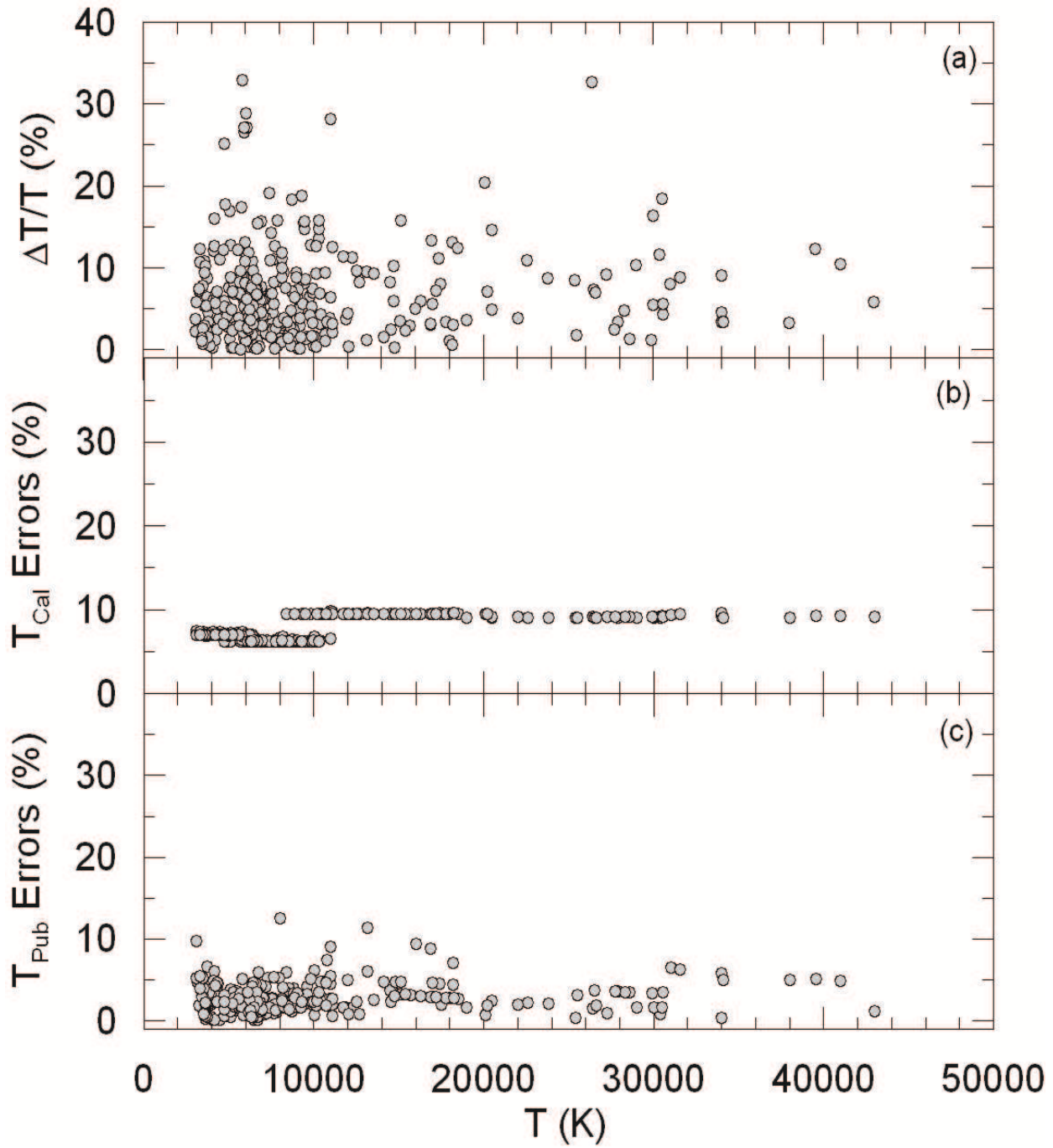


Fig. 12.— a) Comparing absolute relative differences between calculated and published temperatures of larger sample. b) Relative errors of calculated and, c) relative errors of published temperatures.

Table 2: The basic stellar parameters and relative errors for the stars selected for the calibration sample.

ID Star name	α (J2000)	δ (J2000)	Com	M/M_{\odot}	$\Delta M_{err}/M$	R/R_{\odot}	$\Delta R_{err}/R$	T_{eff}	$(T_{eff})_{err}$	$\log L/L_{\odot}$	$\Delta L_{err}/L$	FF(%)	Remark
1 MU Cas	00:15:51.56	+60:25:53.64	Pri	4.657	0.021	4.192	0.012	14750	500	2.873	0.056	37	✓
2 MU Cas	00:15:51.56	+60:25:53.64	Sec	4.575	0.020	3.671	0.011	15100	500	2.799	0.055	33	✓
3 V69-47 Tuc	00:22:52.95	-72:03:40.68	Pri	0.876	0.006	1.316	0.004	5945	150	0.288	0.042	11	X
4 V69-47 Tuc	00:22:52.95	-72:03:40.68	Sec	0.859	0.007	1.163	0.005	5959	150	0.185	0.042	9	X
5 YZ Cas	00:45:39.08	+74:59:17.06	Pri	2.308	0.004	2.547	0.012	9200	300	1.620	0.054	41	✓
6 YZ Cas	00:45:39.08	+74:59:17.06	Sec	1.347	0.007	1.359	0.015	6700	250	0.524	0.061	35	✓
7 NGC188 KR V12	00:52:37.54	+85:10:34.65	Pri	1.102	0.006	1.425	0.013	5900	100	0.344	0.031	27	✓
8 NGC188 KR V12	00:52:37.54	+85:10:34.65	Sec	1.080	0.006	1.374	0.014	5875	100	0.305	0.031	27	✓
9 zet Phe	01:08:23.08	-55:14:44.74	Pri	3.922	0.011	2.853	0.007	14550	350	2.515	0.040	69	✓
10 zet Phe	01:08:23.08	-55:14:44.74	Sec	2.545	0.010	1.854	0.011	11910	200	1.793	0.030	63	✓
11 AI Phe	01:09:34.19	-46:15:56.09	Pri	1.197	0.004	2.935	0.016	6310	150	1.089	0.042	22	X
12 AI Phe	01:09:34.19	-46:15:56.09	Sec	1.238	0.003	1.819	0.013	5010	120	0.272	0.041	15	✓
13 CO And	01:11:24.83	+46:57:49.34	Pri	1.289	0.005	1.727	0.012	6140	130	0.580	0.037	43	✓
14 CO And	01:11:24.83	+46:57:49.34	Sec	1.264	0.006	1.694	0.010	6170	130	0.572	0.036	43	✓
15 V459 Cas	01:11:29.92	+61:08:47.96	Pri	2.015	0.015	2.010	0.006	9140	300	1.403	0.054	26	✓
16 V459 Cas	01:11:29.92	+61:08:47.96	Sec	1.962	0.015	1.966	0.007	9100	300	1.377	0.054	26	✓
17 UV Psc	01:16:55.12	+06:48:42.12	Pri	0.983	0.009	1.117	0.018	5780	100	0.097	0.033	69	✓
18 V505 Per	02:21:12.96	+54:30:36.28	Pri	1.272	0.001	1.288	0.011	6512	21	0.428	0.011	31	✓
19 V505 Per	02:21:12.96	+54:30:36.28	Sec	1.254	0.001	1.267	0.011	6462	12	0.400	0.010	31	✓
20 XY Cet	02:59:33.53	+03:31:03.27	Pri	1.773	0.009	1.876	0.019	7870	115	1.084	0.029	49	✓
21 XY Cet	02:59:33.53	+03:31:03.27	Sec	1.615	0.009	1.776	0.016	7620	125	0.980	0.031	50	✓
22 CW Eri	03:03:59.95	-17:44:16.06	Pri	1.583	0.013	2.093	0.024	6840	86	0.935	0.029	55	✓
23 TZ For	03:14:40.09	-35:33:27.60	Pri	1.945	0.015	3.974	0.023	6350	100	1.363	0.033	22	X
24 TZ For	03:14:40.09	-35:33:27.60	Sec	2.045	0.029	8.349	0.014	5000	100	1.592	0.035	26	X
25 2MASSJ03262072+0312362	03:26:20.73	+03:12:36.29	Pri	0.527	0.004	0.505	0.016	3330	60	-1.553	0.030	31	✓
26 2MASSJ03262072+0312362	03:26:20.73	+03:12:36.29	Sec	0.491	0.002	0.471	0.019	3270	60	-1.638	0.036	31	✓
27 EY Cep	03:40:04.07	+81:01:09.07	Pri	1.524	0.005	1.463	0.007	7090	150	0.686	0.036	22	✓
28 EY Cep	03:40:04.07	+81:01:09.07	Sec	1.500	0.009	1.468	0.007	6970	150	0.660	0.036	22	✓
29 V1229 Tau	03:47:29.45	+24:17:18.04	Pri	2.221	0.012	1.844	0.020	10025	620	1.489	0.097	46	✓
30 V1229 Tau	03:47:29.45	+24:17:18.04	Sec	1.565	0.010	1.587	0.026	7262	380	0.799	0.085	51	✓
31 V1130 Tau	03:50:41.94	+01:33:50.21	Pri	1.306	0.006	1.490	0.007	6650	70	0.591	0.019	82	✓
32 V1130 Tau	03:50:41.94	+01:33:50.21	Sec	1.392	0.006	1.784	0.006	6625	70	0.741	0.019	94	✓
33 IQ Per	03:59:44.68	+48:09:04.50	Pri	3.513	0.011	2.465	0.012	12300	200	2.096	0.029	60	✓
34 IQ Per	03:59:44.68	+48:09:04.50	Sec	1.733	0.012	1.509	0.013	7670	100	0.850	0.025	61	✓
35 CF Tau	04:05:10.13	+22:29:48.17	Pri	1.282	0.007	2.797	0.004	5200	150	0.711	0.048	74	X
36 CF Tau	04:05:10.13	+22:29:48.17	Sec	1.252	0.009	2.048	0.008	6000	150	0.688	0.042	59	X
37 AG Per	04:06:55.83	+33:26:46.93	Pri	4.498	0.030	3.009	0.023	18200	800	2.950	0.073	66	✓
38 AG Per	04:06:55.83	+33:26:46.93	Sec	4.098	0.027	2.616	0.027	17400	800	2.751	0.076	62	✓
39 WW Cam	04:31:25.28	+64:21:45.50	Pri	1.920	0.007	1.913	0.008	8360	140	1.205	0.029	55	✓
40 WW Cam	04:31:25.28	+64:21:45.50	Sec	1.873	0.010	1.810	0.008	8240	140	1.132	0.029	53	✓
41 2MASSJ04480963+0317480	04:48:00.96	+03:17:48.09	Pri	0.567	0.004	0.552	0.014	3920	80	-1.187	0.038	48	✓
42 2MASSJ04480963+0317480	04:48:00.96	+03:17:48.09	Sec	0.532	0.004	0.532	0.011	3810	80	-1.268	0.038	48	✓
43 TYC 4749-560-1	04:53:04.43	-07:00:23.47	Pri	0.834	0.007	0.848	0.006	5340	200	-0.280	0.061	42	✓
44 TYC 4749-560-1	04:53:04.43	-07:00:23.47	Sec	0.828	0.007	0.833	0.006	5125	200	-0.367	0.064	42	✓
45 HP Aur	05:10:21.78	+35:47:46.63	Pri	0.959	0.011	1.052	0.011	5790	80	0.048	0.025	51	✓
46 HP Aur	05:10:21.78	+35:47:46.63	Sec	0.807	0.012	0.823	0.011	5270	90	-0.329	0.030	47	✓
47 V1236 Tau	05:16:28.81	+26:07:38.80	Pri	0.788	0.013	0.766	0.020	4200	200	-0.785	0.077	30	✓
48 V1236 Tau	05:16:28.81	+26:07:38.80	Sec	0.771	0.010	0.803	0.012	4133	250	-0.772	0.094	32	✓
49 CD Tau	05:17:31.15	+20:07:54.63	Pri	1.441	0.011	1.798	0.009	6200	50	0.632	0.016	45	✓
50 CD Tau	05:17:31.15	+20:07:54.63	Sec	1.366	0.012	1.584	0.013	6200	50	0.522	0.017	42	✓
51 EW Ori	05:20:09.15	+02:02:39.97	Pri	1.173	0.009	1.169	0.004	6070	95	0.222	0.027	21	✓
52 EW Ori	05:20:09.15	+02:02:39.97	Sec	1.123	0.008	1.098	0.005	5900	95	0.118	0.027	21	✓
53 2MASS J05282082+0338327	05:28:20.82	+03:38:32.80	Pri	1.366	0.008	1.835	0.005	5103	—	0.312	0.010	43	✓
54 2MASS J05282082+0338327	05:28:20.82	+03:38:32.80	Sec	1.327	0.006	1.735	0.006	4751	26	0.139	0.011	42	✓
55 AS Cam	05:29:46.91	+69:29:45.36	Pri	3.312	0.030	2.617	0.015	12000	600	2.106	0.080	47	✓
56 UX Men	05:30:03.18	-76:14:55.34	Pri	1.235	0.005	1.349	0.010	6200	100	0.383	0.028	33	✓
57 UX Men	05:30:03.18	-76:14:55.34	Sec	1.196	0.006	1.275	0.010	6150	100	0.320	0.029	32	✓
58 TZ Men	05:30:13.89	-84:47:06.37	Pri	2.482	0.010	2.017	0.010	10400	500	1.631	0.077	22	✓
59 TZ Men	05:30:13.89	-84:47:06.37	Sec	1.500	0.007	1.433	0.010	7200	300	0.695	0.067	24	✓
60 V1174 Ori	05:34:27.85	-05:41:37.80	Pri	1.010	0.015	1.347	0.011	4470	120	-0.187	0.046	42	X
61 V1174 Ori	05:34:27.85	-05:41:37.80	Sec	0.731	0.011	1.071	0.010	3615	100	-0.754	0.047	44	X
62 V432 Aur	05:37:32.51	+37:05:12.26	Pri	1.080	0.015	2.464	0.008	6080	85	0.872	0.024	63	X
63 V432 Aur	05:37:32.51	+37:05:12.26	Sec	1.224	0.013	1.232	0.005	6685	93	0.435	0.005	39	✓
64 GG Ori	05:43:10.22	+00:41:14.90	Pri	2.342	0.007	1.852	0.013	9950	200	1.480	0.035	27	✓
65 GG Ori	05:43:10.22	+00:41:14.90	Sec	2.337	0.007	1.830	0.014	9950	200	1.469	0.035	27	✓
66 V1031 Ori	05:47:26.89	-10:31:58.65	Pri	2.281	0.007	4.349	0.008	7850	500	1.809	0.099	78	X
67 V1031 Ori	05:47:26.89	-10:31:58.65	Sec	2.467	0.007	3.006	0.021	8400	500	1.606	0.094	62	✓
68 beta Aur	05:59:31.72	+44:56:50.76	Pri	2.369	0.011	2.762	0.006	9350	200	1.719	0.036	52	✓
69 beta Aur	05:59:31.72	+44:56:50.76	Sec	2.295	0.012	2.568	0.007	9200	200	1.628	0.037	50	✓
70 V1388 Ori	06:10:59.17	+11:59:41.49	Pri	7.421	0.011	5.604	0.007	20500	500	3.697	0.041	86	✓
71 V1388 Ori	06:10:59.17	+11:59:41.49	Sec	5.156	0.006	3.763	0.008	18500	500	3.173	0.045	76	✓
72 FT Ori	06:13:58.15	+21:25:39.18	Pri	2.168	0.010	1.871	0.007	9600	400	1.426	0.067	42	✓
73 FT Ori	06:13:58.15	+21:25:39.18	Sec	1.773	0.011	1.626	0.008	8600	300	1.113	0.057	43	✓
74 V404 CMa	06:15:55.42	-18:44:51.54	Pri	0.750	0.007	0.721	0.019	4200	100	-0.839	0.043	75	✓
75 V404 CMa	06:15:55.42	-18:44:51.54	Sec	0.659									

ID Star name	α (J2000)	δ (J2000)	Com	M/M_{\odot}	$\Delta M_{err}/M$	R/R_{\odot}	$\Delta R_{err}/R$	T_{eff}	$(T_{eff})_{err}$	$\log L/L_{\odot}$	$\Delta L_{err}/L$	FF(%)	Remark
76 RR Lyn	06:26:25.84	+56:17:06.35	Pri	1.935	0.004	2.579	0.008	7570	100	1.292	0.023	29	✓
77 RR Lyn	06:26:25.84	+56:17:06.35	Sec	1.520	0.003	1.596	0.019	6980	100	0.735	0.029	23	✓
78 V578 Mon	06:32:00.61	+04:52:40.90	Pri	10.212	0.005	5.228	0.011	30000	500	4.298	0.030	66	✓
79 V578 Mon	06:32:00.61	+04:52:40.90	Sec	14.482	0.006	4.318	0.016	26400	400	3.910	0.029	68	✓
80 WW Aur	06:32:27.18	+32:27:17.63	Pri	1.964	0.004	1.928	0.006	7960	420	1.127	0.083	51	✓
81 WW Aur	06:32:27.18	+32:27:17.63	Sec	1.814	0.004	1.842	0.006	7670	410	1.023	0.084	52	✓
82 GX Gem	06:46:09.13	+34:24:52.83	Pri	1.488	0.007	2.334	0.005	6194	100	0.857	0.027	51	✓
83 GX Gem	06:46:09.13	+34:24:52.83	Sec	1.467	0.007	2.244	0.005	6166	100	0.815	0.028	50	✓
84 HS Aur	06:51:18.47	+47:40:24.16	Pri	0.898	0.021	1.005	0.023	5350	70	-0.129	0.029	16	✓
85 HI Mon	06:55:49.07	-04:02:35.79	Pri	11.426	0.021	4.775	0.021	30000	500	4.220	0.033	82	✓
86 HI Mon	06:55:49.07	-04:02:35.79	Sec	9.864	0.016	4.645	0.014	29000	500	4.137	0.031	86	✓
87 SW CMa	07:08:15.24	-22:26:25.26	Pri	2.240	0.006	3.015	0.007	8200	150	1.567	0.031	33	✓
88 SW CMa	07:08:15.24	-22:26:25.26	Sec	2.105	0.009	2.496	0.017	8100	150	1.382	0.034	29	✓
89 HW CMa	07:08:21.86	-22:24:29.87	Pri	1.719	0.006	1.649	0.011	7560	150	0.902	0.034	13	✓
90 HW CMa	07:08:21.86	-22:24:29.87	Sec	1.779	0.007	1.668	0.013	7700	150	0.944	0.034	13	✓
91 GZ CMa	07:16:19.21	-16:43:00.10	Pri	2.201	0.011	2.490	0.012	8810	350	1.525	0.065	43	✓
92 GZ CMa	07:16:19.21	-16:43:00.10	Sec	2.001	0.012	2.130	0.019	8531	340	1.334	0.066	40	✓
93 FS Mon	07:24:42.30	-05:09:14.57	Pri	1.632	0.007	2.061	0.006	6715	100	0.890	0.026	66	✓
94 FS Mon	07:24:42.30	-05:09:14.57	Sec	1.462	0.007	1.637	0.007	6550	100	0.646	0.027	59	✓
95 YY Gem	07:34:37.41	+31:52:09.79	Pri	0.598	0.008	0.621	0.010	3820	100	-1.131	0.045	53	✓
96 YY Gem	07:34:37.41	+31:52:09.79	Sec	0.601	0.008	0.605	0.010	3820	100	-1.155	0.041	52	✓
97 2MASSJ07431157+0316220	07:43:11.57	+03:16:22.09	Pri	0.584	0.003	0.559	0.004	3730	90	-1.268	0.038	33	✓
98 2MASSJ07431157+0316220	07:43:11.57	+03:16:22.09	Sec	0.544	0.004	0.512	0.008	3610	90	-1.398	0.041	32	✓
99 PV Pup	07:45:28.73	-14:41:10.20	Pri	1.539	0.008	1.536	0.010	6920	300	0.686	0.070	58	✓
100 PV Pup	07:45:28.73	-14:41:10.20	Sec	1.527	0.009	1.493	0.011	6930	300	0.664	0.070	57	✓
101 V392 Car	07:58:10.48	-60:51:57.20	Pri	1.900	0.013	1.624	0.018	8850	200	1.162	0.041	40	✓
102 V392 Car	07:58:10.48	-60:51:57.20	Sec	1.853	0.013	1.600	0.019	8650	200	1.110	0.041	40	✓
103 AI Hya	08:18:47.46	+00:17:00.16	Pri	1.974	0.020	2.764	0.007	7100	60	1.241	0.016	34	✓
104 AI Hya	08:18:47.46	+00:17:00.16	Sec	2.140	0.019	3.912	0.008	6700	60	1.442	0.017	49	✓
105 NSVS 07394765	08:25:51.30	+24:27:05.10	Pri	0.360	0.014	0.459	0.009	3300	200	-1.658	0.089	22	X
106 NSVS 07394765	08:25:51.30	+24:27:05.10	Sec	0.180	0.022	0.491	0.010	3106	125	-1.699	0.061	40	X
107 TYC 5998-1918-1	08:25:51.60	-16:22:47.30	Pri	0.703	0.004	0.694	0.013	4350	200	-0.810	0.074	39	✓
108 TYC 5998-1918-1	08:25:51.60	-16:22:47.30	Sec	0.687	0.004	0.699	0.019	4090	200	-0.910	0.077	40	✓
109 AY Cam	08:25:51.79	+77:13:06.85	Pri	1.947	0.021	2.784	0.007	7250	100	1.284	0.024	66	✓
110 AY Cam	08:25:51.79	+77:13:06.85	Sec	1.707	0.021	2.034	0.007	7395	100	1.046	0.024	55	✓
111 VV Pyx	08:27:33.27	-20:50:38.25	Pri	2.097	0.009	2.169	0.009	9500	200	1.537	0.036	40	✓
112 HD 71636	08:29:56.31	+37:04:15.48	Pri	1.530	0.006	1.576	0.006	6950	140	0.716	0.034	30	✓
113 HD 71636	08:29:56.31	+37:04:15.48	Sec	1.299	0.005	1.365	0.006	6440	140	0.459	0.037	30	✓
114 CU Cnc	08:31:37.58	+19:23:39.47	Pri	0.427	0.005	0.433	0.012	3160	150	-1.770	0.071	20	✓
115 CU Cnc	08:31:37.58	+19:23:39.47	Sec	0.394	0.003	0.392	0.023	3125	150	-1.886	0.090	19	✓
116 VZ Hya	08:31:41.41	-06:19:07.56	Pri	1.271	0.007	1.315	0.004	6645	150	0.481	0.038	38	✓
117 VZ Hya	08:31:41.41	-06:19:07.56	Sec	1.146	0.005	1.113	0.006	6290	150	0.241	0.040	36	✓
118 TZ Pyx	08:41:08.26	-32:12:03.02	Pri	2.075	0.019	2.356	0.014	7468	203	1.190	0.046	63	✓
119 RS Cha	08:43:12.21	-79:04:12.29	Pri	1.893	0.005	2.168	0.028	7638	76	1.157	0.029	71	✓
120 RS Cha	08:43:12.21	-79:04:12.29	Sec	1.871	0.005	2.379	0.025	7228	72	1.142	0.027	76	✓
121 NSVS 02502726	08:44:11.04	+54:23:47.32	Pri	0.713	0.027	0.675	0.009	4300	200	-0.854	0.074	59	✓
122 CV Vel	09:00:37.99	-51:33:20.06	Pri	6.076	0.012	4.130	0.006	18000	500	3.206	0.046	41	✓
123 CV Vel	09:00:37.99	-51:33:20.06	Sec	5.977	0.012	3.912	0.007	17780	500	3.138	0.046	39	✓
124 PT Vel	09:10:57.72	-43:16:02.93	Pri	2.199	0.007	2.095	0.010	9247	150	1.460	0.029	62	✓
125 PT Vel	09:10:57.72	-43:16:02.93	Sec	1.626	0.006	1.560	0.013	7638	180	0.871	0.041	58	✓
126 KW Hya	09:12:26.04	-07:06:35.38	Pri	1.973	0.018	2.129	0.007	8000	200	1.222	0.042	28	✓
127 KW Hya	09:12:26.04	-07:06:35.38	Sec	1.485	0.011	1.486	0.015	6900	200	0.653	0.049	25	✓
128 2MASS J09381349-0104281	09:38:13.51	-01:04:27.90	Pri	0.761	0.028	0.766	0.017	4360	150	-0.721	0.058	56	✓
129 QX Car	09:54:33.88	-58:25:16.59	Pri	9.246	0.013	4.293	0.014	23800	500	3.725	0.037	47	✓
130 QX Car	09:54:33.88	-58:25:16.59	Sec	8.460	0.014	4.053	0.015	22600	500	3.585	0.039	48	✓
131 HS Hya	10:24:36.77	-19:05:32.96	Pri	1.255	0.006	1.278	0.005	6500	50	0.418	0.014	54	✓
132 HS Hya	10:24:36.77	-19:05:32.96	Sec	1.219	0.006	1.220	0.006	6400	50	0.351	0.014	53	✓
133 ZZ UMa	10:30:03.19	+61:48:41.42	Pri	1.179	0.011	1.518	0.015	5903	60	0.400	0.022	50	✓
134 ZZ UMa	10:30:03.19	+61:48:41.42	Sec	0.960	0.010	1.158	0.011	5097	60	-0.090	0.022	46	✓
135 2MASS J10305521+0334265	10:30:55.21	+03:34:26.57	Pri	0.499	0.004	0.457	0.011	3720	20	-1.444	0.012	28	✓
136 2MASS J10305521+0334265	10:30:55.21	+03:34:26.57	Sec	0.444	0.005	0.427	0.009	3630	20	-1.553	0.015	28	✓
137 RZ Cha	10:42:24.10	-82:02:14.19	Pri	1.506	0.023	2.282	0.009	6457	160	0.910	0.042	60	✓
138 RZ Cha	10:42:24.10	-82:02:14.19	Sec	1.514	0.026	2.282	0.009	6457	160	0.910	0.042	60	✓
139 DW Car	10:43:10.07	-60:02:11.74	Pri	11.341	0.011	4.561	0.010	27900	1000	4.054	0.059	87	✓
140 DW Car	10:43:10.07	-60:02:11.74	Sec	10.626	0.013	4.299	0.013	26500	1000	3.913	0.062	86	✓
141 chi02 Hya	11:05:57.57	-27:17:16.27	Pri	3.605	0.022	4.484	0.009	11750	190	2.537	0.028	86	✓
142 chi02 Hya	11:05:57.57	-27:17:16.27	Sec	2.632	0.019	2.206	0.019	11100	230	1.822	0.038	60	✓
143 EM Car	11:12:04.51	-61:05:42.93	Pri	22.833	0.014	9.356	0.018	34000	2000	5.021	0.093	79	✓
144 EM Car	11:12:04.51	-61:05:42.93	Sec	21.376	0.015	8.345	0.019	34000	2000	4.922	0.093	75	✓
145 LSPM J1112+7626	11:12:42.32	+76:26:56.40	Pri	0.395	0.005	0.381	0.013	3061	162	-1.959	0.073	3	✓
146 LSPM J1112+7626	11:12:42.32	+76:26:56.40	Sec	0.274	0.004	0.300	0.017	2952	163	-2.222	0.067	3	✓
147 FM Leo	11:12:45.09	+00:20:52.84	Pri	1.318	0.005	1.649	0.026	6316	240	0.589	0.065	29	✓
148 EP Cru	12:37:16.75	-56:47:17.38	Pri	5.019	0.026	3.590	0.010	15700	500	2.847	0.053	29	✓
149 EP Cru	12:37:16.75	-56:47:17.38	Sec	4.830	0.027	3.495	0.010	15400	500	2.790	0.053	29	✓
150 IM Vir	12:49:38.70	-06:04:44.86	Pri										

ID Star name	α (J2000)	δ (J2000)	Com	M/M_{\odot}	$\Delta M_{err}/M$	R/R_{\odot}	$\Delta R_{err}/R$	T_{eff}	$(T_{eff})_{err}$	$\log L/L_{\odot}$	$\Delta L_{err}/L$	FF(%)	Remark
151 IM Vir	12:49:38.70	-06:04:44.86	Sec	0.664	0.008	0.681	0.019	4250	130	-0.866	0.051	46	✓
152 eta Mus	13:15:14.94	-67:53:40.52	Pri	3.283	0.012	2.140	0.009	12700	100	2.029	0.016	51	✓
153 eta Mus	13:15:14.94	-67:53:40.52	Sec	3.282	0.012	2.130	0.019	12550	300	2.005	0.043	51	✓
154 SZ Cen	13:50:35.09	-58:29:57.11	Pri	2.272	0.011	4.555	0.005	8000	300	1.883	0.061	75	X
155 SZ Cen	13:50:35.09	-58:29:57.11	Sec	2.311	0.009	3.622	0.006	8280	300	1.743	0.059	64	✓
156 DM Vir	14:07:52.43	-11:09:07.49	Pri	1.454	0.006	1.764	0.010	6500	100	0.698	0.027	37	✓
157 DM Vir	14:07:52.43	-11:09:07.49	Sec	1.448	0.006	1.764	0.010	6500	300	0.698	0.074	37	✓
158 V636 Cen	14:16:57.91	-49:56:42.36	Pri	1.052	0.005	1.024	0.004	5900	85	0.057	0.024	25	✓
159 V636 Cen	14:16:57.91	-49:56:42.36	Sec	0.854	0.004	0.835	0.005	5000	100	-0.408	0.034	25	✓
160 Psi Cen	14:20:33.43	-37:53:07.06	Pri	3.114	0.005	3.634	0.002	10450	300	2.150	0.047	14	✓
161 Psi Cen	14:20:33.43	-37:53:07.06	Sec	1.909	0.016	1.811	0.002	8800	300	1.247	0.055	11	✓
162 AD Boo	14:35:12.78	+24:38:21.35	Pri	1.414	0.006	1.614	0.009	6575	120	0.641	0.031	53	✓
163 AD Boo	14:35:12.78	+24:38:21.35	Sec	1.209	0.005	1.218	0.008	6145	120	0.279	0.033	47	✓
164 GG Lup	15:18:56.37	-40:47:17.60	Pri	4.106	0.010	2.379	0.011	14750	450	2.381	0.051	55	✓
165 GG Lup	15:18:56.37	-40:47:17.60	Sec	2.504	0.010	1.725	0.011	11000	600	1.592	0.086	58	✓
166 GU Boo	15:21:55.17	+33:56:04.20	Pri	0.609	0.011	0.628	0.025	3920	130	-1.076	0.058	69	✓
167 CV Boo	15:26:19.54	+36:58:53.43	Pri	1.045	0.012	1.269	0.018	5760	150	0.202	0.045	77	✓
168 CV Boo	15:26:19.54	+36:58:53.43	Sec	0.995	0.012	1.180	0.019	5670	150	0.111	0.046	75	✓
169 RT CrB	15:38:03.03	+29:29:13.95	Pri	1.344	0.007	4.256	0.017	5134	100	1.053	0.035	73	X
170 RT CrB	15:38:03.03	+29:29:13.95	Sec	1.359	0.007	3.778	0.017	5781	100	1.156	0.032	67	X
171 V335 Ser	15:59:05.76	+00:35:44.55	Pri	2.029	0.005	2.039	0.010	9506	289	1.484	0.050	45	✓
172 V335 Ser	15:59:05.76	+00:35:44.55	Sec	1.844	0.011	1.607	0.006	8872	248	1.157	0.046	39	✓
173 TV Nor	16:04:09.24	-51:32:39.99	Pri	2.048	0.011	1.851	0.006	9120	148	1.328	0.028	23	✓
174 TV Nor	16:04:09.24	-51:32:39.99	Sec	1.661	0.011	1.560	0.009	7798	108	0.907	0.025	23	✓
175 M4-V65	16:23:28.39	-26:30:22.00	Pri	0.803	0.011	1.147	0.009	6088	108	0.210	0.030	43	X
176 M4-V65	16:23:28.39	-26:30:22.00	Sec	0.605	0.007	0.611	0.015	4812	125	-0.745	0.044	31	✓
177 M4-V66	16:23:32.23	-26:31:41.30	Pri	0.784	0.005	0.934	0.005	6162	98	0.053	0.027	18	X
178 M4-V66	16:23:32.23	-26:31:41.30	Sec	0.743	0.005	0.830	0.006	5938	105	-0.114	0.030	16	X
179 M4-V69	16:23:58.01	-26:37:18.00	Pri	0.766	0.007	0.866	0.012	6084	121	-0.035	0.035	5	X
180 M4-V69	16:23:58.01	-26:37:18.00	Sec	0.728	0.005	0.807	0.010	5915	137	-0.145	0.039	5	X
181 V760 Sco	16:24:43.72	-34:53:37.53	Pri	4.969	0.018	3.028	0.020	16900	500	2.827	0.051	70	✓
182 V760 Sco	16:24:43.72	-34:53:37.53	Sec	4.610	0.015	2.656	0.019	16300	500	2.650	0.052	66	✓
183 CM Dra	16:34:20.41	+57:09:43.94	Pri	0.231	0.004	0.253	0.004	3130	70	-2.222	0.067	24	✓
184 CM Dra	16:34:20.41	+57:09:43.94	Sec	0.214	0.005	0.239	0.004	3120	70	-2.301	0.000	24	✓
185 WZ Oph	17:06:39.04	+07:46:57.78	Pri	1.227	0.006	1.401	0.009	6165	100	0.406	0.028	34	✓
186 WZ Oph	17:06:39.04	+07:46:57.78	Sec	1.220	0.005	1.419	0.008	6115	100	0.403	0.029	34	✓
187 V2365 Oph	17:08:45.78	+09:11:10.14	Pri	1.964	0.009	2.191	0.004	9500	200	1.545	0.035	35	✓
188 V2365 Oph	17:08:45.78	+09:11:10.14	Sec	1.055	0.009	0.934	0.004	6400	210	0.119	0.054	26	✓
189 V2368 Oph	17:16:14.26	+02:11:10.33	Pri	2.417	0.007	3.857	0.005	9300	200	2.000	0.036	17	✓
190 V2368 Oph	17:16:14.26	+02:11:10.33	Sec	2.525	0.026	3.740	0.005	9500	200	2.010	0.035	18	✓
191 TX Her	17:18:36.45	+41:53:17.10	Pri	1.607	0.025	1.688	0.018	7534	200	0.916	0.046	54	✓
192 TX Her	17:18:36.45	+41:53:17.10	Sec	1.441	0.021	1.428	0.021	6678	211	0.561	0.054	51	✓
193 LV Her	17:35:32.40	+23:10:30.60	Pri	1.192	0.008	1.358	0.009	6060	150	0.349	0.042	13	✓
194 LV Her	17:35:32.40	+23:10:30.60	Sec	1.169	0.007	1.313	0.008	6030	150	0.311	0.042	13	✓
195 V624 Her	17:44:17.25	+14:24:36.24	Pri	2.277	0.006	3.028	0.010	8150	150	1.560	0.032	55	✓
196 V624 Her	17:44:17.25	+14:24:36.24	Sec	1.876	0.007	2.208	0.014	7945	150	1.242	0.033	48	✓
197 V539 Ara	17:50:28.39	-53:36:44.66	Pri	6.265	0.011	4.436	0.027	18200	1300	3.287	0.111	64	✓
198 V906 Sco	17:53:54.77	-34:45:09.80	Pri	3.370	0.021	4.525	0.008	10400	500	2.333	0.077	82	✓
199 V906 Sco	17:53:54.77	-34:45:09.80	Sec	3.246	0.021	3.518	0.011	10700	500	2.163	0.075	70	✓
200 Z Her	17:58:06.98	+15:08:21.90	Pri	1.312	0.023	2.743	0.029	4977	175	0.618	0.061	62	X
201 V1647 Sgr	17:59:13.47	-36:56:19.84	Pri	2.184	0.018	1.908	0.011	9600	310	1.443	0.053	42	✓
202 V1647 Sgr	17:59:13.47	-36:56:19.84	Sec	1.967	0.015	1.741	0.012	9100	300	1.271	0.055	42	✓
203 V3903 Sgr	18:09:17.70	-23:59:18.22	Pri	27.204	0.020	8.120	0.011	38000	1900	5.091	0.080	91	✓
204 V3903 Sgr	18:09:17.70	-23:59:18.22	Sec	18.964	0.023	6.149	0.010	34100	1700	4.662	0.079	87	✓
205 EG Ser	18:26:02.20	-01:40:51.42	Pri	2.200	0.023	1.689	0.006	9900	200	1.391	0.034	19	✓
206 EG Ser	18:26:02.20	-01:40:51.42	Sec	1.990	0.015	1.549	0.006	9100	200	1.169	0.037	19	✓
207 V451 Oph	18:29:14.04	+10:53:31.44	Pri	2.769	0.022	2.646	0.011	10800	800	1.932	0.113	64	✓
208 V451 Oph	18:29:14.04	+10:53:31.44	Sec	2.351	0.021	2.032	0.015	9800	500	1.534	0.081	57	✓
209 V413 Ser	18:35:08.21	+00:02:34.82	Pri	3.654	0.014	3.200	0.016	11100	300	2.145	0.046	69	✓
210 V413 Ser	18:35:08.21	+00:02:34.82	Sec	3.318	0.012	2.921	0.017	10350	280	1.944	0.046	68	✓
211 V1331 Aql	18:44:12.79	-01:33:15.56	Pri	10.079	0.011	4.253	0.007	25400	100	3.830	0.009	80	✓
212 V1331 Aql	18:44:12.79	-01:33:15.56	Sec	5.282	0.019	4.043	0.007	20100	140	3.379	0.014	96	✓
213 YY Sgr	18:44:35.86	-19:23:22.71	Pri	3.482	0.026	2.344	0.021	14125	670	2.293	0.077	52	✓
214 BF Dra	18:50:59.35	+69:52:57.48	Pri	1.413	0.002	2.999	0.006	6360	150	1.121	0.039	35	X
215 BF Dra	18:50:59.35	+69:52:57.48	Sec	1.374	0.002	2.763	0.006	6400	150	1.061	0.039	34	X
216 DI Her	18:53:26.24	+24:16:40.80	Pri	5.173	0.019	2.679	0.019	16980	800	2.729	0.076	22	✓
217 DI Her	18:53:26.24	+24:16:40.80	Sec	4.524	0.013	2.479	0.020	15135	715	2.462	0.077	23	✓
218 HP Dra	18:54:53.48	+51:18:29.79	Pri	1.056	0.005	1.340	0.009	6000	150	0.320	0.042	19	✓
219 HP Dra	18:54:53.48	+51:18:29.79	Sec	1.024	0.007	1.028	0.010	5895	150	0.059	0.043	15	✓
220 V1182 Aql	18:55:23.13	+09:20:48.08	Pri	30.884	0.019	9.059	0.020	43000	500	5.401	0.026	96	✓
221 FL Lyr	19:12:04.86	+46:19:26.87	Pri	1.218	0.013	1.282	0.023	6150	100	0.324	0.033	44	✓
222 V565 Lyr	19:20:49.10	+37:46:09.30	Pri	0.995	0.003	1.101	0.006	5600	95	0.029	0.029	11	✓
223 V565 Lyr	19:20:49.10	+37:46:09.30	Sec	0.929	0.003	0.971	0.009	5430	125	-0.133	0.039	10	✓
224 V568 Lyr	19:20:54.30	+37:45:34.70	Pri	1.075	0.007	1.400	0.011	5665	100	0.258	0.031	15	✓
225 V568 Lyr	19:20:54.30	+37:45:34.70	Sec	0.827	0.005	0.768	0.008	4900	1				

ID Star name	α (J2000)	δ (J2000)	Com	M/M_{\odot}	$\Delta M_{err}/M$	R/R_{\odot}	$\Delta R_{err}/R$	T_{eff}	$(T_{eff})_{err}$	$\log L/L_{\odot}$	$\Delta L_{err}/L$	FF(%)	Remark
226 V1430 Aql	19:21:48.49 +04:32:56.92	Pri	0.957	0.010	1.101	0.009	5262	150	-0.079	0.047	70	✓	
227 V1430 Aql	19:21:48.49 +04:32:56.92	Sec	0.859	0.023	0.851	0.012	4930	100	-0.416	0.035	60	✓	
228 UZ Dra	19:25:55.05 +68:56:07.15	Pri	1.345	0.015	1.311	0.023	6210	110	0.361	0.035	35	✓	
229 UZ Dra	19:25:55.05 +68:56:07.15	Sec	1.236	0.016	1.150	0.017	5985	110	0.183	0.034	34	✓	
230 V2080 Cyg	19:26:47.95 +50:08:43.77	Pri	1.190	0.014	1.596	0.005	6000	75	0.472	0.022	35	✓	
231 V2080 Cyg	19:26:47.95 +50:08:43.77	Sec	1.156	0.015	1.599	0.005	5987	75	0.470	0.022	36	✓	
232 V885 Cyg	19:32:49.86 +30:01:17.03	Pri	2.000	0.015	2.487	0.005	8375	150	1.436	0.030	64	✓	
233 V885 Cyg	19:32:49.86 +30:01:17.03	Sec	2.228	0.012	3.591	0.008	8150	150	1.708	0.031	97	✓	
234 KIC 6131659	19:37:06.98 +41:26:12.86	Pri	0.922	0.008	0.880	0.003	5660	140	-0.146	0.041	9	✓	
235 KIC 6131659	19:37:06.98 +41:26:12.86	Sec	0.685	0.007	0.640	0.009	4780	105	-0.717	0.037	9	✓	
236 V1143 Cyg	19:38:41.18 +54:58:25.66	Pri	1.388	0.012	1.347	0.017	6460	100	0.453	0.030	22	✓	
237 V1143 Cyg	19:38:41.18 +54:58:25.66	Sec	1.344	0.010	1.324	0.017	6400	100	0.422	0.030	22	✓	
238 V453 Cyg	20:06:34.97 +35:44:26.28	Pri	14.377	0.014	8.564	0.006	26600	500	4.518	0.032	76	✓	
239 V453 Cyg	20:06:34.97 +35:44:26.28	Sec	11.119	0.012	5.497	0.011	25500	800	4.060	0.052	63	✓	
240 2MASSJ20115132+0337194	20:11:51.40 +03:37:20.00	Pri	0.557	0.002	0.519	0.021	3690	80	-1.347	0.037	53	✓	
241 2MASSJ20115132+0337194	20:11:51.40 +03:37:20.00	Sec	0.535	0.002	0.456	0.015	3610	80	-1.495	0.039	49	✓	
242 MY Cyg	20:20:03.39 +33:56:35.02	Pri	1.805	0.017	2.215	0.009	7050	200	1.037	0.047	46	✓	
243 MY Cyg	20:20:03.39 +33:56:35.02	Sec	1.794	0.017	2.275	0.009	7000	200	1.048	0.048	48	✓	
244 V399 Vul	20:25:10.80 +21:29:18.84	Pri	7.550	0.011	6.498	0.005	19000	320	3.694	0.029	64	✓	
245 V399 Vul	20:25:10.80 +21:29:18.84	Sec	5.440	0.006	3.506	0.025	18250	520	3.088	0.051	48	✓	
246 BP Vul	20:25:33.25 +21:02:17.97	Pri	1.737	0.009	1.853	0.008	7709	150	1.037	0.033	58	✓	
247 BP Vul	20:25:33.25 +21:02:17.97	Sec	1.408	0.006	1.489	0.009	6823	150	0.635	0.037	55	✓	
248 V442 Cyg	20:27:52.30 +30:47:28.30	Pri	1.560	0.013	2.072	0.014	6900	82	0.941	0.024	60	✓	
249 V442 Cyg	20:27:52.30 +30:47:28.30	Sec	1.407	0.014	1.662	0.018	6808	79	0.727	0.025	53	✓	
250 IO Aqr	20:40:45.47 +00:56:21.02	Pri	1.624	0.012	2.538	0.024	6600	—	1.040	0.075	70	✓	
251 V379 Cep	20:43:13.38 +57:06:50.39	Pri	10.873	0.022	7.986	0.015	22025	428	4.130	0.035	10	✓	
252 V379 Cep	20:43:13.38 +57:06:50.39	Sec	6.233	0.021	3.070	0.013	20206	374	3.149	0.033	7	✓	
253 CG Cyg	20:58:13.45 +35:10:29.66	Pri	0.948	0.013	0.896	0.015	5260	185	-0.258	0.058	70	✓	
254 CG Cyg	20:58:13.45 +35:10:29.66	Sec	0.821	0.016	0.846	0.017	4720	66	-0.496	0.028	72	✓	
255 V1061 Cyg	21:07:20.52 +52:02:58.42	Pri	1.281	0.012	1.616	0.011	6180	100	0.534	0.029	50	✓	
256 V1061 Cyg	21:07:20.52 +52:02:58.42	Sec	0.931	0.008	0.974	0.021	5300	150	-0.173	0.049	40	✓	
257 EI Cep	21:28:28.21 +76:24:12.59	Pri	1.772	0.004	2.898	0.017	6750	100	1.195	0.029	38	✓	
258 EI Cep	21:28:28.21 +76:24:12.59	Sec	1.680	0.004	2.330	0.019	6950	100	1.056	0.029	32	✓	
259 2MASS J21295384-5620038	21:29:54.00 -56:20:03.87	Pri	0.839	0.020	0.847	0.014	4750	150	-0.484	0.052	65	✓	
260 2MASS J21295384-5620038	21:29:54.00 -56:20:03.87	Sec	0.714	0.018	0.720	0.024	4220	180	-0.830	0.070	63	✓	
261 EE Peg	21:40:01.88 +09:11:05.11	Pri	2.151	0.009	2.103	0.014	8700	200	1.357	0.040	49	✓	
262 EE Peg	21:40:01.88 +09:11:05.11	Sec	1.332	0.008	1.321	0.008	6450	300	0.433	0.074	46	✓	
263 EK Cep	21:41:21.51 +69:41:34.11	Pri	2.024	0.010	1.579	0.009	9000	200	1.167	0.038	27	✓	
264 EK Cep	21:41:21.51 +69:41:34.11	Sec	1.122	0.009	1.315	0.011	5700	190	0.215	0.055	37	✓	
265 VZ Cep	21:50:11.14 +71:26:38.30	Pri	1.402	0.011	1.558	0.008	6670	160	0.635	0.040	69	✓	
266 BG Ind	21:58:30.08 -59:00:43.71	Pri	1.428	0.006	2.290	0.007	6353	270	0.885	0.069	83	✓	
267 BG Ind	21:58:30.08 -59:00:43.71	Sec	1.293	0.006	1.680	0.023	6653	233	0.696	0.060	70	✓	
268 CM Lac	22:00:04.45 +44:33:07.74	Pri	1.971	0.030	1.509	0.020	9000	300	1.128	0.057	52	✓	
269 BW Aqr	22:23:15.93 -15:19:56.22	Pri	1.479	0.014	2.057	0.019	6350	100	0.791	0.031	34	✓	
270 BW Aqr	22:23:15.93 -15:19:56.22	Sec	1.377	0.015	1.788	0.022	6450	100	0.696	0.032	31	✓	
271 WX Cep	22:31:15.78 +63:31:21.55	Pri	2.324	0.020	3.997	0.008	8150	225	1.801	0.046	73	✓	
272 WX Cep	22:31:15.78 +63:31:21.55	Sec	2.533	0.019	2.708	0.009	8872	250	1.611	0.047	57	✓	
273 RW Lac	22:44:57.10 +49:39:27.57	Pri	0.928	0.006	1.193	0.003	5760	100	0.148	0.029	18	X	
274 RW Lac	22:44:57.10 +49:39:27.57	Sec	0.870	0.005	0.970	0.004	5560	150	-0.093	0.044	16	✓	
275 AH Cep	22:47:52.94 +65:03:43.80	Pri	15.565	0.013	6.385	0.017	29900	1000	4.466	0.056	89	✓	
276 AH Cep	22:47:52.94 +65:03:43.80	Sec	13.714	0.015	5.864	0.022	28600	1000	4.315	0.060	88	✓	
277 V364 Lac	22:52:14.81 +38:44:44.64	Pri	2.334	0.006	3.308	0.011	8250	150	1.658	0.032	43	✓	
278 V364 Lac	22:52:14.81 +38:44:44.64	Sec	2.296	0.011	2.986	0.012	8500	150	1.621	0.031	40	✓	
279 EF Aqr	23:01:19.09 -06:26:15.35	Pri	1.244	0.006	1.338	0.009	6150	65	0.362	0.020	38	✓	
280 EF Aqr	23:01:19.09 -06:26:15.35	Sec	0.946	0.006	0.956	0.013	5185	110	-0.227	0.037	35	✓	
281 CW Cep	23:04:02.22 +63:23:48.76	Pri	11.797	0.012	5.524	0.022	28300	1000	4.245	0.060	70	✓	
282 CW Cep	23:04:02.22 +63:23:48.76	Sec	11.067	0.013	5.030	0.024	27700	1000	4.126	0.061	69	✓	
283 PV Cas	23:10:02.58 +59:12:06.15	Pri	2.757	0.018	2.298	0.009	10200	250	1.710	0.041	66	✓	
284 PV Cas	23:10:02.58 +59:12:06.15	Sec	2.816	0.022	2.257	0.007	10200	250	1.695	0.041	66	✓	
285 RT And	23:11:10.10 +53:01:33.04	Pri	1.240	0.024	1.268	0.012	6095	214	0.299	0.058	83	✓	
286 RT And	23:11:10.10 +53:01:33.04	Sec	0.907	0.022	0.906	0.014	4732	110	-0.432	0.040	75	✓	
287 V396 Cas	23:13:35.98 +56:44:17.20	Pri	2.397	0.009	2.592	0.005	9225	150	1.640	0.028	39	✓	
288 V396 Cas	23:13:35.98 +56:44:17.20	Sec	1.901	0.008	1.779	0.006	8550	120	1.181	0.024	33	✓	
289 2MASS J23143816+0339493	23:14:38.16 +03:39:49.33	Pri	0.469	0.004	0.441	0.005	3460	180	-1.602	0.079	26	✓	
290 2MASS J23143816+0339493	23:14:38.16 +03:39:49.33	Sec	0.383	0.003	0.374	0.005	3320	180	-1.824	0.079	26	✓	
291 IT Cas	23:42:01.40 +51:44:36.80	Pri	1.330	0.007	1.603	0.009	6470	110	0.607	0.030	39	✓	
292 IT Cas	23:42:01.40 +51:44:36.80	Sec	1.328	0.006	1.569	0.025	6470	110	0.588	0.035	38	✓	
293 BK Peg	23:47:08.46 +26:33:59.92	Pri	1.414	0.005	1.985	0.004	6265	85	0.736	0.023	37	✓	
294 BK Peg	23:47:08.46 +26:33:59.92	Sec	1.257	0.004	1.472	0.012	6320	30	0.492	0.013	31	✓	
295 AL Scl	23:55:16.58 -31:55:17.28	Pri	3.617	0.030	3.241	0.015	13550	350	2.502	0.045	61	✓	
296 AL Scl	23:55:16.58 -31:55:17.28	Sec	1.703	0.023	1.401	0.014	10300	360	1.297	0.058	50	✓	

(X) Probable non main-sequence star (locates above ZAMS line in Fig. 1).

Table 3: Classical MLRs for the four mass domains.

Domain	N	Mass range	Equation	R	σ	α
Low mass	57	$0.38 < M/M_{\odot} \leq 1.05$	$\log L = 4.841(132) \times \log M - 0.026(25)$	0.980	0.121	4.841
Intermediate mass	146	$1.05 < M/M_{\odot} \leq 2.40$	$\log L = 4.328(90) \times \log M - 0.002(20)$	0.970	0.108	4.328
High mass	42	$2.4 < M/M_{\odot} \leq 7$	$\log L = 3.962(203) \times \log M + 0.120(112)$	0.951	0.165	3.962
Very high mass	23	$7 < M/M_{\odot} < 32$	$\log L = 2.726(203) \times \log M + 1.237(228)$	0.946	0.158	2.726

Table 4: Comparing linear, quadratic and cubic MLRs of the calibration sample as a whole (268 main-sequence stars).

Equation	R	σ
$\log L = +4.040(32) \times (\log M) - 0.002(14)$	0.992	0.187
$\log L = -0.705(41) \times (\log M)^2 + 4.655(42) \times (\log M) - 0.025(10)$	0.992	0.130
$\log L = -0.125(84) \times (\log M)^3 - 0.535(121) \times (\log M)^2 + 4.634(45) \times (\log M) - 0.033(11)$	0.992	0.130

Table 5: Standard deviations on M-L diagram and corresponding relative uncertainties.

Domain	Mass range	σ	$\Delta L/L(\%)$	$(\Delta L/L)/4$	$(\Delta R/R)/2$	$\Delta T/T$	α	$\Delta M/M(\%)$
Low mass	$0.38 < M/M_{\odot} \leq 1.05$	0.121	27.86	6.96	1.5	7.12	4.841	5.76
Intermediate mass	$1.05 < M/M_{\odot} \leq 2.40$	0.108	24.87	6.22	1.5	6.39	4.328	5.75
High mass	$2.40 < M/M_{\odot} \leq 7.00$	0.165	37.99	9.50	1.5	9.62	3.962	9.59
Very high mass	$7 < M/M_{\odot} < 32$	0.158	36.38	9.10	1.5	9.22	2.726	13.34

Table 6: Comparing the calculated and the published temperatures.

T_{eff} range (K)	N	Mean standard difference (K)	Mean calculated error (K)	Mean published error (K)
(2750, 5000]	37	345	291	117
(5000, 10000]	168	441	453	162
(10000, 15000]	24	975	1109	392
(15000, 43000]	39	2283	2203	746

Mean standard difference = $\sqrt{\frac{\sum(T_{cal} - T_{pub})^2}{N}}$. Summation over all stars in the range given.

Table 7: Comparing published and calculated (empirical) effective temperatures.

ID Star	α (J2000)	δ (J2000)	Com	$\Delta M/M$	$\Delta R/R$	T_{eff}	ΔT_{eff}	$\Delta T/T$	Published temperatures		This study		
									Ref.	T_{eff}	ΔT_{eff}	$\Delta T/T$	
1 DV Psc	00:13:09.20	+05:35:43.06	Pri	0.028	0.044	4450	—	0.002	2007MNRAS.382.1133Z	4286	313	0.073	
2 DV Psc	00:13:09.20	+05:35:43.06	Sec	0.021	0.039	3614	8	0.002	2007MNRAS.382.1133Z	3223	233	0.072	
3 MU Cas	00:15:51.56	+60:25:53.64	Pri	0.021	0.012	14750	500	0.034	2004AJ....128.1840L	13876	1321	0.095	
4 MU Cas	00:15:51.56	+60:25:53.64	Sec	0.020	0.011	15100	500	0.033	2004AJ....128.1840L	14569	1386	0.095	
5 YZ Cas	00:45:39.08	+74:59:17.06	Pri	0.004	0.012	9200	300	0.033	1981ApJ...251..591L	8937	558	0.062	
6 YZ Cas	00:45:39.08	+74:59:17.06	Sec	0.007	0.015	6700	250	0.037	1981ApJ...251..591L	6832	428	0.063	
7 NGC188 KR V12	00:52:37.54	+85:10:34.65	Pri	0.006	0.013	5900	100	0.017	2009AJ....137.5086M	5370	336	0.063	
8 NGC188 KR V12	00:52:37.54	+85:10:34.65	Sec	0.006	0.014	5875	100	0.017	2009AJ....137.5086M	5350	335	0.063	
9 V364 Cas	00:52:43.01	+50:28:10.16	Pri	0.056	0.006	7816	86	0.011	2009IBVS.5884...1N	8018	499	0.062	
10 zet Phe	01:08:23.08	-55:14:44.74	Pri	0.011	0.007	14550	350	0.024	1983A&A...118..255A	14188	1348	0.095	
11 zet Phe	01:08:23.08	-55:14:44.74	Sec	0.010	0.011	11910	200	0.017	1983A&A...118..255A	11468	1091	0.095	
12 AI Phe	01:09:34.19	-46:15:56.09	Sec	0.003	0.013	5010	120	0.024	1988A&A...196..128A	5390	337	0.063	
13 CO And	01:11:24.83	+46:57:49.34	Pri	0.005	0.012	6140	130	0.021	2010AJ....139.2347L	5779	361	0.062	
14 CO And	01:11:24.83	+46:57:49.34	Sec	0.006	0.010	6170	130	0.021	2010AJ....139.2347L	5713	356	0.062	
15 V459 Cas	01:11:29.92	+61:08:47.96	Pri	0.015	0.006	9140	300	0.033	2004AJ....128.1340L	8686	541	0.062	
16 V459 Cas	01:11:29.92	+61:08:47.96	Sec	0.015	0.007	9100	300	0.033	2004AJ....128.1340L	8533	531	0.062	
17 2MASSJ01132817-3821024	01:13:28.17	-38:21:02.50	Pri	0.049	0.034	3750	250	0.067	2012MNRAS.425.1245H	4075	292	0.072	
18 2MASSJ01132817-3821024	01:13:28.17	-38:21:02.50	Sec	0.043	0.054	3085	300	0.097	2012MNRAS.425.1245H	3200	239	0.075	
19 UV Psc	01:16:55.12	+06:48:42.12	Pri	0.009	0.018	5780	100	0.017	1997AJ....114.1195P	5271	370	0.070	
20 UV Psc	01:16:55.12	+06:48:42.12	Sec	0.007	0.036	4750	80	0.017	1997AJ....114.1195P	4494	323	0.072	
21 V615 Per	02:19:01.57	+57:07:19.30	Sec	0.016	0.049	11000	500	0.045	2004MNRAS.349..547S	14101	1383	0.098	
22 V618 Per	02:19:11.78	+57:06:41.10	Pri	0.013	0.042	11000	1000	0.091	2004MNRAS.349..547S	11277	740	0.066	
23 V618 Per	02:19:11.78	+57:06:41.10	Sec	0.016	0.052	8000	1000	0.125	2004MNRAS.349..547S	8121	547	0.067	
24 V505 Per	02:21:12.96	+54:30:36.28	Pri	0.001	0.011	6512	21	0.003	2008A&A...480..465T	6596	412	0.062	
25 V505 Per	02:21:12.96	+54:30:36.28	Sec	0.001	0.011	6462	12	0.002	2008A&A...480..465T	6549	409	0.062	
26 AG Ari	02:26:26.96	+12:53:55.81	Pri	0.032	0.010	10300	250	0.024	2007MNRAS.380.1422I	8904	555	0.062	
27 AG Ari	02:26:26.96	+12:53:55.81	Sec	0.033	0.011	9800	230	0.023	2007MNRAS.380.1422I	9163	572	0.062	
28 XY Cet	02:59:33.53	+03:31:03.27	Pri	0.009	0.019	7870	115	0.015	2011MNRAS.414.3740S	7829	492	0.063	
29 XY Cet	02:59:33.53	+03:31:03.27	Sec	0.009	0.016	7620	125	0.016	2011MNRAS.414.3740S	7273	456	0.063	
30 CW Eri	03:03:59.95	-17:44:16.06	Pri	0.013	0.024	6840	86	0.013	1983AJ....88.1242P	6556	415	0.063	
31 CW Eri	03:03:59.95	-17:44:16.06	Sec	0.008	0.045	6561	100	0.015	1983AJ....88.1242P	6257	414	0.066	
32 AE For	03:08:06.66	-24:45:37.74	Pri	0.006	0.045	4100	—	0.001	2013MNRAS.429.1840R	4017	294	0.073	
33 AE For	03:08:06.66	-24:45:37.74	Sec	0.005	0.047	4055	6	0.001	2013MNRAS.429.1840R	4048	298	0.074	
34 TV Cet	03:14:36.51	+02:45:16.40	Pri	0.038	0.013	6902	150	0.022	2010NewA...15..356B	6738	421	0.062	
35 TV Cet	03:14:36.51	+02:45:16.40	Sec	0.040	0.008	6575	150	0.023	2010NewA...15..356B	6735	420	0.062	
36 2MASSJ03262072+0312362	03:26:20.73	+03:12:36.29	Pri	0.004	0.016	3330	60	0.018	2011ApJ...728..48K	3687	258	0.070	
37 2MASSJ03262072+0312362	03:26:20.73	+03:12:36.29	Sec	0.002	0.019	3270	60	0.018	2011ApJ...728..48K	3504	246	0.070	
38 EY Cep	03:40:04.07	+81:01:09.07	Pri	0.005	0.007	7090	150	0.021	2006AJ....131.2664L	7526	469	0.062	
39 EY Cep	03:40:04.07	+81:01:09.07	Sec	0.009	0.007	6970	150	0.022	2006AJ....131.2664L	7385	460	0.062	
40 V1229 Tau	03:47:29.45	+24:17:18.04	Pri	0.012	0.020	10025	620	0.062	2007A&A...463..579G	10076	634	0.063	
41 V1229 Tau	03:47:29.45	+24:17:18.04	Sec	0.010	0.026	7262	380	0.052	2007A&A...463..579G	7437	472	0.063	
42 V1130 Tau	03:50:41.94	+01:33:50.21	Pri	0.006	0.007	6650	70	0.011	2010A&A...510A..91C	6310	393	0.062	
43 V1130 Tau	03:50:41.94	+01:33:50.21	Sec	0.006	0.006	6625	70	0.011	2010A&A...510A..91C	6179	385	0.062	
44 IQ Per	03:59:44.68	+48:09:04.50	Pri	0.011	0.012	12300	200	0.016	1985ApJ...295..569L	13686	1302	0.095	
45 IQ Per	03:59:44.68	+48:09:04.50	Sec	0.012	0.013	7670	100	0.013	1985ApJ...295..569L	8516	532	0.062	
46 AG Per	04:06:55.83	+33:26:46.93	Pri	0.030	0.023	18200	800	0.044	1994A&A...291..795G	15824	1514	0.096	
47 AG Per	04:06:55.83	+33:26:46.93	Sec	0.027	0.027	17400	800	0.046	1994A&A...291..795G	15475	1485	0.096	
48 SZ Cam	04:07:49.29	+62:19:58.58	Pri	0.038	0.006	30360	—	0.008	2012A&A...539A.139T	26826	2441	0.091	
49 SZ Cam	04:07:49.29	+62:19:58.58	Sec	0.036	0.018	27244	255	0.009	2012A&A...539A.139T	24747	2262	0.091	
50 WW Cam	04:31:25.28	+64:21:45.50	Pri	0.007	0.008	8360	140	0.017	2002AJ....123.1013L	8450	526	0.062	
51 WW Cam	04:31:25.28	+64:21:45.50	Sec	0.010	0.008	8240	140	0.017	2002AJ....123.1013L	8458	527	0.062	
52 2MASSJ04480963+0317480	04:48:00.96	+03:17:48.09	Pri	0.004	0.014	3920	80	0.020	2011ApJ...728..48K	3853	270	0.070	
53 2MASSJ04480963+0317480	04:48:00.96	+03:17:48.09	Sec	0.004	0.011	3810	80	0.021	2011ApJ...728..48K	3633	254	0.070	
54 TYC 4749-560-1	04:53:04.43	-07:00:23.47	Pri	0.007	0.006	5340	200	0.037	2011A&A...526A..29H	4958	346	0.070	
55 TYC 4749-560-1	04:53:04.43	-07:00:23.47	Sec	0.007	0.006	5125	200	0.039	2011A&A...526A..29H	4959	346	0.070	
56 HP Aur	05:10:21.78	+35:47:46.63	Pri	0.011	0.011	5790	80	0.014	2005AstL...31..117K	5272	368	0.070	
57 HP Aur	05:10:21.78	+35:47:46.63	Sec	0.012	0.011	5270	90	0.017	2005AstL...31..117K	4837	338	0.070	
58 V1236 Tau	05:16:28.81	+26:07:38.80	Pri	0.013	0.020	4200	200	0.048	2006ApJ...651.1155B	4871	343	0.070	
59 V1236 Tau	05:16:28.81	+26:07:38.80	Sec	0.010	0.012	4133	250	0.060	2006ApJ...651.1155B	4633	324	0.070	
60 CD Tau	05:17:31.15	+20:07:54.63	Pri	0.011	0.009	6200	50	0.008	1999MNRAS.309..199R	6390	398	0.062	
61 CD Tau	05:17:31.15	+20:07:54.63	Sec	0.012	0.013	6200	50	0.008	1999MNRAS.309..199R	6425	402	0.063	
62 AR Aur	05:18:18.90	+33:46:02.45	Pri	0.040	0.020	10950	300	0.027	1994A&A...282..787N	11377	1087	0.096	
63 AR Aur	05:18:18.90	+33:46:02.45	Sec	0.041	0.020	10350	300	0.029	1994A&A...282..787N	10485	660	0.063	
64 EW Ori	05:20:09.15	+02:02:39.97	Pri	0.009	0.004	6070	95	0.016	2010A&A...511A..22C	6343	395	0.062	
65 EW Ori	05:20:09.15	+02:02:39.97	Sec	0.008	0.005	5900	95	0.016	2010A&A...511A..22C	6243	388	0.062	
66 2MASS J05282082+0338327	05:28:20.82	+03:38:32.80	Pri	0.008	0.005	5103	—	0.005	2008A&A...481..747S	5970	371	0.062	
67 2MASS J05282082+0338327	05:28:20.82	+03:38:32.80	Sec	0.006	0.006	4751	26	0.005	2008A&A...481..747S	5950	370	0.062	
68 AS Cam	05:29:46.91	+69:29:45.36	Pri	0.030	0.015	12000	600	0.050	1997ApJ...475..798K	12530	1194	0.095	
69 AS Cam	05:29:46.91	+69:29:45.36	Sec	0.040	0.020	10700	520	0.049	1997ApJ...475..798K	10901	1041	0.095	
70 UX Men	05:30:03.18	-76:14:55.34	Pri	0.005	0.010	6200	100	0.016	1989A&A...211..346A	6243	389	0.062	
71 UX Men	05:30:03.18												

ID Star	α (J2000)	δ (J2000)	Com	$\Delta M/M$	$\Delta R/R$	T_{eff}	ΔT_{eff}	$\Delta T/T$	Published temperatures			This study			
									Ref.	T_{eff}	ΔT_{eff}	$\Delta T/T$			
76 GG Ori	05:43:10.22	+00:41:14.90	Pri	0.007	0.013	9950	200	0.020	2000AJ....120..3226T	10648	666	0.063			
77 GG Ori	05:43:10.22	+00:41:14.90	Sec	0.007	0.014	9950	200	0.020	2000AJ....120..3226T	10687	669	0.063			
78 V1031 Ori	05:47:26.89	-10:31:58.65	Sec	0.007	0.021	8400	500	0.060	1990A&A...228..365A	8733	835	0.096			
79 beta Aur	05:59:31.72	+44:56:50.76	Pri	0.011	0.006	9350	200	0.021	1994A&A...291..777N	8828	549	0.062			
80 beta Aur	05:59:31.72	+44:56:50.76	Sec	0.012	0.007	9200	200	0.022	1994A&A...291..777N	8847	551	0.062			
81 V1388 Ori	06:10:59.17	+11:59:41.49	Pri	0.011	0.007	20500	500	0.024	2009AJ....137..3222W	19495	1774	0.091			
82 V1388 Ori	06:10:59.17	+11:59:41.49	Sec	0.006	0.008	18500	500	0.027	2009AJ....137..3222W	16199	1540	0.095			
83 FT Ori	06:13:58.15	+21:25:39.18	Pri	0.010	0.007	9600	400	0.042	2011AJ....141..195S	9745	607	0.062			
84 FT Ori	06:13:58.15	+21:25:39.18	Sec	0.011	0.008	8600	300	0.035	2011AJ....141..195S	8409	524	0.062			
85 V404 CMa	06:15:55.42	-18:44:51.54	Pri	0.007	0.019	4200	100	0.024	2009AcA....59..385R	4729	332	0.070			
86 V404 CMa	06:15:55.42	-18:44:51.54	Sec	0.008	0.025	3940	20	0.005	2009AcA....59..385R	4158	294	0.071			
87 IM Mon	06:23:01.47	-03:16:37.11	Pri	0.044	0.013	17500	350	0.020	2011PASJ....63..1079B	18892	1799	0.095			
88 IM Mon	06:23:01.47	-03:16:37.11	Sec	0.048	0.013	14500	550	0.038	2011PASJ....63..1079B	13294	1266	0.095			
89 RR Lyn	06:26:25.84	+56:17:06.35	Pri	0.004	0.008	7570	100	0.013	2002ARep..46..119K	7339	457	0.062			
90 RR Lyn	06:26:25.84	+56:17:06.35	Sec	0.003	0.019	6980	100	0.014	2002ARep..46..119K	7185	452	0.063			
91 V578 Mon	06:32:00.61	+04:52:40.90	Pri	0.005	0.011	30000	500	0.017	2000A&A...358..553H	25090	2286	0.091			
92 V578 Mon	06:32:00.61	+04:52:40.90	Sec	0.006	0.016	26400	400	0.015	2000A&A...358..553H	35028	3198	0.091			
93 WW Aur	06:32:27.18	+32:27:17.63	Pri	0.004	0.006	7960	420	0.053	2005MNRAS.363..529S	8626	537	0.062			
94 WW Aur	06:32:27.18	+32:27:17.63	Sec	0.004	0.006	7670	410	0.053	2005MNRAS.363..529S	8098	504	0.062			
95 SV Cam	06:41:19.07	+82:16:02.42	Pri	0.041	0.036	6038	58	0.010	2002A&A...386..548K	7780	504	0.065			
96 GX Gem	06:46:09.13	+34:24:52.83	Pri	0.007	0.005	6194	100	0.016	2008AJ....135..1757S	5806	361	0.062			
97 GX Gem	06:46:09.13	+34:24:52.83	Sec	0.007	0.005	6166	100	0.016	2008AJ....135..1757S	5831	363	0.062			
98 HS Aur	06:51:18.47	+47:40:24.16	Pri	0.021	0.023	5350	70	0.013	1986AJ....91..383P	4981	352	0.071			
99 HS Aur	06:51:18.47	+47:40:24.16	Sec	0.019	0.034	5200	72	0.014	1986AJ....91..383P	5191	372	0.072			
100 HI Mon	06:55:49.07	-04:02:35.79	Pri	0.021	0.021	30000	500	0.017	2011AJ....142..5W	28341	2595	0.092			
101 HI Mon	06:55:49.07	-04:02:35.79	Sec	0.016	0.014	29000	500	0.017	2011AJ....142..5W	25996	2371	0.091			
102 LT CMa	07:04:02.62	-12:17:17.37	Pri	0.036	0.019	17000	500	0.029	2010PASJ....62..1291B	17945	1713	0.095			
103 LT CMa	07:04:02.62	-12:17:17.37	Sec	0.042	0.024	13140	800	0.061	2010PASJ....62..1291B	14391	1378	0.096			
104 SW CMa	07:08:15.24	-22:26:25.26	Pri	0.006	0.007	8200	150	0.018	2012A&A...537A..117T	7953	495	0.062			
105 SW CMa	07:08:15.24	-22:26:25.26	Sec	0.009	0.017	8100	150	0.019	2012A&A...537A..117T	8172	513	0.063			
106 HW CMa	07:08:21.86	-22:24:29.87	Pri	0.006	0.011	7560	150	0.020	2012A&A...537A..117T	8075	504	0.062			
107 HW CMa	07:08:21.86	-22:24:29.87	Sec	0.007	0.013	7700	150	0.019	2012A&A...537A..117T	8333	521	0.063			
108 GZ CMa	07:16:19.21	-16:43:00.10	Pri	0.011	0.012	8810	350	0.040	1985AJ....90..1324P	8587	536	0.062			
109 GZ CMa	07:16:19.21	-16:43:00.10	Sec	0.012	0.019	8531	340	0.040	1985AJ....90..1324P	8375	527	0.063			
110 TYC 176-2950-1	07:16:25.56	+05:48:53.33	Sec	0.008	0.017	—	—	—		5505	386	0.070			
111 CW CMa	07:21:52.53	-23:47:37.43	Pri	0.010	0.021	—	—	—		9294	586	0.063			
112 CW CMa	07:21:52.53	-23:47:37.43	Sec	0.010	0.039	—	—	—		8979	585	0.065			
113 FS Mon	07:24:42.30	-05:09:14.57	Pri	0.007	0.006	6715	100	0.015	2000AJ....119..1389L	6829	425	0.062			
114 FS Mon	07:24:42.30	-05:09:14.57	Sec	0.007	0.007	6550	100	0.015	2000AJ....119..1389L	6802	424	0.062			
115 YY Gem	07:34:37.41	+31:52:09.79	Pri	0.008	0.010	3820	100	0.026	2002ApJ...567..1140T	3874	271	0.070			
116 YY Gem	07:34:37.41	+31:52:09.79	Sec	0.008	0.010	3820	100	0.026	2002ApJ...567..1140T	3949	276	0.070			
117 2MASSJ07431157+0316220	07:43:11.57	+03:16:22.09	Pri	0.003	0.004	3730	90	0.024	2011ApJ...728..48K	3968	276	0.070			
118 2MASSJ07431157+0316220	07:43:11.57	+03:16:22.09	Sec	0.004	0.008	3610	90	0.025	2011ApJ...728..48K	3805	265	0.070			
119 PV Pup	07:45:28.73	-14:41:10.20	Pri	0.008	0.010	6920	300	0.043	1984A&A...132..219V	7423	463	0.062			
120 PV Pup	07:45:28.73	-14:41:10.20	Sec	0.009	0.011	6930	300	0.043	1984A&A...132..219V	7466	466	0.062			
121 V392 Car	07:58:10.48	-60:51:57.20	Pri	0.013	0.018	8850	200	0.023	2001A&A...374..204D	9068	570	0.063			
122 V392 Car	07:58:10.48	-60:51:57.20	Sec	0.013	0.019	8650	200	0.023	2001A&A...374..204D	8892	559	0.063			
123 AI Hya	08:18:47.46	+00:17:00.16	Pri	0.020	0.007	7100	60	0.008	1988AJ....95..190P	7244	451	0.062			
124 AI Hya	08:18:47.46	+00:17:00.16	Sec	0.019	0.008	6700	60	0.009	1988AJ....95..190P	6645	414	0.062			
125 TYC 5998-1918-1	08:25:51.60	-16:22:47.30	Pri	0.004	0.013	4350	200	0.046	2011A&A...526A..29H	4457	312	0.070			
126 TYC 5998-1918-1	08:25:51.60	-16:22:47.30	Sec	0.004	0.019	4090	200	0.049	2011A&A...526A..29H	4319	304	0.070			
127 AY Cam	08:25:51.79	+77:13:06.85	Pri	0.021	0.007	7250	100	0.014	2004AJ....128..1319W	7112	443	0.062			
128 AY Cam	08:25:51.79	+77:13:06.85	Sec	0.021	0.007	7395	100	0.014	2004AJ....128..1319W	7216	449	0.062			
129 VV Pyx	08:27:33.27	-20:50:38.25	Pri	0.009	0.009	9500	200	0.021	1984A&A...134..147A	8731	544	0.062			
130 HD 71636	08:29:56.31	+37:04:15.48	Pri	0.006	0.006	6950	140	0.020	2006AJ....132..2489H	7282	453	0.062			
131 HD 71636	08:29:56.31	+37:04:15.48	Sec	0.005	0.006	6440	140	0.022	2006AJ....132..2489H	6555	408	0.062			
132 CU Cnc	08:31:37.58	+19:23:39.47	Pri	0.005	0.012	3160	150	0.047	2003A&A...398..239R	3086	216	0.070			
133 CU Cnc	08:31:37.58	+19:23:39.47	Sec	0.003	0.023	3125	150	0.048	2003A&A...398..239R	2943	208	0.071			
134 VZ Hya	08:31:41.41	-06:19:07.56	Pri	0.007	0.004	6645	150	0.023	2008A&A...487..1095C	6523	406	0.062			
135 VZ Hya	08:31:41.41	-06:19:07.56	Sec	0.005	0.006	6290	150	0.024	2008A&A...487..1095C	6339	395	0.062			
136 TZ Pyx	08:41:08.26	-32:12:03.02	Pri	0.019	0.014	7468	203	0.027	2011MNRAS.412..1787D	8282	518	0.063			
137 TZ Pyx	08:41:08.26	-32:12:03.02	Sec	0.039	0.015	7521	208	0.028	2011MNRAS.412..1787D	8596	538	0.063			
138 RS Cha	08:43:12.21	-79:04:12.29	Pri	0.005	0.028	7638	76	0.010	2000MNRAS.313...99R	7817	498	0.064			
139 RS Cha	08:43:12.21	-79:04:12.29	Sec	0.005	0.025	7228	72	0.010	2000MNRAS.313...99R	7369	467	0.063			
140 NSVS 02502726	08:44:11.04	+54:23:47.32	Pri	0.027	0.009	4300	200	0.047	2009NewA...14..496C	4597	321	0.070			
141 del Vel	08:44:42.23	-54:42:31.76	Pri	0.008	0.013	9450	—	—	2011A&A...532A..50M						

ID Star	α (J2000)	δ (J2000)	Com	$\Delta M/M$	$\Delta R/R$	T_{eff}	ΔT_{eff}	$\Delta T/T$	Published temperatures		This study		
									Ref.	T_{eff}	ΔT_{eff}	$\Delta T/T$	
151 2MASS J09381349-0104281	09:38:13.51	-01:04:27.90	Sec	0.028	0.017	4360	150	0.034	2011A&A...527A..14H	4670	328	0.070	
152 DU Leo	09:44:11.38	+25:21:11.41	Pri	0.021	0.025	—	—	—		4823	341	0.071	
153 QX Car	09:54:33.88	-58:25:16.59	Pri	0.013	0.014	23800	500	0.021	1983A&A...121..271A	25874	2360	0.091	
154 QX Car	09:54:33.88	-58:25:16.59	Sec	0.014	0.015	22600	500	0.022	1983A&A...121..271A	25065	2287	0.091	
155 HS Hya	10:24:36.77	-19:05:32.96	Pri	0.006	0.005	6500	50	0.008	1997AJ...114..2764T	6526	406	0.062	
156 HS Hya	10:24:36.77	-19:05:32.96	Sec	0.006	0.006	6400	50	0.008	1997AJ...114..2764T	6473	403	0.062	
157 ZZ UMa	10:30:03.19	+61:48:41.42	Pri	0.011	0.015	5903	60	0.010	1997A&AS..125..529C	5597	350	0.063	
158 ZZ UMa	10:30:03.19	+61:48:41.42	Sec	0.010	0.011	5097	60	0.012	1997A&AS..125..529C	5031	352	0.070	
159 2MASS J10305521+0334265	10:30:55.21	+03:34:26.57	Pri	0.004	0.011	3720	20	0.005	2011ApJ...728..48K	3628	253	0.070	
160 2MASS J10305521+0334265	10:30:55.21	+03:34:26.57	Sec	0.005	0.009	3630	20	0.006	2011ApJ...728..48K	3258	227	0.070	
161 RZ Cha	10:42:24.10	-82:02:14.19	Pri	0.023	0.009	6457	160	0.025	1975A&A...44..349A	5949	371	0.062	
162 RZ Cha	10:42:24.10	-82:02:14.19	Sec	0.026	0.009	6457	160	0.025	1975A&A...44..349A	5983	373	0.062	
163 DW Car	10:43:10.07	-60:02:11.74	Pri	0.011	0.010	27900	1000	0.036	2007A&A...461..1077S	28851	2628	0.091	
164 DW Car	10:43:10.07	-60:02:11.74	Sec	0.013	0.013	26500	1000	0.038	2007A&A...461..1077S	28428	2592	0.091	
165 UW LMi	10:43:30.20	+28:41:09.08	Pri	0.019	0.041	6500	250	0.038	2004A&A...413..635M	5992	392	0.065	
166 UW LMi	10:43:30.20	+28:41:09.08	Sec	0.019	0.050	6500	250	0.038	2004A&A...413..635M	5929	397	0.067	
167 GZ Leo	11:02:02.27	+22:35:45.50	Pri	0.012	0.038	5120	—	—	2000AJ...120..3265F	5772	417	0.072	
168 GZ Leo	11:02:02.27	+22:35:45.50	Sec	0.012	0.036	5120	—	—	2000AJ...120..3265F	5570	401	0.072	
169 chi02 Hya	11:05:57.57	-27:17:16.27	Pri	0.022	0.009	11750	190	0.016	1978A&A...67..15C	10411	990	0.095	
170 chi02 Hya	11:05:57.57	-27:17:16.27	Sec	0.019	0.019	11100	230	0.021	1978A&A...67..15C	10869	1037	0.095	
171 EM Car	11:12:04.51	-61:05:42.93	Pri	0.014	0.018	34000	2000	0.059	1989A&A...213..183A	32454	2966	0.091	
172 EM Car	11:12:04.51	-61:05:42.93	Sec	0.015	0.019	34000	2000	0.059	1989A&A...213..183A	32854	3004	0.091	
173 LSPM J1112+7626	11:12:42.32	+76:26:56.40	Pri	0.005	0.013	3061	162	0.053	2011ApJ...742..123I	2994	209	0.070	
174 FM Leo	11:12:45.09	+00:20:52.84	Pri	0.005	0.026	6316	240	0.038	2010MNRAS.402..2242R	6058	385	0.064	
175 FM Leo	11:12:45.09	+00:20:52.84	Sec	0.005	0.032	6190	211	0.034	2010MNRAS.402..2242R	6166	396	0.064	
176 EP Cru	12:37:16.75	-56:47:17.38	Pri	0.026	0.010	15700	500	0.032	2013ApJ...767..32A	16148	1536	0.095	
177 EP Cru	12:37:16.75	-56:47:17.38	Sec	0.027	0.010	15400	500	0.032	2013ApJ...767..32A	15755	1498	0.095	
178 IM Vir	12:49:38.70	-06:04:44.86	Pri	0.012	0.015	5570	100	0.018	2009ApJ...707..671M	5393	378	0.070	
179 IM Vir	12:49:38.70	-06:04:44.86	Sec	0.008	0.019	4250	130	0.031	2009ApJ...707..671M	4199	295	0.070	
180 HY Vir	13:08:29.92	-02:40:44.38	Pri	0.005	0.003	7870	—	—	2011AJ...142..185L	6627	412	0.062	
181 HY Vir	13:08:29.92	-02:40:44.38	Sec	0.004	0.005	6546	—	—	2011AJ...142..185L	6730	419	0.062	
182 eta Mus	13:15:14.94	-67:53:40.52	Pri	0.012	0.009	12700	100	0.008	2007MNRAS.382..609B	13736	1306	0.095	
183 eta Mus	13:15:14.94	-67:53:40.52	Sec	0.012	0.019	12550	300	0.024	2007MNRAS.382..609B	13764	1314	0.095	
184 SZ Cen	13:50:35.09	-58:29:57.11	Sec	0.009	0.006	8280	300	0.036	1977A&A...55..401G	7505	467	0.062	
185 ZZ Boo	13:56:09.52	+25:55:07.36	Pri	0.006	0.032	6670	30	0.004	1983AJ...88..1242P	6593	423	0.064	
186 ZZ Boo	13:56:09.52	+25:55:07.36	Sec	0.006	0.032	6670	30	0.004	1983AJ...88..1242P	6382	410	0.064	
187 BH Vir	13:58:24.86	-01:39:38.95	Pri	0.015	0.041	6100	100	0.016	2004A&A...424..993K	6217	407	0.065	
188 BH Vir	13:58:24.86	-01:39:38.95	Sec	0.014	0.036	5500	200	0.036	2004A&A...424..993K	5707	411	0.072	
189 DM Vir	14:07:52.43	-11:09:07.49	Pri	0.006	0.010	6500	100	0.015	1996A&A...314..864L	6514	406	0.062	
190 DM Vir	14:07:52.43	-11:09:07.49	Sec	0.006	0.010	6500	300	0.046	1996A&A...314..864L	6485	404	0.062	
191 V636 Cen	14:16:57.91	-49:56:42.36	Pri	0.005	0.004	5900	85	0.014	2009A&A...502..253C	5977	416	0.070	
192 V636 Cen	14:16:57.91	-49:56:42.36	Sec	0.004	0.005	5000	100	0.020	2009A&A...502..253C	5142	358	0.070	
193 Psi Cen	14:20:33.43	-37:53:07.06	Pri	0.005	0.002	10450	300	0.029	2006A&A...456..651B	10003	950	0.095	
194 Psi Cen	14:20:33.43	-37:53:07.06	Sec	0.016	0.002	8800	300	0.034	2006A&A...456..651B	8631	537	0.062	
195 AD Boo	14:35:12.78	+24:38:21.35	Pri	0.006	0.009	6575	120	0.018	2008A&A...487..1095C	6607	412	0.062	
196 AD Boo	14:35:12.78	+24:38:21.35	Sec	0.005	0.008	6145	120	0.020	2008A&A...487..1095C	6420	400	0.062	
197 ASAS J150145-5242.2	15:01:44.67	-52:42:10.81	Pri	0.012	0.049	—	—	—		6301	421	0.067	
198 ASAS J150145-5242.2	15:01:44.67	-52:42:10.81	Sec	0.012	0.050	—	—	—		6372	427	0.067	
199 GG Lup	15:18:56.37	-40:47:17.60	Pri	0.010	0.011	14750	450	0.031	1993A&A...277..439A	16259	1547	0.095	
200 GG Lup	15:18:56.37	-40:47:17.60	Sec	0.010	0.011	11000	600	0.055	1993A&A...277..439A	11699	1113	0.095	
201 GU Boo	15:21:55.17	+33:56:04.20	Pri	0.011	0.025	3920	130	0.033	2005ApJ...631..1120L	3938	279	0.071	
202 GU Boo	15:21:55.17	+33:56:04.20	Sec	0.010	0.032	3810	130	0.034	2005ApJ...631..1120L	3869	277	0.072	
203 CV Boo	15:26:19.54	+36:58:53.43	Pri	0.012	0.018	5760	150	0.026	2008AJ...136..2158T	5325	374	0.070	
204 CV Boo	15:26:19.54	+36:58:53.43	Sec	0.012	0.019	5670	150	0.026	2008AJ...136..2158T	5204	366	0.070	
205 alpha CrB	15:34:41.27	+26:42:52.90	Sec	0.027	0.044	5800	300	0.052	1986AJ...91..1428T	5416	396	0.073	
206 ASAS J155259-6637.8	15:52:58.42	-66:37:47.26	Sec	0.002	0.054	—	—	—		5864	397	0.068	
207 V335 Ser	15:59:05.76	+00:35:44.55	Pri	0.005	0.010	9506	289	0.030	2011NewA...16..412B	8689	542	0.062	
208 V335 Ser	15:59:05.76	+00:35:44.55	Sec	0.011	0.006	8872	248	0.028	2011NewA...16..412B	8826	549	0.062	
209 TV Nor	16:04:09.24	-51:32:39.99	Pri	0.011	0.006	9120	148	0.016	1997A&A...324..137N	9212	573	0.062	
210 TV Nor	16:04:09.24	-51:32:39.99	Sec	0.011	0.009	7798	108	0.014	1997A&A...324..137N	8000	499	0.062	
211 M4-V65	16:23:28.39	-26:30:22.00	Sec	0.007	0.015	4812	125	0.026	2013AJ...145..43K	3961	277	0.070	
212 M4-V66	16:23:32.23	-26:31:41.30	Sec	0.005	0.006	5938	105	0.018	2013AJ...145..43K	4358	304	0.070	
213 M4-V69	16:23:58.01	-26:37:18.00	Pri	0.007	0.012	6084	121	0.020	2013AJ...145..43K	4427	309	0.070	
214 M4-V69	16:23:58.01	-26:37:18.00	Sec	0.005	0.010	5915	137	0.023	2013AJ...145..43K	4312	301	0.070	
215 V760 Sco	16:24:43.72	-34:53:37.53	Pri	0.018	0.020	16900	500	0.030	1985A&A...151..329A	17409	1663	0.096	
216 V760 Sco	16:24:43.72	-34:53:37.53	Sec	0.015	0.019	16300	500	0.031	1985A&A...151..329A	17258	1647	0.095	
217 V1034 Sco	16:54:19.85	-41:50:09.40	Pri	0.025	0.060	34000	150	0.004	2005A&A...441..213S	30919	2961	0.096	
218 WZ Oph	17:06:39.04	+07:46:57.78	Pri	0.006	0.009	6165	100	0.016	2008A&A...487..1095C	6083	379	0.062	
219 WZ Oph	17:06:39.04	+07:46:57.78	Sec	0.005	0.008	6115	100	0.016	2008A&A...487..1095C	6007	374	0.062	
220 V2365 Oph	17:08:45.78	+09:11:10.14	Pri	0.009	0.004	9500	200	0.021	2008MNRAS.384..331I	8092	503	0.062	
221 V2365 Oph	17:08:45.78	+09:11:10.14	Sec	0.009	0.004	6400	210	0.033	2008MNRAS.384..331I	6279	438	0.070	
222 V2368 Oph													

ID Star	α (J2000)	δ (J2000)	Com	$\Delta M/M$	$\Delta R/R$	T_{eff}	ΔT_{eff}	$\Delta T/T$	Published temperatures		This study		
									Ref.	T_{eff}	ΔT_{eff}	$\Delta T/T$	
226 TX Her	17:18:36.45	+41:53:17.10	Pri	0.025	0.018	7534	200	0.027	2011NewA...16..498E	7420	466	0.063	
227 TX Her	17:18:36.45	+41:53:17.10	Sec	0.021	0.021	6678	211	0.032	2011NewA...16..498E	7170	452	0.063	
228 LV Her	17:35:32.40	+23:10:30.60	Pri	0.008	0.009	6060	150	0.025	2009AJ...138.1622T	5988	373	0.062	
229 LV Her	17:35:32.40	+23:10:30.60	Sec	0.007	0.008	6030	150	0.025	2009AJ...138.1622T	5963	371	0.062	
230 V624 Her	17:44:17.25	+14:24:36.24	Pri	0.006	0.010	8150	150	0.018	1984AJ....89.1057P	8078	504	0.062	
231 V624 Her	17:44:17.25	+14:24:36.24	Sec	0.007	0.014	7945	150	0.019	1984AJ....89.1057P	7671	480	0.063	
232 BD-00 3357	17:46:19.42	-00:18:38.10	Sec	0.022	0.053	6425	30	0.005	2006AN...327..899D	6888	466	0.068	
233 V539 Ara	17:50:28.39	-53:36:44.66	Pri	0.011	0.027	18200	1300	0.071	1983A&A...118..255A	18095	1736	0.096	
234 V906 Sco	17:53:54.77	-34:45:09.80	Pri	0.021	0.008	10400	500	0.048	1997A&A...326..709A	9694	922	0.095	
235 V906 Sco	17:53:54.77	-34:45:09.80	Sec	0.021	0.011	10700	500	0.047	1997A&A...326..709A	10594	1008	0.095	
236 Z Her	17:58:06.98	+15:08:21.90	Pri	0.043	0.032	6397	75	0.012	1988AJ....95.1242P	7090	455	0.064	
237 V1647 Sgr	17:59:13.47	-36:56:19.84	Pri	0.018	0.011	9600	310	0.032	1985A&A...145..206A	9727	607	0.062	
238 V1647 Sgr	17:59:13.47	-36:56:19.84	Sec	0.015	0.012	9100	300	0.033	1985A&A...145..206A	9093	568	0.062	
239 V3903 Sgr	18:09:17.70	-23:59:18.22	Pri	0.020	0.011	38000	1900	0.050	1997A&A...327.1094V	39253	3577	0.091	
240 V3903 Sgr	18:09:17.70	-23:59:18.22	Sec	0.023	0.010	34100	1700	0.050	1997A&A...327.1094V	35274	3213	0.091	
241 EG Ser	18:26:02.20	-01:40:51.42	Pri	0.023	0.006	9900	200	0.020	1993AJ...105.2291T	10421	649	0.062	
242 EG Ser	18:26:02.20	-01:40:51.42	Sec	0.015	0.006	9100	200	0.022	1993AJ...105.2291T	9762	608	0.062	
243 V451 Oph	18:29:14.04	+10:53:31.44	Pri	0.022	0.011	10800	800	0.074	1986A&A...167..287C	10436	993	0.095	
244 V451 Oph	18:29:14.04	+10:53:31.44	Sec	0.021	0.015	9800	500	0.051	1986A&A...167..287C	10208	639	0.063	
245 RX Her	18:30:39.26	+12:36:40.34	Pri	0.033	0.045	11100	—	0.006	1980A&AS...42..285J	10746	1049	0.098	
246 RX Her	18:30:39.26	+12:36:40.34	Sec	0.028	0.056	10016	71	0.007	1980A&AS...42..285J	10176	694	0.068	
247 V413 Ser	18:35:08.21	+00:02:34.82	Pri	0.014	0.016	11100	300	0.027	2008MNRAS.389..205C	12490	1191	0.095	
248 V413 Ser	18:35:08.21	+00:02:34.82	Sec	0.012	0.017	10350	280	0.027	2008MNRAS.389..205C	11881	1133	0.095	
249 V1331 Aql	18:44:12.79	-01:33:15.56	Pri	0.011	0.007	25400	100	0.004	2005MNRAS.360..915L	27570	2509	0.091	
250 V1331 Aql	18:44:12.79	-01:33:15.56	Sec	0.019	0.007	20100	140	0.007	2005MNRAS.360..915L	16006	1521	0.095	
251 YY Sgr	18:44:35.86	-19:23:22.71	Pri	0.033	0.012	14800	700	0.047	1997AJ....113.1091L	14837	1412	0.095	
252 YY Sgr	18:44:35.86	-19:23:22.71	Sec	0.026	0.021	14125	670	0.047	1997AJ....113.1091L	13912	1329	0.096	
253 BD+03 3821	18:52:40.31	+04:03:11.75	Pri	0.027	0.008	13140	1500	0.114	2009A&A...508.1375M	13293	1264	0.095	
254 BD+03 3821	18:52:40.31	+04:03:11.75	Sec	0.040	0.010	12044	100	0.008	2009A&A...508.1375M	12001	1141	0.095	
255 DI Her	18:53:26.24	+24:16:40.80	Pri	0.019	0.019	16980	800	0.047	1982ApJ...254..203P	19261	1839	0.095	
256 DI Her	18:53:26.24	+24:16:40.80	Sec	0.013	0.020	15135	715	0.047	1982ApJ...254..203P	17533	1674	0.095	
257 HP Dra	18:54:53.48	+51:18:29.79	Pri	0.005	0.009	6000	150	0.025	2010AJ...140..129M	5288	330	0.062	
258 HP Dra	18:54:53.48	+51:18:29.79	Sec	0.007	0.010	5895	150	0.025	2010AJ...140..129M	5773	403	0.070	
259 V1182 Aql	18:55:23.13	+09:20:48.08	Pri	0.019	0.020	43000	500	0.012	2005ApJS..161..171M	40520	3708	0.092	
260 V1182 Aql	18:55:23.13	+09:20:48.08	Sec	0.024	0.037	30500	500	0.016	2005ApJS..161..171M	36105	3351	0.093	
261 V805 Aql	19:06:18.20	-11:38:57.33	Pri	0.019	0.057	8185	330	0.040	1981ApJ...244..541P	8904	609	0.068	
262 V526 Sgr	19:08:15.03	-31:20:54.94	Pri	0.031	0.011	10140	190	0.019	1997AJ....113.1091L	10185	636	0.062	
263 V526 Sgr	19:08:15.03	-31:20:54.94	Sec	0.036	0.013	8710	100	0.011	1997AJ....113.1091L	8091	506	0.063	
264 KIC 4247791-1	19:08:39.57	+39:22:36.96	Pri	0.012	0.004	—	—	—	—	6470	402	0.062	
265 KIC 4247791-1	19:08:39.57	+39:22:36.96	Sec	0.007	0.004	—	—	—	—	5925	369	0.062	
266 FL Lyr	19:12:04.86	+46:19:26.87	Pri	0.013	0.023	6150	100	0.016	1986AJ....91..383P	6309	399	0.063	
267 FL Lyr	19:12:04.86	+46:19:26.87	Sec	0.011	0.031	5300	95	0.018	1986AJ....91..383P	5506	393	0.071	
268 V565 Lyr	19:20:49.10	+37:46:09.30	Pri	0.003	0.006	5600	95	0.017	2011A&A...525A...2B	5388	376	0.070	
269 V565 Lyr	19:20:49.10	+37:46:09.30	Sec	0.003	0.009	5430	125	0.023	2011A&A...525A...2B	5280	369	0.070	
270 V568 Lyr	19:20:54.30	+37:45:34.70	Pri	0.007	0.011	5665	100	0.018	2008A&A...492..171G	5274	329	0.062	
271 V568 Lyr	19:20:54.30	+37:45:34.70	Sec	0.005	0.008	4900	100	0.020	2008A&A...492..171G	5157	360	0.070	
272 V1430 Aql	19:21:48.49	+04:32:56.92	Pri	0.010	0.009	5262	150	0.029	2012NewA...17..498L	5140	359	0.070	
273 V1430 Aql	19:21:48.49	+04:32:56.92	Sec	0.023	0.012	4930	100	0.020	2012NewA...17..498L	5130	359	0.070	
274 UZ Dra	19:25:55.05	+68:56:07.15	Pri	0.015	0.023	6210	110	0.018	1989AJ....97..822L	6945	439	0.063	
275 UZ Dra	19:25:55.05	+68:56:07.15	Sec	0.016	0.017	5985	110	0.018	1989AJ....97..822L	6767	425	0.063	
276 V2080 Cyg	19:26:47.95	+50:08:43.77	Pri	0.014	0.005	6000	75	0.013	2008MNRAS.384..331I	5514	343	0.062	
277 V2080 Cyg	19:26:47.95	+50:08:43.77	Sec	0.015	0.005	5987	75	0.013	2008MNRAS.384..331I	5338	332	0.062	
278 WTS 19e-3-08413	19:32:43.20	+36:36:53.50	Pri	0.054	0.046	3506	140	0.040	2012MNRAS.426.1507B	3233	237	0.073	
279 V885 Cyg	19:32:49.86	+30:01:17.03	Pri	0.015	0.005	8375	150	0.018	2004AJ...128.1324L	7746	482	0.062	
280 V885 Cyg	19:32:49.86	+30:01:17.03	Sec	0.012	0.008	8150	150	0.018	2004AJ...128.1324L	7245	451	0.062	
281 WTS 19b-2-01387	19:34:15.50	+36:28:27.30	Pri	0.038	0.026	3498	100	0.029	2012MNRAS.426.1507B	3474	246	0.071	
282 WTS 19b-2-01387	19:34:15.50	+36:28:27.30	Sec	0.035	0.027	3436	100	0.029	2012MNRAS.426.1507B	3389	240	0.071	
283 WTS 19c-3-01405	19:36:40.70	+36:42:46.00	Pri	0.056	0.048	3309	130	0.039	2012MNRAS.426.1507B	3065	226	0.074	
284 KIC 6131659	19:37:06.98	+41:26:12.86	Pri	0.008	0.003	5660	140	0.025	2012ApJ...761..157B	5496	383	0.070	
285 KIC 6131659	19:37:06.98	+41:26:12.86	Sec	0.007	0.009	4780	105	0.022	2012ApJ...761..157B	4498	314	0.070	
286 V1143 Cyg	19:38:41.18	+54:58:25.66	Pri	0.012	0.017	6460	100	0.015	1987A&A...174..107A	7089	445	0.063	
287 V1143 Cyg	19:38:41.18	+54:58:25.66	Sec	0.010	0.017	6400	100	0.016	1987A&A...174..107A	6905	433	0.063	
288 V541 Cyg	19:42:29.45	+31:19:40.20	Pri	0.040	0.016	9885	230	0.023	1998AJ....115..801L	10039	629	0.063	
289 V541 Cyg	19:42:29.45	+31:19:40.20	Sec	0.036	0.022	9955	230	0.023	1998AJ....115..801L	10280	649	0.063	
290 V1765 Cyg	19:48:50.60	+33:26:14.22	Pri	0.014	0.037	—	—	—	—	22861	2122	0.093	
291 V1765 Cyg	19:48:50.60	+33:26:14.22	Sec	0.020	0.037	—	—	—	—	26655	2474	0.093	
292 V380 Cyg	19:50:37.33	+40:35:59.13	Sec	0.036	0.019	20500	500	0.024	2000ApJ...544..409G	23501	2149	0.091	
293 BD-20 5728	19:51:12.79	-20:30:10.21	Pri	0.005	0.047	—	—	—	—	5976	397	0.066	
294 KIC 10935310	19:51:39.82	+48:19:55.38	Pri	0.031	0.011	4320	100	0.023	2013MNRAS.429..85C	4535	317	0.070	
295 V477 Cyg	20:05:27.69	+31:58:18.11	Sec	0.052	0.031	6700	235	0.035	1992A&A...260..227G	6944	445	0.064	
296 V453 Cyg	20:06:34.97	+35:44:26.28	Pri	0.0									

ID Star	α (J2000)	δ (J2000)	Com	$\Delta M/M$	$\Delta R/R$	T_{eff}	ΔT_{eff}	$\Delta T/T$	Published temperatures		This study		
									Ref.	T_{eff}	ΔT_{eff}	$\Delta T/T$	
301 V478 Cyg	20:19:38.75	+38:20:09.20	Pri	0.054	0.016	30550	1070	0.035	1991AJ....101..600P	29246	2670	0.091	
302 V478 Cyg	20:19:38.75	+38:20:09.20	Sec	0.055	0.016	30550	1070	0.035	1991AJ....101..600P	28824	2632	0.091	
303 MY Cyg	20:20:03.39	+33:56:35.02	Pri	0.017	0.009	7050	200	0.028	2009AJ....137.2949T	7346	458	0.062	
304 MY Cyg	20:20:03.39	+33:56:35.02	Sec	0.017	0.009	7000	200	0.029	2009AJ....137.2949T	7200	449	0.062	
305 V399 Vul	20:25:10.80	+21:29:18.84	Pri	0.011	0.005	19000	320	0.017	2012NewA...17..215C	18318	1667	0.091	
306 V399 Vul	20:25:10.80	+21:29:18.84	Sec	0.006	0.025	18250	520	0.028	2012NewA...17..215C	17697	1695	0.096	
307 BP Vul	20:25:33.25	+21:02:17.97	Pri	0.009	0.008	7709	150	0.019	2003AJ....126.1905L	7704	480	0.062	
308 BP Vul	20:25:33.25	+21:02:17.97	Sec	0.006	0.009	6823	150	0.022	2003AJ....126.1905L	6848	427	0.062	
309 V442 Cyg	20:27:52.30	+30:47:28.30	Pri	0.013	0.014	6900	82	0.012	1987AJ....94..712L	6486	406	0.063	
310 V442 Cyg	20:27:52.30	+30:47:28.30	Sec	0.014	0.018	6808	79	0.012	1987AJ....94..712L	6477	407	0.063	
311 MP Del	20:28:26.57	+11:43:14.52	Pri	0.055	0.019	7400	120	0.016	2008MNRAS.390..958I	5986	376	0.063	
312 MP Del	20:28:26.57	+11:43:14.52	Sec	0.059	0.019	6927	120	0.017	2008MNRAS.390..958I	5842	367	0.063	
313 V456 Cyg	20:28:50.84	+39:09:13.69	Pri	0.032	0.012	7750	100	0.013	2014AJ....147..149B	8725	545	0.062	
314 V456 Cyg	20:28:50.84	+39:09:13.69	Sec	0.032	0.014	6755	400	0.059	2014AJ....147..149B	7804	488	0.063	
315 IO Aqr	20:40:45.47	+00:56:21.02	Pri	0.012	0.024	6600	—	0.045	2004A&A...417..689D	6121	388	0.063	
316 V379 Cep	20:43:13.38	+57:06:50.39	Pri	0.022	0.015	22025	428	0.019	2007A&A...463.1061H	21187	1934	0.091	
317 V379 Cep	20:43:13.38	+57:06:50.39	Sec	0.021	0.013	20206	374	0.019	2007A&A...463.1061H	21641	2060	0.095	
318 Y Cyg	20:52:03.58	+34:39:27.47	Pri	0.023	0.050	31000	2000	0.065	1995AJ....297..127H	33493	3159	0.094	
319 Y Cyg	20:52:03.58	+34:39:27.47	Sec	0.017	0.053	31570	2000	0.063	1995AJ....297..127H	34363	3255	0.095	
320 CG Cyg	20:58:13.45	+35:10:29.66	Pri	0.013	0.015	5260	185	0.035	1994AJ....108.1091P	5633	395	0.070	
321 CG Cyg	20:58:13.45	+35:10:29.66	Sec	0.016	0.017	4720	66	0.014	1994AJ....108.1091P	4871	342	0.070	
322 V1061 Cyg	21:07:20.52	+52:02:58.42	Pri	0.012	0.011	6180	100	0.016	2006ApJ...640.1018T	5934	370	0.062	
323 V1061 Cyg	21:07:20.52	+52:02:58.42	Sec	0.008	0.021	5300	150	0.028	2006ApJ...640.1018T	5286	372	0.070	
324 EI Cep	21:28:28.21	+76:24:12.59	Pri	0.004	0.017	6750	100	0.015	2000AJ....119.1942T	6295	395	0.063	
325 EI Cep	21:28:28.21	+76:24:12.59	Sec	0.004	0.019	6950	100	0.014	2000AJ....119.1942T	6627	417	0.063	
326 2MASS J21295384-5620038	21:29:54.00	-56:20:03.87	Pri	0.020	0.014	4750	150	0.032	2011A&A...527A..14H	4997	350	0.070	
327 2MASS J21295384-5620038	21:29:54.00	-56:20:03.87	Sec	0.018	0.024	4220	180	0.043	2011A&A...527A..14H	4459	315	0.071	
328 EE Peg	21:40:01.88	+09:11:05.11	Pri	0.009	0.014	8700	200	0.023	1984ApJ...281..268L	9114	570	0.063	
329 EE Peg	21:40:01.88	+09:11:05.11	Sec	0.008	0.008	6450	300	0.047	1984ApJ...281..268L	6846	426	0.062	
330 EK Cep	21:41:21.51	+69:41:34.11	Pri	0.010	0.009	9000	200	0.022	1987ApJ...313L..81P	9848	614	0.062	
331 EK Cep	21:41:21.51	+69:41:34.11	Sec	0.009	0.011	5700	190	0.033	1987ApJ...313L..81P	5699	356	0.062	
332 OO Peg	21:41:37.70	+14:39:30.75	Pri	0.018	0.037	8770	150	0.017	2001A&A...378..477M	7161	464	0.065	
333 OO Peg	21:41:37.70	+14:39:30.75	Sec	0.018	0.036	8683	180	0.021	2001A&A...378..477M	8725	565	0.065	
334 VZ Cep	21:50:11.14	+71:26:38.30	Pri	0.011	0.008	6670	160	0.024	2009AJ....137..507T	6663	415	0.062	
335 VZ Cep	21:50:11.14	+71:26:38.30	Sec	0.007	0.038	5720	120	0.021	2009AJ....137..507T	6268	407	0.065	
336 BG Ind	21:58:30.08	-59:00:43.71	Pri	0.006	0.007	6353	270	0.042	2011MNRAS.414.2479R	5607	349	0.062	
337 BG Ind	21:58:30.08	-59:00:43.71	Sec	0.006	0.023	6653	233	0.035	2011MNRAS.414.2479R	5879	372	0.063	
338 CM Lac	22:00:04.45	+44:33:07.74	Pri	0.030	0.020	9000	300	0.033	2012Ap&SS.340..281L	9788	616	0.063	
339 BW Aqr	22:23:15.93	-15:19:56.22	Pri	0.014	0.019	6350	100	0.016	1991A&A...246..397C	6145	386	0.063	
340 BW Aqr	22:23:15.93	-15:19:56.22	Sec	0.015	0.022	6450	100	0.016	1991A&A...246..397C	6100	385	0.063	
341 WX Cep	22:31:15.78	+63:31:21.55	Pri	0.020	0.008	8150	225	0.028	1987AJ....93..672P	7188	448	0.062	
342 WX Cep	22:31:15.78	+63:31:21.55	Sec	0.019	0.009	8872	250	0.028	1987AJ....93..672P	9444	898	0.095	
343 LL Aqr	22:34:42.15	-03:35:58.17	Pri	0.047	0.015	6680	160	0.024	2008MNRAS.390..958I	6233	390	0.063	
344 LL Aqr	22:34:42.15	-03:35:58.17	Sec	0.048	0.016	6200	160	0.026	2008MNRAS.390..958I	6054	424	0.070	
345 RW Lac	22:44:57.10	+10:49:39:27.57	Pri	0.006	0.003	5760	100	0.017	2005AJ....130.2838L	4757	331	0.070	
346 RW Lac	22:44:57.10	+10:49:39:27.57	Sec	0.005	0.004	5560	150	0.027	2005AJ....130.2838L	4879	340	0.070	
347 DH Cep	22:46:54.11	+58:05:03.50	Pri	0.052	0.035	41000	2000	0.049	1996A&A...314..165H	36706	3400	0.093	
348 DH Cep	22:46:54.11	+58:05:03.50	Sec	0.054	0.035	39550	2000	0.051	1996A&A...314..165H	34698	3214	0.093	
349 AH Cep	22:47:52.94	+65:03:43.80	Pri	0.013	0.017	29900	1000	0.033	1990A&A...236..409H	30257	2764	0.091	
350 AH Cep	22:47:52.94	+65:03:43.80	Sec	0.015	0.022	28600	1000	0.035	1990A&A...236..409H	28962	2653	0.092	
351 V364 Lac	22:52:14.81	+38:44:44.64	Pri	0.006	0.011	8250	150	0.018	1999AJ....118.1831T	7938	495	0.062	
352 V364 Lac	22:52:14.81	+38:44:44.64	Sec	0.011	0.012	8500	150	0.018	1999AJ....118.1831T	8208	513	0.063	
353 EF Aqr	23:01:19.09	-06:26:15.35	Pri	0.006	0.009	6150	65	0.011	2012A&A...540A..64V	6318	394	0.062	
354 EF Aqr	23:01:19.09	-06:26:15.35	Sec	0.006	0.013	5185	110	0.021	2012A&A...540A..64V	5439	380	0.070	
355 CW Cep	23:04:02.22	+63:23:48.76	Pri	0.012	0.022	28300	1000	0.035	1991A&A...241..98C	26930	2467	0.092	
356 CW Cep	23:04:02.22	+63:23:48.76	Sec	0.013	0.024	27700	1000	0.036	1991A&A...241..98C	27019	2479	0.092	
357 PV Cas	23:10:02.58	+59:12:06:15	Pri	0.018	0.009	10200	250	0.025	1995AJ....109.2680B	11150	1060	0.095	
358 PV Cas	23:10:02.58	+59:12:06:15	Sec	0.022	0.007	10200	250	0.025	1995AJ....109.2680B	11489	1092	0.095	
359 RT And	23:11:10.10	+53:01:33.04	Pri	0.024	0.012	6095	214	0.035	1994AJ....108.1091P	6467	404	0.062	
360 RT And	23:11:10.10	+53:01:33.04	Sec	0.022	0.014	4732	110	0.023	1994AJ....108.1091P	5310	372	0.070	
361 V396 Cas	23:13:35.98	+56:44:17.20	Pri	0.009	0.005	9225	150	0.016	2004AJ...128.3005L	9230	574	0.062	
362 V396 Cas	23:13:35.98	+56:44:17.20	Sec	0.008	0.006	8550	120	0.014	2004AJ...128.3005L	8669	540	0.062	
363 2MASS J23143816+0339493	23:14:38.16	+03:39:49.33	Pri	0.004	0.005	3460	180	0.052	2011ApJ...728..48K	3426	239	0.070	
364 2MASS J23143816+0339493	23:14:38.16	+03:39:49.33	Sec	0.003	0.005	3320	180	0.054	2011ApJ...728..48K	2911	203	0.070	
365 AR Cas	23:30:01.94	+58:32:56.11	Pri	0.034	0.012	17200	500	0.029	1999A&A...345..855H	15964	1519	0.095	
366 AR Cas	23:30:01.94	+58:32:56.11	Sec	0.032	0.019	8150	200	0.025	1999A&A...345..855H	8964	564	0.063	
367 V731 Cep	23:37:43.55	+64:18:11.20	Pri	0.038	0.016	10700	200	0.019	2008MNRAS.390..399B	11709	1116	0.095	
368 V731 Cep	23:37:43.55	+64:18:11.20	Sec	0.042	0.015	9265	220	0.024	2008MNRAS.390..399B	9408	589	0.063	
369 IT Cas	23:42:01.40	+51:44:36.80	Pri	0.007	0.009	6470	110	0.017	1997AJ....114.1206L	6205	387	0.062	
370 IT Cas	23:42:01.40	+51:44:36.80	Sec	0.006	0.025	6470	110	0.017	1997AJ....114.1206L	6262	397	0.063	
371 BK Peg	23:47:08.46	+26:33:59.92	Pri	0.005</td									